JOURNAL OF
The Electrochemical Society

VOLUME 99 NUMBER 5

May, 1949

Published Monthly by
THE ELECTROCHEMICAL SOCIETY

Journal of The Electrochemical Society

Number 5 **May 1949** Volume 95

Current Affairs

Editorial:
Moving the Decimal Point Over 93C
Section News 94C
Personals 98C
Letters to the Editor 98C
Book Reviews 99C
New Members 101C
Recent Patents 102C
Employment Situations 102C

Feature Section

A Report from President Lee 103C
The Profession of Electrochemistry
III. The Electrochemical Engineer. *C. L. Mantell* 104C

Technical Notes and Reviews

Possible Role of the Solid Surface in Electroless Plating. *E. E. Glenn, Jr., E. L. Cook, and N. Hackerman* 110C

Technical Papers

Deposition of Metals on Aluminum. *S. Heiman* 205
Effect of Non-Condensable Gases on Corrosion of Nickel in Steam Condensate. *W. A. Wesley and H. R. Copson* 226
Long-Term Deterioration in Certain Phosphors. *E. F. Lowry* 242
Double and Triple Activated Magnesium Pyrophosphate Phosphors. *H. G. Froelich* 254
Fluorescence of Silicate Phosphors III. *K. H. Butler* 267
Electron Affinity of the Carbon Atom. *G. Glockler and J. W. Sauerwald* 282
Thermionic Emission from Carbon. *G. Glockler and J. W. Sauerwald* 292

EDITORIAL STAFF

H. H. Uhlig
Editor

Eleanor Reid
Managing Editor

H. B. Linford
U. B. Thomas
Associate Editors

R. M. Burns
Consultant

PUBLICATION COMMITTEE

H. J. Read
Chairman

J. M. Bialosky
Paul S. Brellier
N. C. Cahoon
C. L. Faust
H. C. Froelich
A. E. Pavlish
E. B. Sanigar
Sherlock Swann, Jr.
Archie J. Weith

Published monthly by The Electrochemical Society, Inc., Mt. Royal and Guilford Aves., Baltimore 2, Md. Editorial office, 235 W. 102nd Street, New York 25, N. Y. Statements and opinions given in articles and papers in the Journal of The Electrochemical Society are those of the contributors and The Electrochemical Society assumes no responsibility for them. Subscription $7.50 to members and $10 to non-members. Single copies $0.75 to members, $1.00 to non-members. Copyright 1949 by The Electrochemical Society.

Entered as second class matter November 15, 1947, at the Post Office at Baltimore, Maryland, under the act of August 24, 1912.

DEPOSITION OF METALS ON ALUMINUM BY IMMERSION FROM SOLUTIONS CONTAINING FLUORIDES[1]

SAMUEL HEIMAN[2]

University of Pennsylvania, Philadelphia, Pennsylvania

ABSTRACT

A new process has been developed for depositing zinc, cadmium, and tin by chemical displacement upon aluminum. The immersion solutions contain the metal sulfate and either hydrofluoric acid or the fluoride anion. The deposited metals have good appearance, sound structure, and excellent adhesion to the aluminum, which does not depend on any roughening of the aluminum surface. The bond between the zinc deposit and aluminum is the best of the metals deposited and is greater than the cohesive strength of the aluminum base metal. The zinc immersion deposit may thus be used as a base for plating other metals. The effectiveness of the method results from the extraordinarily high solubility of the oxide film on the aluminum in solutions containing the fluoride anion in acid environment. This is shown from published solubility data and is demonstrated by potential measurements.

INTRODUCTION

Electroplated coatings upon aluminum have assumed an important place among the finishes for this metal because the light weight and low cost of aluminum are combined with the specific desirable properties of the plated coating. Thus, aluminum is plated with silver for increased surface conductivity on contracts and electronic parts, with cadmium and nickel for improved solderability, brass for bonding to rubber, heavy chromium for wear resistance, and decorative chromium on nickel for improved appearance and abrasion resistance. The applications are manifold and continually increasing.

The present status of the art is the culmination of years of research in an effort to obtain deposits as adherent and as smooth as those obtained in other plating processes. Since 1890, over 150 patents and 300 papers have been devoted to this subject; all but a few yield unsatisfactory results. The difficulty in plating on aluminum results from the high potential of the metal which ordinarily tends to produce loosely adherent immersion deposits and the ever-present surface oxide film. The problem has been attacked by five general methods:

(a) *Etching the surface.* Aluminum may be etched in a mixture of nitric and hydrofluoric acids and then nickel plated (1). The adhesion of the nickel to the aluminum depended to a large extent on the keying action of the nickel deposit in the pits in the aluminum surface.

[1] Manuscript received December 14, 1948. This paper, based upon a thesis presented to the faculty of the Graduate School of the University of Pennsylvania, Philadelphia, Pennsylvania, by the author in partial fulfillment of the requirements for the degree of Doctor of Philosophy, prepared for delivery before the Chicago Meeting, October 12 to 15, 1949.

[2] Chief Chemist, Philadelphia Rust-Proof Company, Philadelphia, Pennsylvania.

(b) *Deposition of a bonding metal by electrochemical displacement.* The aluminum oxide film may be replaced by a metal deposited on the aluminum by electrochemical displacement. The immersion coating then serves as a base for the subsequent electrodeposition of other metals. Several processes have been proposed for depositing nickel (1), iron (2, 3, 4), and manganese (5) from hydrochloric acid solutions. In these processes, however, the aluminum was pitted by the hydrochloric acid and the adhesion attained was more the result of a mechanical keying action in the pits in the aluminum than a true adhesion of the two metals. The process involving the deposition of zinc by immersion on the aluminum from a highly alkaline zincate solution has been much more successful in securing the highest degree of adhesion without pitting the base metal (6, 7, 8, 9, 10).

(c) *Anodic treatment.* The natural oxide coating on aluminum may be replaced by a relatively thick, porous, anodic oxide coating (11, 12, 13, 14). The electroplated metal adheres to the aluminum by virtue of properly filling the pores of the oxide coating and this type of adhesion is thus similar to the mechanical keying action described above in (a).

(d) *Special plating solutions.* Various methods have been proposed for plating zinc (15), cadmium (16), copper (17, 18), and nickel (19) directly on aluminum, usually from solutions of special composition, but none of these coatings has the degree of adhesion required. Zinc (20, 21) and chromium (22, 23) have been reported to be plated directly on certain alloys of aluminum to a limited extent.

(e) *Miscellaneous methods.* Copper has been deposited by immersion on aluminum from molten cuprous chloride at 450°C. (24, 25). A high degree of adhesion is obtained but the physical properties, resulting from heat treatment of the aluminum, are adversely affected and the process, in general, is more difficult than those described above.

Of all the methods which have been devised and studied, only two produce smooth and adherent deposits and are used commercially today. They are the zinc immersion process and the anodic coating process. The former process is much more widely used because it is applicable to more alloys, requires less equipment and time, and the conditions are less critical.

PRELIMINARY EXPERIMENTAL WORK

An initial purpose of this research was to electroplate or deposit by immersion metals other than zinc and obtain a deposit equal to or better in quality than that obtained by the zinc immersion process. A study of copper was undertaken first and an intensive study of cyanide copper solutions was made. This type of solution has the advantage of being alkaline for the removal of the aluminum oxide and having a cyanide complex to decrease the copper ion concentration and favor immersion deposits of good structure. Fair adhesion was obtained on 24ST alloy but only poor adhesion on 2S aluminum.

At this point it was decided to study only immersion deposits on aluminum. It is probable that the metal electrodeposited upon aluminum during the first few seconds of plating contains a certain amount of metal which has been deposited by immersion. If this immersion deposit is not adherent to the aluminum, the plated coating will probably not be adherent. Furthermore, it would be reasonable to expect that a solution

from which satisfactory immersion deposits might be obtained would be suitable, with little or no modification, for plating that metal upon aluminum. It was decided, therefore, to direct this investigation toward finding satisfactory immersion coatings on aluminum to be used as a base for subsequent plating of copper.

Considerable exploratory work was carried out in an effort to obtain immersion cadmium coatings which would be a satisfactory base for plating. Cyanide cadmium solutions were tested over a wide range of conditions. The cadmium immersion deposits had excellent appearance and structure, but copper subsequently electroplated on these coatings blistered. The separation occurred between the cadmium and aluminum.

Since efforts to deposit copper and cadmium from alkaline solutions were unsuccessful, attention was directed toward the acid type solutions. Such a solution must contain a compound which has a solvent action on the aluminum oxide. The formation of a complex compound containing the metal is desirable in order to decrease the rate of deposition by immersion and to favor sound immersion deposits. Hydrofluoric acid and the fluoride salts have these properties to a striking degree; accordingly, they were investigated.

LITERATURE

The use of hydrofluoric acid for the cleaning and pickling of aluminum has been known for many years. For this purpose, it was found that hydrofluoric acid works better in combination with nitric acid (26, 27). This mixture is used commercially today to clean aluminum and produces a smooth, semi-bright surface on the aluminum. Fluorides have also been recommended in various combinations for cleaning aluminum kitchen and chemical ware (28, 29, 30, 31).

Mellor (32) states that in the reaction of aluminum with hydrofluoric acid, the aluminum fluoride which is produced has a low solubility, so that a protective coating of the fluoride may remain on the metal when the concentration of the acid is great enough.

Ephraim (34) points out that aluminum fluoride prepared in the dry way is remarkably insoluble in water and resists boiling sulfuric acid and alkalies. It dissolves slightly in hydrofluoric acid with the formation of a complex fluoride. Aluminum hydroxide, however, dissolves easily in hydrofluoric acid with no tendency to reprecipitate the fluoride.

Hess and coworkers (35, 36) investigated the use of dilute hydrofluoric acid and other materials for removing the irregular, gross oxide film on aluminum surfaces prior to spot welding. The thickness and condition of the oxide film was determined and expressed in terms of the electric contact resistance between two specimens of aluminum. When the contact resistance was plotted as a function of time of treatment, a "V"-shaped curve was obtained. The contact resistance first fell as the original oxide film was removed; then there was a period of equilibrium during which the surface contact resistance remained low; and, finally, the surface resistance rose again as another film, presumable insoluble reaction products, built up on the surface.

Work (1, 20) utilized a dip in dilute hydrofluoric acid to prepare aluminum for plating. He used a 5 per cent solution for fifteen seconds and

noted that this method does not specially roughen the surface. The hydrofluoric acid treatment was said to dissolve the oxide and make the surface uniformly active. For treatment of silicon-bearing aluminum alloys, a mixture of 3 parts concentrated nitric acid and 1 part hydrofluoric acid by volume has been recommended; but the latter acid is a solvent for the silicon and the mixture has a strong tendency to etch the aluminum.

Thomas and coworkers (37, 38) studied the effect of certain acids upon the rates of dissolution of certain hydrous alumina specimens. Part of their data is given in Fig. 1.

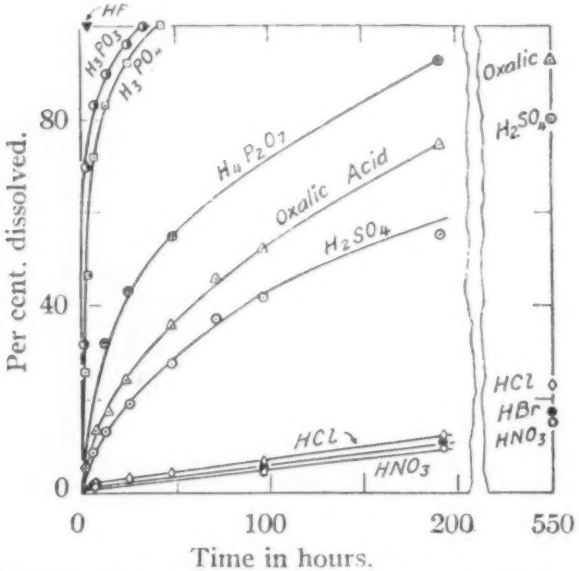

FIG. 1. The dissolution of $Al_2O_3 \cdot 2.89\ H_2O$ in diverse acids. This graph (from Reference 37) contrasts the rates of dissolution of 260 mg. of 100-mesh $Al_2O_3 \cdot 2.89\ H_2O$ at 25° in 200 ml. of 0.2*N* solution (H_3PO_3 and H_3PO_4 were 0.1M) of the acids indicated on the curves. The oxide dissolved completely in the 0.2*N* HF in about 6 minutes and in the 0.2*N* H_2SiF_6 in about 2 hours. (Reprinted by permission from the *Journal of The American Chemical Society*)

Other data by Clay and Thomas show that the rate of dissolution of hydrous alumina in an acid solution is dependent upon the nature and concentration of the anions present and upon the temperature at which the oxides were prepared.

The extraordinarily high rate of dissolution of hydrous alumina in the hydrofluoric acid solution, or in acid solutions containing the fluoride ion, is indeed striking. The application of hydrofluoric acid and fluorides in solutions for the deposition of metals on aluminum was, therefore, strongly indicated. On the other hand, the relatively low solubility of the oxide in hydrochloric acid may account for the lack of true adhesion of the metals deposited on aluminum from solutions containing this acid (1, 2, 3, 4, 5).

According to Thomas and coworkers, the differences in dissolution rates are neither a function of the hydrogen ion activity, nor of diffusibility, or valence of the ions. It is postulated that the explanation lies in (a) the coördination structure of the oxide and (b) the specific nature of the anions. The formula $Al_2O_3 \cdot xH_2O$ does not adequately represent the formula of hydrous alumina; they are complex polyolated and polyoxolated structures. While oxonium ions readily convert the hydroxo groups present to aquo groups, the ol and oxo bridges, however, are very resistant to attack. Before an oxonium ion can react with an ol or oxo link, it is necessary to form an intermediate link (an aluminum-anion complex), the formation of which renders the ol and oxo groups reactive toward oxonium ion. The formation of this intermediate complex is the rate-determining factor in the dissolution process.

Thus, the catalytic effect of an anion in acid solutions upon the rate of dissolution of hydrous alumina depends upon the specific property of that anion to bind coördinatively and form stable complexes with the aluminum ion. The fluoride anion possesses this property to a high degree.

The mechanism of the catalytic effect of anions in the dissolution of hydrous alumina in acid solutions is as follows: When an anion, such as fluoride ion, which forms a complex with an aluminum ion in acid solution approaches the aluminum ion in an ol $\underset{(\mathrm{AlOAl})}{\overset{\mathrm{H}}{}}$ link, the bond between the aluminum and the oxygen will be broken. This may be shown in the following manner:

$$\mathrm{F^-} \rightarrow \mathrm{Al} \cdots \underset{\mathrm{OAl.}}{\overset{\mathrm{H}}{}}$$

The ol group has now been converted into an hydroxo group which readily reacts with a proton from an oxonium ion in the solution.

Hydrofluoric acid in combination with either nitric acid or ferric sulfate is used widely in dissolving oxide scale on stainless steel. Percival and coworkers (39) offer a theory for the high rate of solution of metal oxides in hydrofluoric acid which is similar to that made above by Thomas. The specific effectiveness of the fluoride ion in stainless steel pickling is considered to be due to its complex-forming tendency as a result of its free electron pairs and its relatively small radius with consequent high charge density. The stages in the process may be represented briefly as follows: (a) formation of a metal-fluoride complex; (b) loosening of the metal-oxygen bond; and (c) reaction of oxygen with protons from oxonium ions in solution to form water.

POTENTIAL OF ALUMINUM IN VARIOUS ELECTROLYTES

Although the data of Thomas and coworkers were obtained from solubility measurements of hydrous alumina in various acid solutions, it would be interesting to check their results electrochemically. Aluminum placed in a normal solution of aluminum ions does not exhibit its true reversible potential of -1.69 volts (40, 41, 42). The apparent potential which is observed is considerably lower than the reversible potential, and this is caused by the film of oxide on the surface which introduces a high resistance or polarization effect. According to Thomas, those anions in acid solutions

which form stable complexes with aluminum will dissolve aluminum oxide. However, a solution with both these properties should, according to electrochemical considerations, raise the apparent potential of the aluminum immersed in it. Accordingly, potential measurements were made of aluminum in various electrolytes in an effort to find some correlation or tendency of these electrolytes to act as solvents for the natural oxide on the surface of the aluminum. The potential of aluminum immersed in various electrolytes was measured against a specially designed saturated calomel half cell (43) by the compensation method, using a Leeds and Northrup Type 2651 potentiometer. The potential readings were converted to the hydrogen scale by adding +0.246 volts.

The 2S aluminum panels were cleaned in hydrofluoric and nitric acids

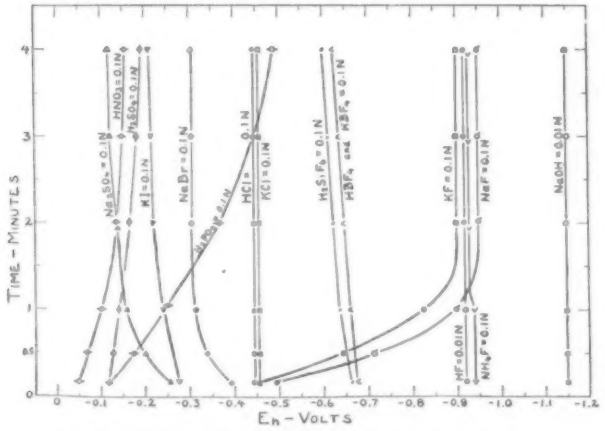

FIG. 2. Potential of aluminum in various electrolytes

as described later in the section headed "Standard Procedure" and then immersed in the electrolyte at 25° C. Two hundred ml. of the 0.1*N* solution under investigation were contained in 250 ml. beakers. The tip of the calomel cell was lightly pressed against the panel and cell voltage readings were taken at appropriate time intervals up to four minutes. The results are plotted in Fig. 2. Most of the curves are the average of two sets of measurements. The reproducibility of the measurements was usually about ±10 millivolts.

Gassing at the surface of the aluminum immersed in the 0.1*N* sodium hydroxide and 0.1*N* hydrofluoric acids interfered with the sensitivity of the potential determinations. Consequently, this work was repeated with more dilute solutions (0.01*N*) where there was much less gassing and steady readings were obtained.

It will be observed that the aluminum in the 0.01*N* sodium hydroxide solution exhibits the highest potential value of −1.15 volts. This value is closest to the reversible figure of −1.69 and this may be taken as an

indication that sodium hydroxide has the greatest ability to dissolve the aluminum oxide and thus decrease its resistance.

The fluorides are next in effectiveness and the aluminum has an apparent potential of approximately −0.90 to −0.95 volts in both 0.01*N* hydrofluoric acid and 0.1*N* solutions of sodium, potassium, and ammonium fluoride. A high solvent action of fluorides for aluminum oxide compared to other anions is indicated.

Following in decreasing order are fluoboric acid, potassium fluoborate, and fluosilicic acid at approximately −0.65 volts, hydrochloric acid and potassium chloride at −0.45 volts, sodium bromide at −0.3 volts, potassium iodide at −0.2 volts, and sulfuric acid, sodium sulfate, and nitric acid at −0.15 volts.

The fact that aluminum has approximately the same potential in either an acid or its corresponding salt indicates that the anion is the most important factor in dissolving the oxide film on aluminum (i.e., in reducing the passivity of aluminum), and not the acidity of the environment in which the anion is present. This was demonstrated for the acids and salts of the fluoride, fluoborate, chloride, and sulfate anions. This agrees with the work of Thomas cited above who found that the rate of dissolution of hydrous aluminum oxide is a specific property of the anion present in a solution and not of the acidity.

The data from Fig. 1 showing the relative solvent power of anions on hydrous alumina are listed in decreasing order in Table I. In presenting the potential data given in Fig. 2, the solution containing hydroxide, in which the aluminum exhibited the highest potential, is given first and the others are listed in decreasing order.

Inspection of Table I indicates a close correlation between the Thomas data and the potential data, although the position of the sulfate ion is anomalous. The greater the solvent action of an anion for the oxide film on the aluminum, the higher the potential of the aluminum in a solution containing this anion, i.e., the closer the potential is to the reversible potential of −1.69 volts.

PRELIMINARY EXPERIMENTAL WORK WITH SOLUTIONS CONTAINING HYDROFLUORIC ACID

Exploratory tests were carried out in which, in general, hydrofluoric acid was added to solutions of various metal salts, and the quality and adhesion of the immersion deposits produced on the aluminum were noted and studied. The metals studied were zinc, cadmium, tin, and copper.

During the course of this exploratory work, modifications and improvements were constantly made and these will be discussed before presenting the standard procedure which finally was evolved.

The aluminum panels were 2 inch x 0.875 inch x 0.051 inch (5.08 cm. x 2.22 cm. x 0.130 cm.) and had a total area of 0.025 sq. ft. (0.23 sq. dm.). The chemicals were reagent grade and in most of this research, commercially pure aluminum (2S)[3] was used.

Cleaning the aluminum.—A standard method for preparing aluminum for plating by the zinc immersion process using sodium hydroxide followed by nitric acid proved to be satisfactory in the initial work, although it etches

[3] For composition of this metal, see Appendix.

the surface of the aluminum. The procedure was as follows: (a) cleaner = sodium hydroxide, 50 g./l., 30 seconds at 80°C.; (b) nitric acid (sp.gr. = 1.42), 70 per cent by volume, 15 seconds, for film removal.

The chrome pickle procedure described by Bengston (21) also was satisfactory.

A dilute hydrofluoric acid dip for the purpose of removing gross oxide and activating the surface of the aluminum prior to the immersion dip yielded the best results. It was found that any treatment prior to the hydrofluoric acid was not significant and could be reduced to a degreasing operation using either a solvent, such as trichlorethylene, or an inhibited alkaline cleaner. Thus, the aluminum could be pre-cleaned in sodium hydroxide or in the chrome pickle, but these treatments are not essential. The concentration of the hydrofluoric acid was not critical and time of treatment may vary from one to three minutes at a temperature of 25°C. The surface of the 2S aluminum was not roughened seriously by this dip.

TABLE I. *Comparison of the relative solvent power of anions on hydrous alumina and the relative potentials of aluminum in solutions containing these anions.*

Rative solvent power of anions on hydrous alumina. Data from Clay and Thomas (37).	Relative potentials of aluminum in solutions containing different anions. Data from Fig. 2.
	OH
F	F
SiF_6	SiF_6 and BF_4
PO_4	
SO_4	
Cl	Cl and PO_4
Br	Br
	I
NO_3	SO_4 and NO_3

Film removal.—The film remaining on the aluminum after the reaction with the dilute hydrofluoric acid consists of the metals which were alloyed with the aluminum. It may be removed readily by dissolving in 70 per cent by volume nitric acid at room temperature. The time is not critical and may vary from ten to twenty seconds. This process is followed by a cold water rinse. Warm or hot water should not be used in any rinse process because of the tendency to form a relatively heavy oxide film on the aluminum which may interfere with the subsequent immersion process.

Immersion process.—In the early exploratory work, metal chlorides were evaluated in combination with hydrofluoric acid. It was soon found that, in general, better deposits were obtained when the heavy metal sulfate was used instead of the chloride. Considerable work was carried out to determine the specific effects of variation in the concentrations of the metal sulfate and hydrofluoric acid on the quality of the metal immersion deposits.

Addition agents were found to be valuable in improving the structure and adhesion of the immersion deposits and consequently were studied in some detail. Glue was used in the cadmium and early zinc work, whereas glue, goulac, and purified residue acid[4] were used in the tin solutions.

[4] Purified residue acid is a mixture of high boiling coal tar phenols and was obtained from the Reilly Tar and Chemical Corporation, Indianapolis, Indiana. It had the following distillation range: I. B. P. = 102°; 5% = 212°; 10% = 222°; 30% = 232°; 50% = 235°; 70% = 238°; E. P. = 90% = 276°C.

Mild agitation of the panel in the immersion solution was found to have a beneficial effect and, therefore, was made standard practice in all of the work.

The quality and structure of the immersion deposits were determined by visual inspection and by rubbing the deposit where the aluminum panel had been bent through 180 degrees. More complete evaluation of the adhesion of the zinc film to the aluminum was obtained by qualitative and quantitative adhesion tests on the heavy copper deposit subsequently plated on the zinc.

Plating on the immersion deposit.—In the exploratory work, copper was plated directly on the zinc film from a copper pyrophosphate plating solution (45). However, poor adhesion between the zinc and the copper frequently occurred, and it appeared that the zinc deposited from the acid solution was more active than that deposited from the zincate solution and that this contributed to the poor adhesion. This difficulty was eliminated entirely by the use of a special cyanide copper strike on the zinc prior to the plating from the copper pyrophosphate bath.

The best results were obtained with zinc immersion coatings and the poorest with copper; the cadmium and tin coatings were intermediate in the degree of adhesion on aluminum. Consequently, the most intensive work was carried out with zinc deposits.

STANDARD PROCEDURE

On the basis of the preliminary research described above, the following standard procedure was selected and used in the experimental work with zinc, cadmium, tin, and copper immersion baths containing hydrofluoric acid or fluoride salts.

(a) Cleaner
  Bath:
    Inhibited alkaline cleaner ..... 45 g./l.
  Time ..... 3–5 minutes
  Temperature ..... 80°–90°C.
(b) Cold water rinse
(c) Acid dip
  Bath:
    Hydrofluoric acid 0.5*N*
  Time ..... 2–3 minutes
  Temperature ..... 25°C.
(d) Cold water rinse
(e) Film removal
  Bath:
    Nitric acid (sp. gr. 1.42) ..... 70% by volume
  Time ..... 10–20 seconds
  Temperature ..... 25°C.
(f) Cold water rinse
(g) Immersion dip
  Bath:
    For compositions studied, see next section on "Immersion Baths."
  Time ..... 5–60 seconds
  Temperature ..... 25°C.
  Mild agitation
(h) Cold water rinse
(i) Copper strike
  Bath:
    Copper cyanide ..... 20.0 g./l.
    Sodium cyanide ..... 23.0 g./l.
    Sodium carbonate ..... 30.0 g./l.
    "Free" sodium cyanide ..... 0.3 g./l.

Temperature	25°C.
pH	10
Current density	20–30 amp./sq.ft. (2.2–3.2 amp./sq.dm.) for 10 seconds, then 5 amp./sq.ft. (0.54 amp./sq.dm.) for about one minute

(j) Cold water rinse
(k) Copper plate
Bath:

Copper pyrophosphate solution	(44, 45)
Current density	30 amp./sq.ft. (3.2 amp./sq.dm.)
Time	18 minutes.
Thickness copper	0.0005 inch (0.013 mm.)

(l) Cold water rinse
(m) Nickel plate. (Plated only for adhesion tests, described later)
Bath:

Nickel sulfate	240 g./l.
Nickel chloride	45 g./l.
Boric acid	30 g./l.
Sodium lauryl sulfate	2 g./l.
Temperature	55°C.
pH	5.2
Current density	30 amp./sq.ft. (3.2 amp./sq.dm.)
Time	20 minutes
Thickness nickel	0.0005 inch (0.013 mm.)

(n) Preliminary qualitative adhesion tests
(1) Panel bent in half through 180 degrees. Peeling or flaking of deposit observed especially at the bend.
(2) Heating tests.
Oven test: 150°C. for 15 minutes
Furnace test: 300°C. for 2 hours
Examine under a microscope (15×) for blisters

IMMERSION BATHS

ZINC SULFATE-HYDROFLUORIC ACID SYSTEM

Effect of varying zinc sulfate and hydrofluoric acid concentrations.—The results of furnace tests on panels prepared and plated according to the standard procedure are recorded in Fig. 3. The concentration of zinc sulfate was studied up to the saturation value ($7N$). The hydrofluoric acid concentration was also studied over a wide range in order to establish the lower and upper limits of its effectiveness.

There is a considerable area of concentrations of the two components at which excellent deposits may be obtained. The minimum hydrofluoric concentration is about $0.2N$. The permissible concentration of hydrofluoric acid increases up to a maximum of $2.5N$ with increase in the zinc sulfate concentration. For general plating purposes, a bath composition well within the desirable area may be taken, for example:

$$ZnSO_4 \cdot 7H_2O = 5.0N \text{ (718.9 g./l.)}$$
$$HF = 1.0N \text{ (35.0 ml./l. of 48\% acid)}$$

The zinc immersion deposits obtained in the preferred area had a clean, uniform, gray color. Spotty or streaked deposits were obtained from

solutions containing excess hydrofluoric acid and were an indication of inferior adhesion of the plated coating.

In the initial work with this system, relatively low zinc concentrations such as 0.1 and 0.5*N* were studied. The results were only fair. The addition of hydrolyzed glue effected a decided improvement; the zinc film had a better structure, there was much less gassing, and the copper deposit had better adhesion. This beneficial effect of the glue is ascribed to its effect on increasing the hydrogen overvoltage on the zinc film and to the improvement in physical structure of the zinc film. Subsequently, the zinc sulfate-hydrofluoric acid-glue system was studied over a wide range of concentrations. Later it was found that at the higher zinc concentrations, such as 3 to 7*N*, the presence of glue had a deleterious effect at the higher

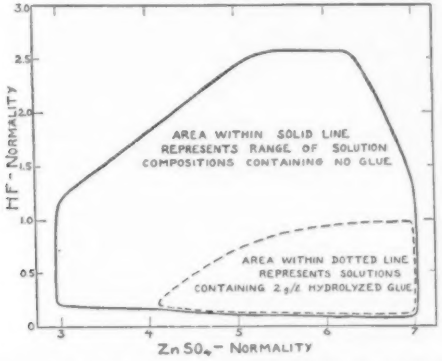

FIG. 3. Effect of composition of the zinc sulfate-hydrofluoric acid system on the adhesion of the zinc deposited by immersion on 2S aluminum. The standard procedure was used for preparing aluminum and for plating 0.0005 inch copper upon the zinc deposit. Aluminum processed in solution compositions within areas defined by solid and dotted lines passed the bend and furnace tests (300°C. for 2 hours) for adhesion.

Solid line—solutions contained no glue; dotted line—solutions contained 2 g./l. hydrolyzed glue.

HF concentrations. The overall picture may be seen in Fig. 3. The presence of glue considerably reduced the range of satisfactory zinc sulfate-hydrofluoric acid concentrations.

Zinc sulfate-fluoride salt system.—It was shown in the work of Clay and Thomas (37) that while certain acids, particularly hydrofluoric acid, are effective solvents for hydrous alumina, it is the anion of these acids which is the effective agent. This was indicated also by the potential study described above where it was found that aluminum exhibited approximately the same potential in either hydrofluoric acid or fluoride salt solutions.

Accordingly, various fluoride salts in combination with zinc sulfate were evaluated as immersion dip solutions. The aluminum panels were treated by the standard procedure and the plated coatings evaluated for adhesion by the bend and furnace tests. The results of these tests are given in Table II.

From the above data it is seen that the fluoride salts are just as effective as hydrofluoric acid. Neither hydrofluoric acid nor the fluoride salts were effective below a concentration of 0.2*N* and the plated coatings blistered in the furnace. While the zinc sulfate solutions and hydrofluoric acid were miscible in all proportions, there was a maximum solubility of the fluoride salts in the 5*N* zinc sulfate solution. The precipitate which formed at the fluoride salt concentrations given in Table II was probably the zinc alkali fluoride complex or possibly zinc hydroxide or basic zinc sulfate. This fixes an upper limit to the fluoride range at which good deposits are obtained, and this is much narrower than that obtained with hydrofluoric acid. On the other hand, a convenient way of maintaining a fixed fluoride concentration is available by keeping the solution saturated with the fluoride salt. Furthermore, the salt is easier to handle than the acid both for preparing the solution and making additions.

Study of the hydrofluoric acid dip.—The effect of varying the temperature and concentration of the hydrofluoric acid dip was studied for its effect on the quality of the zinc immersion coating as measured by the furnace test on the copper electrodeposits. The standard experimental procedure was otherwise the same as previously described.

TABLE II

Fluoride salt	Concentration of fluoride salt mixed with 5*N* $ZnSO_4 \cdot 7H_2O$ at which	
	Copper deposits on zinc film passed furnace test	Precipitate formed $ZnSO_4 \cdot 7H_2O$-fluoride salt mixture
Sodium fluoride, NaF	0.2*N*–0.4*N*	0.4*N*
Potassium fluoride, $KF \cdot 2H_2O$	0.2*N*–0.4*N*	0.4*N*
Ammonium fluoride, NH_4F	0.2*N*–1.0*N*	1.0*N*
Ammonium acid fluoride, $NH_4F \cdot HF$	0.2*N*–1.0*N*	1.0*N*

Tests were made with 0.5*N* hydrofluoric acid at 40°C. and the results compared with those obtained at the standard 25°C. It was found that, in general, the activity of the reaction of hydrofluoric acid on aluminum at 40°C. was approximately twice that at 25°C., and the minimum time in the acid dip, therefore, could be halved.

The effect of acid concentration was studied with 0.5*N*, 1.5*N*, and 3.0*N* hydrofluoric acid solutions at 25°C. There was a considerable increase in the activity of the acid with increase in strength. With a fifteen second dip in 3.0*N* acid, a 2S aluminum panel plated according to the standard procedure passed the furnace test.

The concentration, temperature, and time in the hydrofluoric acid dip for activating the aluminum surface are not critical and the dip is effective under a wide range of conditions. The optimum conditions must be determined for each article plated, depending on its alloy composition and surface condition.

In general, the 0.5*N* solution at room temperature is recommended and the time of dip should be sufficient to activate the surface and permit maximum adhesion without removing too much metal and possibly etching the aluminum.

Effect of time in the zinc sulfate-hydrofluoric acid immersion dip.—The effect of variation in the time of immersion of the aluminum in the zinc immersion solution consisting of 5*N* zinc sulfate and 1*N* hydrofluoric acid was studied. The standard plating procedure was followed and the copper electroplates were evaluated in the furnace test.

The immersion time was not critical and satisfactory deposits were obtained when the time varied from 10 seconds to 2 minutes. The zinc films had a uniform gray color. On the basis of this work, the preferred time in the zinc immersion solution was 30 to 60 seconds.

Temperature of the zinc sulfate-hydrofluoric acid immersion dip.—The temperature of the standard 5*N* zinc sulfate—1*N* hydrofluoric acid immersion solution was 25°C. in all of the previous experimental work. The effect of raising the temperature of this solution to 45°C. on the quality of the final copper electroplate was studied and evaluated by the furnace test. The higher temperature had the effect of giving a heavier zinc coating and decreased the permissible immersion time from 2 minutes at 25°C. to 20 seconds. The immersion solution should, therefore, be kept at room temperature, preferably between 20° and 25°C.

Immersion deposits upon various aluminum alloys.—The following aluminum alloys were plated using the standard procedure given above: 24ST, 52S, 61ST.[5] These alloys were chosen as representative of the various types of wrought aluminum alloys.

Excellent zinc immersion deposits were obtained with all the alloys. Several specimens of each alloy were plated with both 0.0005 inch of copper and 0.0005 inch of nickel and these panels were tested by the bend test, furnace test, hack saw test, and grinding wheel test. All panels passed these tests.

Rate of zinc deposition by immersion.—Data showing the rate of growth of the zinc film in two different types of zinc immersion solutions are given in Fig. 4. The solutions tested had the following composition:

(a) Zinc sulfate-hydrofluoric acid system

$ZnSO_4 \cdot 7H_2O = 5.0N$ (718.9 g./l.)

HF = 0.5*N* (17.5 ml./l. of 48% acid)

(b) Zincate system (21)

ZnO = 2.46*N* (100 g./l.)

NaOH = 12.5*N* (500 g./l.)

The panels were prepared according to the standard procedure and immersed in the zinc solutions for varying lengths of time. The weight of the zinc coating was determined by weighting the panels before and after stripping in 50 per cent by volume nitric acid.

It is observed that the initial rate of growth of the zinc film is somewhat slower in the $ZnSO_4$-HF system than in the zincate bath, but eventually a slightly thicker film is produced on the panel immersed in the fluoride bath. The thickness of the zinc coating undoubtedly depends on several other factors, such as the base metal composition and the condition of the surface of the aluminum resulting from previous metallurgical and chemical and cleaning treatments.

Adhesion tests.—Qualitative adhesion tests were made on the 2S aluminum, and several aluminum alloys, which were pretreated and plated ac-

[5] For composition of these alloys, see Appendix.

cording to the standard procedure. The zinc immersion solution had the following composition: zinc sulfate = $5N$; hydrofluoric acid = $1N$. The alloys tested were 2S, 24ST, 52S, and 61ST; these alloys were chosen as being representative of the various types of wrought aluminum. The various panels were plated with either 0.0005 inch copper or 0.0005 inch copper plus 0.0005 inch nickel. After each adhesion test, the panels were examined under a 15× microscope for evidence of blistering or separation of the plated coating from the basis metal.

The various copper plated panels were subjected to the following tests:

(a) *Bend test* (46). The panel was bent through 180 degrees and then hammered flat.

(b) *Furnace test* (47). The panel was heated in a furnace at 300°C. for two hours.

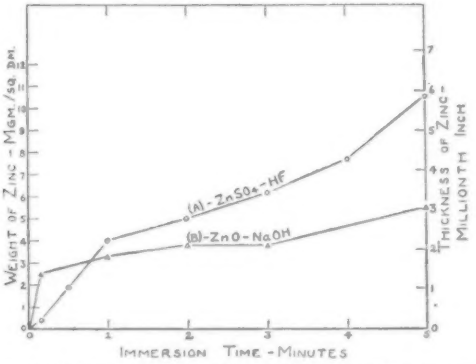

FIG. 4. Thickness of zinc deposited by immersion upon 2S aluminum as a function of time. Standard procedure used for cleaning aluminum. Bath compositions: curve A—$ZnSO_4 \cdot 7H_2O = 5N$; HF = $0.5N$; curve B—ZnO = 100 g./l.; NaOH = 500 g./l.

(c) *Solder test* (48). A 0.040 inch diameter copper wire was soldered to the panel and then pulled to the breaking point. In all these tests the fracture took place in the solder and the plate did not lift off the base metal.

(d) *Burnishing test* (49). The panel was burnished with the peen of a hammer having a one pound head.

The various copper and nickel plated panels were subjected to the following tests:

(e) *Hammering test* (50). The panel was struck vigorous blows with a hammer.

(f) *Sawing test* (51). The panel was cut with a hack saw.

(g) *Grinding wheel test* (52). The end of the panel was held perpendicularly against a 10 inch diameter, 70 grit emery wheel revolving at 1800 r.p.m.

In all of these tests with the 2S and various aluminum alloys, there were no signs of blistering or separation of the plated coating from the base metal.

Quantitative data on the adhesion of the plated copper and nickel coat-

ings on aluminum were obtained by the Ollard method (54) as refined by E. J. Roehl (55). The aluminum test cylinder was prepared for plating by the standard procedure, using the 5*N* $ZnSO_4$-1*N* HF immersion dip solution and then plated with 0.0005 inch copper and 0.1 inch nickel from the high speed Pinner-Kinnaman bath (56). In three different tensile tests, the fracture occurred in the aluminum base metal and not at the bond between the aluminum and plated coating. The Ollard test values were 19,880; 19,300 and 19,070 psi compared to the ultimate strength of 2S½H aluminum, 17,000 psi.

CADMIUM SULFATE-HYDROFLUORIC ACID SYSTEM

The preliminary investigation on the deposition of cadmium by immersion on aluminum from alkaline cyanide solutions was not successful. The deposits themselves were adherent and had good structure but copper electrodeposits on them blistered. In view of its successful application to zinc deposition described above, hydrofluoric acid should be applicable to the deposition of other metals which are near zinc and aluminum in the EMF series, especially cadmium. The purpose of this work was to explore the possibilities of depositing cadmium on aluminum from acid type solutions containing hydrofluoric acid.

Certain information, learned from the zinc deposition work, was found to be applicable to the research on the cadmium. For example, the precleaning in hydrofluoric acid and the cyanide copper strike were found desirable and useful.

On the other hand, exploratory work with the cadmium sulfate-hydrofluoric acid system showed that certain experimental precautions were necessary. They were:

(a) An addition agent was required. Cadmium deposits from the cadmium sulfate-hydrofluoric acid system were found to be coarse-grained and spotty. The addition of glue to this system resulted in a considerable improvement in the structure of the deposit. Further improvement was noted with hydrolyzed glue, which gave better deposits and much less suspended matter. The optimum concentration of hydrolyzed glue was 1 to 2 g./l.

(b) Good agitation of the aluminum panel in the cadmium solution was necessary to obtain deposits of uniform, sound structure.

(c) The time of dip was important and more critical than with zinc. If the immersion time was too long, the quality of the immersion deposit deteriorated, both in regard to the appearance and structure of the deposit, and the adhesion as measured by qualitative tests on the copper plate. The maximum allowable immersion time decreased as the ratio of hydrofluoric acid to cadmium sulfate increased. In general, the preferred time of immersion ranged from five to fifteen seconds.

(d) For testing the adhesion of the copper deposits on the cadmium immersion coating in this exploratory work, main reliance was placed on the bend test. Although the oven and furnace tests were also used, there is some doubt as to their validity because the brittle alloy of cadmium and copper which is formed when cadmium plated brass or copper is heated to 100°C. will itself cause blistering (53).

In the experimental work to be described, the standard pre-cleaning and

copper plating procedure was used. The cadmium immersion dip procedure was as follows:

Aluminum	= 2S
Immersion dip:	
Cadmium sulfate	= Concentration varied
Hydrofluoric acid	= Concentration varied
Hydrolyzed glue	= 2 g./l.
Time	= 5–15 seconds
Temperature	= 25° C.
Agitation of panel	= Fairly vigorous

Having established the preferred experimental conditions, a series of tests were made to determine the optimum concentrations of cadmium

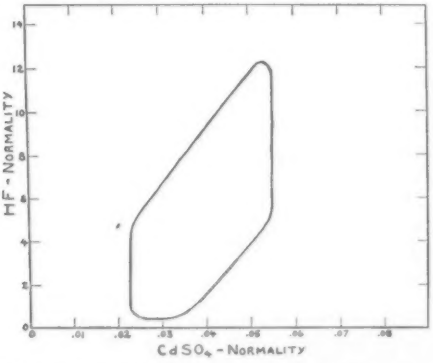

FIG. 5. Effect of composition of the cadmium sulfate-hydrofluoric acid system on the adhesion of the cadmium deposited by immersion on 2S aluminum. Standard procedure, used for preparing aluminum and for plating 0.0005 inch copper upon the cadmium deposit. Aluminum processed in solution compositions within areas defined by solid line passed the bend and oven tests (150°C. for 15 minutes) for adhesion.

sulfate and hydrofluoric acid. The bend test and oven test were used as criteria for the adhesion of the copper deposit and the results are given in Fig. 5. The following conclusions may be drawn from these data:

(a) The results were much better with this system than with the cyanide cadmium solution. These cadmium immersion deposits had excellent color and structure and could not be rubbed off. Furthermore, these deposits could act as bases for heavy copper electrodeposits which did not flake or blister when subjected to the bend and oven tests. Extensive qualitative and quantitative adhesion tests similar to those made with the zinc deposits were not made in this study.

(b) The "area" of metal sulfate-hydrofluoric acid concentrations in which adherent copper deposits were obtained was much smaller with the cadmium immersion coatings than the zinc. The effective cadmium

concentration is low compared to the zinc and ranges from about 0.02 to 0.055*N*. A preferred composition is as follows:

$CdSO_4$	= 0.035*N* (3.6 g./l.)
HF	= 3.0*N* (105.0 ml./l. of 48% acid)
Hydrolyzed glue	= 2.0 g./l.

TIN SULFATE-HYDROFLUORIC ACID SYSTEM

Tin may be deposited by immersion on aluminum from stannate solutions and this process is used commercially for tin coating aluminum pistons (57, 58). The lubricating qualities imparted by the tin serve to reduce scuffing and decrease engine break-in time. Laboratory evaluation of this process indicated that while sound tin deposits may be obtained, the conditions are relatively critical and copper electroplated on these tin coatings blistered, indicating relatively poor adhesion of the tin on the aluminum.

The successful application of fluorides to the deposition of zinc by immersion on aluminum indicated the possibility of obtaining good tin deposits from such a system. This application of fluorides should also be favored by the existence of fluoride tin complexes.

The exploratory work with this tin system was simplified by the general experience gained in the work with zinc and especially with cadmium to which it was even more similar. Stannous sulfate-hydrofluoric acid mixtures were studied with and without addition agents. The quality of the deposits was evaluated by inspecting the tin coatings and by bend and oven heating tests of the copper electroplates over the tin coatings. The results were as follows:

(a) Without addition agents, a heavy, black, pulverulent deposit of tin was precipitated on the aluminum and could be easily wiped off. The addition of glue and cresylic acid, the classical addition agents in the tin sulfate electroplating bath, to the stannous sulfate-hydrofluoric acid system resulted in sound, homogeneous tin deposits. Further improvement was effected by using a mixture of hydrolyzed glue, goulac, and purified residue acid. These addition agents were added to the $SnSO_4$-HF solution in the order given above and with vigorous stirring. The solution was filtered through coarse filter paper to remove suspended matter and excess purified residue acid.

(b) Good agitation of the aluminum in the tin solution is essential for sound tin immersion deposits. Lack of agitation may result in dark streaks in the tin and subsequently poor adhesion of the copper plate.

(c) The optimum time of immersion of the aluminum in the tin solution is important for good results and is relatively critical. The preferred time of immersion varies with the concentrations of stannous sulfate and hydrofluoric acid. The lower the $SnSO_4$ and the higher the HF concentrations, the shorter the time for good tin deposits. In general, the immersion time should not be longer than 10 seconds.

Following the exploratory work, a series of tests were made to determine the range of $SnSO_4$ and HF concentrations at which the best tin immersion deposits may be obtained. The standard procedure was exactly

as outlined for zinc above. The special data for the tin immersion solution were as follows:

Aluminum	= 2S
Immersion dip:	
Stannous sulfate	= Concentration varied from 0.5 to 2.5*N*
Hydrofluoric acid	= Concentration varied from 0.25 to 5.0*N*
Hydrolyzed glue	= 1.0 g./l.
Goulac	= 0.2 g./l.
Purified residue acid	= 1.3 ml./l.
Time	= 5–10 seconds
Temperature	= 25° C.
Agitation of panel	= Fairly vigorous

The following conclusions appear justified:

(a) Excellent tin immersion deposits on aluminum may be obtained from this system over a wide range of concentrations of stannous sulfate and hydrofluoric acid. Based on the experimental work carried out, the following limits for the area of good tin deposits were found: At the lowest $SnSO_4$ concentration of 0.5*N*, the range of HF concentrations were 0.5 to 2.0*N* and for the highest $SnSO_4$ concentration of 2.5*N*, the range of HF concentrations were 1.5 to 4.0*N*. The other values fell within this area. In all probability, this area could be extended, especially toward more concentrated stannous sulfate solutions.

(b) A preferred composition for depositing tin on aluminum by immersion would be:

$SnSO_4$	= 1.5*N* (161.1 g./l.)
HF	= 2.0*N* (70.0 ml./l. of 48% acid)
Hydrolyzed glue	= 1.0 g./l.
Goulac	= 0.2 g./l.
Purified residue acid	= 1.3 ml./l.

(c) The tin deposits are not so good as the zinc immersion deposits as a basis for further plating, but they are much better for this purpose than the tin immersion from the stannate bath.

COPPER SULFATE-HYDROFLUORIC ACID SYSTEM

The various efforts to plate or deposit copper by immersion upon aluminum described earlier were unsuccessful. The successful application of fluorides in the zinc, cadmium, and tin work, however, led to a consideration of the use of fluorides in copper deposition. Both cuprous and cupric fluorides are insoluble in water; but whereas the cuprous fluoride is either insoluble in or is decomposed by the common acids, including hydrofluoric acid, the cupric fluoride is soluble in this acid forming the double salt $CuF_2 \cdot 5HF$ (33).

Some exploratory work was carried out with the copper sulfate-hydrofluoric acid system in an effort to deposit copper by immersion on aluminum. The standard pre-cleaning and plating procedure given earlier and the general experience gained from the earlier fluoride work were utilized

in these tests. The general data on the copper immersion dip solution and the range of the conditions which were tested were as follows:

Aluminum	= 28
Immersion dip:	
Copper sulfate	= 0.1 to 3.0*N*
Hydrofluoric acid	= 0.1 to 1.0*N*
Hydrolyzed glue	= 0 to 2 g./l.
Time	= 5–60 seconds
Temperature	= 25°C.
Agitation of panel	= None to fairly vigorous agitation

In all the conditions tested, the adhesion of the copper deposited on the aluminum was nil and no preferred composition can be given. Depending upon the structure of the copper, the deposits could be either wiped or peeled off the aluminum. Over the range of the experimental conditions tested, no trends or indications pointing to improved adhesion were found. The addition of glue generally improved the structure of the immersion copper deposits.

The poor results with copper deposits on aluminum compared with the excellent zinc deposits may be caused by the following factors:

(a) The greater potential difference between aluminum immersed in copper solutions compared to zinc solutions. This probably causes a higher speed of deposition of copper on aluminum compared to zinc and, consequently, less time for the fluoride anions to completely dissolve the oxide film, the presence of which causes the poor adhesion.

(b) The copper immersion deposit has a greater tendency than the zinc deposit to promote galvanic attack of the aluminum base metal by the solution through the pores in the deposit. The gas and other reaction products from this attack would contribute toward the poor adhesion.

CONCLUSIONS

1. A new method has been developed for depositing metals by electrochemical displacement upon aluminum. Using this method, the deposition of zinc, cadmium, and tin by immersion on various alloys of aluminum has been successfully demonstrated.

2. The immersion deposits have sound structure and such an unusually high degree of adhesion to the aluminum that they may be used as a base for the subsequent electrodeposition of other metals. The bond between the zinc immersion deposit and the aluminum, for example, was found to be greater than the cohesive strength of the aluminum base metal.

3. The immersion solutions contain the fluoride anion which has a very high solvent action on the surface oxide on the aluminum, the presence of which normally prevents adherent immersion coatings on aluminum.

4. This high solubility effect of the fluoride anion on aluminum oxide has been demonstrated by potential measurements.

5. The solutions for preparing immersion deposits of a given metal consist of the metal sulfate, hydrofluoric acid, or a fluoride salt and, in specific cases, organic addition agents.

6. The preferred composition and conditions for depositing zinc by im-

mersion on aluminum are as follows: zinc sulfate = $5N$; hydrofluoric acid = $1N$; time of dip = 30–60 seconds; temperature = 25°C.

7. A process for electroplating upon aluminum which utilizes a zinc film as a basis for subsequent electrodeposition of other metals appears to be at least equal in quality and simplicity to the zincate process which is the best commercial method now in use for plating upon aluminum.

8. The preferred composition and conditions for depositing cadmium by immersion upon aluminum are: cadmium sulfate = $0.035N$; hydrofluoric acid = $0.3N$; hydrolyzed glue = 2 g./l.; time of dip = 5–15 seconds; temperature = 25°C.

9. The preferred composition and conditions for depositing tin by immersion are: stannous sulfate = $1.5N$; hydrofluoric acid = $2.0N$; hydrolyzed glue = 1 g./l.; goulac = 0.2 g./l.; purified residue acid = 1.3 ml./l.; time of dip = 5–10 seconds; temperature = 25°C.

10. These immersion deposits of tin have better adhesion to the aluminum than those obtained by the commercial stannate process.

11. Although some success was attained with 24ST aluminum, extensive efforts to electroplate copper directly on 2S aluminum or to deposit it by immersion were unsuccessful. The adhesion of the copper to the aluminum was invariably poor.

APPENDIX

Nominal composition of wrought aluminum alloys

Alloy	Percentage of alloying elements Aluminum and normal impurities constitute remainder				
	Copper	Silicon	Manganese	Magnesium	Chromium
2S*					
24ST**	4.5		0.6	1.5	
52S				2.5	0.25
61ST**	0.25	0.6		1.0	0.25

* 2S is commercially pure aluminum and contains normal impurities: 0.3% silicon (max.), 0.3-1% iron, 0.2% copper (max.), 0.05% manganese (max.), and 0.10% zinc (max.).

** T designates heat-treated temper.

ACKNOWLEDGMENT

The author wishes to express the great debt of gratitude and sincere thanks due to Dr. Hiram S. Lukens, Director of the Department of Chemistry and Chemical Engineering, University of Pennsylvania, under whose able guidance this work was conducted and who gave generously of his time, advice, and encouragement.

The author is also indebted to Mr. M. G. Herbach and Mr. L. F. Hirsch for their generous permission to use the laboratory facilities of the Philadelphia Rust-Proof Company.

Any discussion of this paper will appear in the discussion section of Volume 96 of the TRANSACTIONS of the Society.

REFERENCES

1. H. K. WORK, *Trans. Electrochem. Soc.*, 53, 361 (1928).
2. J. CANAC AND E. TASSILLY, *Compt. rend.*, 158, 119 (1914).

3. M. Ballay, *Trans. Electrochem. Soc.*, **62**, 91 (1932).
4. Finckh, G. m. b. H., Brit. Pat. 465,078 (1937).
5. A. Mazuir, *Ann. chim. anal.*, **2**, 335 (1920).
6. E. H. Hewitson (To Eastman Kodak Co.) U. S. Pat. 1,627,900, May 10, 1927.
7. J. Korpiun (To Schering-Kahlbaum A. G.) U. S. Pat. 2,142,564, Jan. 3, 1939.
8. B. K. Braund and H. Sutton, *Trans. Faraday Soc.*, **31**, 1595 (1935).
9. R. A. Ehrhardt and J. M. Guthrie, *Monthly Rev. Am. Electroplaters' Soc.*, **34**, 421 (1947).
10. W. R. Meyer, *Monthly Rev. Am. Electroplaters' Soc.*, **33**, 269 (1946).
11. W. J. Travers, U. S. Pat. 1,971,761, Aug. 28, 1934.
12. J. Fischer, *Metallwirtschaft*, **11**, 473 (1932).
13. J. Fischer (To Siemens & Halske, A. G.) U. S. Pat. 2,036,962, Apr. 7, 1936.
14. E. M. Julick and W. A. Mehmel (To Bell Telephone Laboratories, Inc.) U. S. Pat. 2,430,468, Nov. 11, 1947.
15. H. C. Cocks, *Trans. Faraday Soc.*, **26**, 517 (1930).
16. H. Sutton and A. J. Sidery, *J. Inst. Metals*, **38**, 241, II, 1927.
17. A. Lodyguine, *Trans. Electrochem. Soc.*, **7**, 153 (1905).
18. T. C. Cole, U. S. Pat. 1,515,658, Nov. 18, 1924.
19. W. J. Travers, U. S. Pat. 1,256,954, Feb. 19, 1918.
20. H. K. Work, *Trans. Electrochem. Soc.*, **60**, 117 (1931).
21. H. Bengston, *Trans. Electrochem. Soc.*, **88**, 307 (1945).
22. H. K. Work and C. J. Slunder, *Trans. Electrochem. Soc.*, **59**, 429 (1931).
23. W. H. Bowden (To Maytag Co.) U. S. Pat. 1,988,645, Jan. 22, 1935.
24. A. G. Betts, U. S. Pat. 675,584, June 4, 1900.
25. H. N. Gilbert (To E. I. duPont deNemours & Co., Inc.) U. S. Pat. 2,398,738, April 16, 1946.
26. A. V. Davis, U. S. Pat. 528,513, Oct. 30, 1894.
27. G. R. Cornwall (To Cornwall Printing Press Co.) U. S. Pat. 590,966, Oct. 5, 1897.
28. R. H. Brown and R. B. Mears (To Aluminum Company of America) U. S. Pat. 2,316,219, April 13, 1943.
29. ———, *ibid.*, U. S. Pat. 2,316,220, April 13, 1943.
30. J. R. Akers and R. B. Meabs, *Soap and Sanit. Chemicals*, **17**, 25 (1941).
31. W. M. Humphrey, U. S. Pat. 2,257,960, Oct. 7, 1941.
32. J. W. Mellor, "A Comprehensive Treatise on Inorganic and Theoretical Chemistry," Vol. V, p. 210, Longmans, Green and Co., London (1924).
33. ———, *ibid.*, Vol. III, p. 154.
34. F. Ephraim, "Inorganic Chemistry," edited by P. C. L. Thorne and E. R. Roberts, 4th Ed., p. 275. Interscience Publishers, Inc., New York (1943).
35. W. F. Hess, R. A. Wyant, and B. L. Averbach, *Welding J., Research Suppl.*, **21**, 257-s (1942).
36. ———, *ibid.*, **23**, 417-s (1944).
37. J. P. Clay and A. W. Thomas, *J. Am. Chem. Soc.*, **60**, 2384 (1938).
38. R. P. Graham and A. W. Thomas, *ibid.*, **69**, 816 (1947).
39. J. O. Percival, C. P. Dyer, and M. H. Taylor, *Ind. Eng. Chem.*, **30**, 1529 (1941).
40. L. Kahlenberg and J. A. Montgomery, *Trans. Electrochem. Soc.*, **36**, 277 (1920).
41. W. M. Latimer and B. S. Greensfelder, *J. Am. Chem. Soc.*, **50**, 2202 (1938).
42. G. B. Clark and G. V. Akimov, *Compt. rend. acad. sci. U.R.S.S.*, **30**, 805 (1941).
43. A. K. Graham, *Trans. Electrochem. Soc.*, **52**, 157 (1927).
44. J. Starek (To United Chromium, Inc.) U. S. Pat. 2,250,556, July 29, 1941.
45. T. G. Coyle, *Proc. Am. Electroplaters' Soc.*, 113 (1941).
46. A. L. Ferguson and E. F. Stephen, *Monthly Rev. Am. Electroplaters' Soc.*, **32**, 1144 (1945).
47. ———, *ibid.*, **32**, 1237 (1945).
48. ———, *ibid.*, **33**, 295 (1946).
49. ———, *ibid.*, **32**, 1144 (1945).
50. ———, *ibid.*, **32**, 1147 (1945).
51. ———, *ibid.*, **32**, 1244 (1945).
52. ———, *ibid.*, **32**, 1244 (1945).
53. ———, *ibid.*, **33**, 183 (1946).
54. E. A. Ollard, *Trans. Faraday Soc.*, **21**, 81 (1925).
55. E. J. Roehl, *Iron Age*, **146**, 17-20, 30-33 (1940).
56. W. L. Pinner and R. B. Kinnaman, *Monthly Rev. Am. Electroplaters' Soc.*, **32**, 227 (1945).
57. D. Brown, V. Shulberg, and G. Bell, *Automotive Inds.*, **75**, 884 (1936).
58. E. V. Blackman and M. P. Mikula (To Aluminum Company of America) U. S. Pat. 2,377,606, June 5, 1945.

EFFECT OF NON-CONDENSABLE GASES ON CORROSION OF NICKEL IN STEAM CONDENSATE[1]

W. A. WESLEY AND H. R. COPSON

Research Laboratory, The International Nickel Company, Inc., Bayonne, New Jersey

ABSTRACT

The corrosive conditions to which chemical evaporator tubes may be exposed on the steam side were simulated in corrosion tests run in hot water saturated with mixtures of carbon dioxide and air under pressure. These showed that appreciable corrosion of nickel can occur in a critical range of composition of the non-condensable gases, namely from about 55 to 90 per cent carbon dioxide by volume. In the presence of iron corrosion products, this range is broadened to include 40 to about 90 per cent carbon dioxide. Outside the critical range, nickel owes its good resistance to development of a passive film. Corrosion of nickel can be prevented by removing air or carbon dioxide from steam until their ratio is no longer critical. Inconel, tin, and stainless steel were resistant to attack under all the experimental conditions. Zinc and some copper alloys were also tested.

There are abundant data in the literature on the corrosion of steel in steam condensates and this information is well summarized in the "Corrosion Handbook" (1). Unfortunately, this is of little assistance in explaining the behavior of nickel. The corrosion rate of nickel in cold water saturated with carbon dioxide under pressure is very low, only 0.3 per cent that of steel in tests by Rhodes and Clark (2). In water containing only dissolved air, the rate is also very low (3). The literature was searched again at the time of preparing this paper, but the only data on corrosion of nickel in waters with intermediate concentrations of carbon dioxide and air were some from the work to be described below, which were quoted by members of the authors' own company (3, 4, 8).

FIELD OBSERVATIONS

Thinning of the walls of nickel tubes in commercial caustic evaporators has been observed occasionally to an extent indicating corrosion rates on the steam side in the range 100 to 150 mdd, but only in the first effect in a series of evaporators or in the preheaters. In all these cases, heat was supplied by steam direct from the boilers. The second and third effects of such evaporators were heated by steam released from caustic solutions in the previous effect, hence steam substantially free of carbon dioxide. Some sporadic analyses of non-condensable gases in the steam chests of caustic evaporators were available from plant records. These served to show that the range of carbon dioxide contents of the gas in first effect evaporators can be very wide indeed, namely, from 0.3 to 87 per cent by volume. The balance of the non-condensable gas in all cases was nitrogen

[1] Manuscript received December 28, 1948. This paper prepared for delivery before the Philadelphia Meeting, May 4 to 7, 1949.

and oxygen in the ratio of about 4 to 1. There was no correlation of gas analysis with known incidence of corrosion of the nickel tubes, except that low carbon dioxide contents were definitely safer.

APPARATUS

It is a generally accepted principle of corrosion testing that control of the concentration of dissolved gases in a solution is better if the solution is maintained saturated with respect to the gas phase than if an attempt is made to maintain a lesser concentration. If this results in too high a concentration of a reactive gas in solution, then it is customary to dilute the

TABLE I. *Estimated solubility of gases in water at 35 psi gage pressure*

	Estimated absorption coefficient*	
	At 70°C.	At 120°C.
Carbon dioxide	0.30	0.15
Oxygen	0.01833	0.0165

Composition of non-condensable gases—% by vol.			Solubility in ml. per 1,000 ml. water			
			At 70°C.		At 120°C.	
CO_2	O_2	N_2	CO_2	O_2	CO_2	O_2
0	20	80	0	11.3	0	4.7
10	18	72	92	10.2	21	4.2
20	16	64	184	9.0	43	3.8
30	14	56	276	7.9	64	3.3
40	12	48	368	6.8	85	2.8
50	10	40	460	5.7	107	2.3
60	8	32	554	4.5	128	1.9
70	6	24	645	3.4	149	1.4
80	4	16	737	2.3	170	0.9
90	2	8	831	1.1	192	0.5
100	0	0	922	0	214	0

* Absorption coefficient = vol. of gas reduced to 0° and 760 mm. absorbed by one vol. water when the partial pressure of the gas itself, not including water vapor, amounts to 760 mm.

gas phase with an inert gas such as nitrogen. In the present work, it was decided to work with a gas phase containing only carbon dioxide, air, and water vapor. Dilution with additional nitrogen was not included because the analyses of non-condensable gases in the steam chests of the commercial plants always showed a nitrogen to oxygen ratio of about 4 to 1, and it was believed that under the most corrosive conditions the condensate approached equilibrium with the gas phase.

The solubility of these gases in the liquid phase depends upon their partial pressures in the steam and upon the temperature and pressure of the system. By plotting known absorption coefficients for carbon dioxide and oxygen (5) on semilogarithmic graph paper versus 1/T, the coefficients at the desired research temperatures of 70°C. and 120°C. were extrapolated

or interpolated. The solubilities given in Table I were computed from the estimated absorption coefficients for a total gas phase gage pressure of 35 psi or absolute pressure of 2570 mm. mercury.

The construction of the test apparatus was illustrated in principle by one of the authors on page 962 of the "Corrosion Handbook" (9). A photograph of the cover of the actual apparatus is shown in Fig. 1. This cover was bolted pressure-tight on a pressed steel pot, which was surrounded by an oil bath. The pot was 8 inches (18.3 cm.) in diameter and 12 inches (30.4 cm.) deep and served as the corrosion chamber. Test specimens were mounted on a central shaft rotated at 16 rpm at such a distance that the linear speed of a point on the specimen surface was either 8.4 or 14.7 ft. per min. (2.56 or 4.5 meters per min.). This difference in speed had no apparent effect upon the observed corrosion rates. The method of mounting specimens can be seen in Fig. 1. Specimens were insulated from the metal parts by glass rods and porcelain washers. Total area of each specimen was 0.305 sq. dm. It was possible to mount 16 specimens on the shaft at one time, but fewer than this were usually employed.

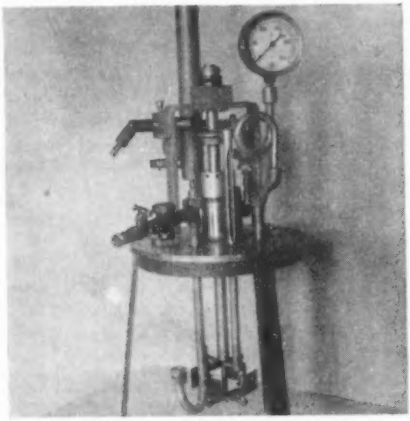

FIG. 1. Cover of corrosion apparatus

Attached to the cover were the inlet for non-condensable gases, a condensor to provide an outlet for the gases, a thermometer well, a safety valve, and a pressure gage.

The gases flowed from a cylinder through a reducing valve, a flowmeter, and a filter into the corrosion chamber. The gas stream was subdivided into small bubbles by means of a perforated nickel tip on the end of the inlet tube. By manipulating a needle valve in the outlet tube, the rate of flow of gases could be easily controlled while the pressure was adjusted by the reducing valve. The pressure was controlled at 35 psi plus or minus 0.5 psi.

The mixed non-condensable gases were purchased in low pressure cylinders holding 55 cu. ft. at about 210 psi. Much higher pressures could not

be used because the carbon dioxide might liquefy and then the composition of the gas leaving the cylinder would not be known. Numerous analyses of the gases as purchased showed the stated composition to be accurate within $\pm\frac{1}{2}$ per cent. Since the cylinders were filled with mixtures of carbon dioxide and air, the composition of a given non-condensable gas mixture is sufficiently defined by merely stating the per cent carbon dioxide present by volume.

As originally designed, the interior of the corrosion chamber was entirely of nickel. The pot itself was nickel-plated. In preliminary tests, it was found that the nickel surfaces corroded and they were replaced wherever possible with Inconel. In the final tests, the area of metal surface below the water level, when the chamber contained its normal 5 liters of water, consisted of 2.5 sq. dm. of nickel and about 20 sq. dm. of Inconel in contact with the water.

STANDARD PROCEDURE

The usual procedure is given here in detail, deviation from it being noted later when necessary:

The oil bath surrounding the corrosion chamber was heated to the desired temperature and this temperature maintained by an automatic regulator. Five liters of distilled water were placed in the chamber and allowed to heat for at least 1 hr. The cover containing four weighed specimens of each kind of metal included in the test was then mounted and the flow of gas through the water started immediately. It was held constant at one l./min. thereafter. The cover was bolted tight as rapidly as possible and rotation of the specimens started. These operations consumed about 10 minutes.

The desired temperature of the water was not reached for from $\frac{1}{2}$ to 1 hr., but after this it remained constant within ± 1°C. Analyses of the exit gases in several runs showed that they were of the desired composition after the first $\frac{1}{2}$ hr. After 2 hr. the test was interrupted, the pressure released, and the cover removed. Two specimens of each kind of metal were removed and two additional weighed pieces inserted in their places. The cover was replaced as rapidly as possible, so that the time required for the interruption was not more than 15 to 25 min. The test was then continued for another 20 hr.

Thus, for each run, duplicate specimens were exposed for the first 2 hr., others for the last 20 hr., and still others for the entire 22 hr.

The general shape of the specimens can be seen in Fig. 1. They were 3.2 by 3.8 by 0.08 cm. in dimensions with two small drilled tabs for mounting. Before use, they were resurfaced with emery, pumice scrubbed, washed in alcohol and ether, dried and weighed. After a corrosion test, they were cleaned by rubbing gently with the fingers dabbed with Sapolio, washed in alcohol and ether, dried and reweighed. This treatment removed all corrosion product safely.

The test pieces were cut from regular commercial sheet metals, whose nominal compositions can be found in modern handbooks.

EFFECT OF TEMPERATURE

The corrosion rate of nickel was determined by the standard procedure with an 80 per cent carbon dioxide gas composition at seven temperatures

from 30° to 135°C. The results are plotted in Fig. 2. At this gas composition and at 35 psi gage pressure, the most corrosive temperature range was 55° to 85°C.

The corrosion rate in the 2 hr. test period was always higher than in the 20 and 22 hr. test periods. At the lowest and highest temperatures, namely 30° and 135°C, respectively, practically all the corrosion occurred in the first 2 hr. or less. At intermediate temperatures, the corrosion rates became more nearly constant with time. Rapid drops in corrosion rates with time seemed attributable to the formation of protective films or to the nickel becoming passive. As the boiling point (138°C.) was ap-

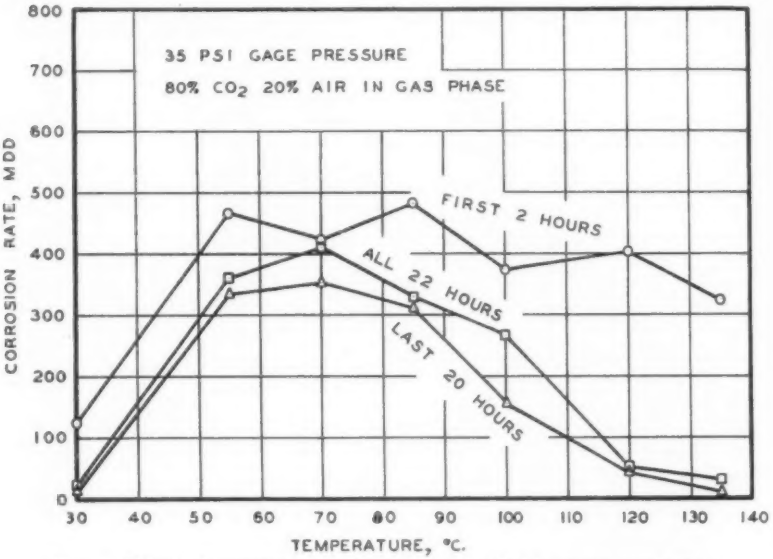

FIG. 2. Effect of temperature on corrosion of nickel in steam condensate

proached, the decreasing solubility of the gases was an important factor affecting the corrosion

EFFECT OF COMPOSITION OF NON-CONDENSABLE GASES

The corrosion rate of nickel was determined by the standard procedure with the carbon dioxide content of the gas phase varying stepwise from 100 to 0 per cent by volume. The determinations were made at 70°C. and at 120°C., and the results are plotted in Fig. 3 and 4, respectively.

At 70°C. and 35 psi gage pressure, the corrosion rate of nickel increased rapidly as the oxygen content of the gases increased from 0 to 6 or 8 per cent. There was then a sharp break in the curve, and with more than 10 per cent oxygen (or with less than 50 per cent carbon dioxide), practically no corrosion of nickel occurred. With 60 per cent carbon dioxide, corro-

sion was rapid for 2 hr., but the corrosion rate then dropped off quickly with time. At 70 and 80 per cent carbon dioxide, the 20 and 22 hr. corrosion rates approached the 2 hr. rate, and it appeared that the corrosion rate of nickel would continue at a high rate under these conditions. At all other concentrations of carbon dioxide, the corrosion rate decreased markedly with time.

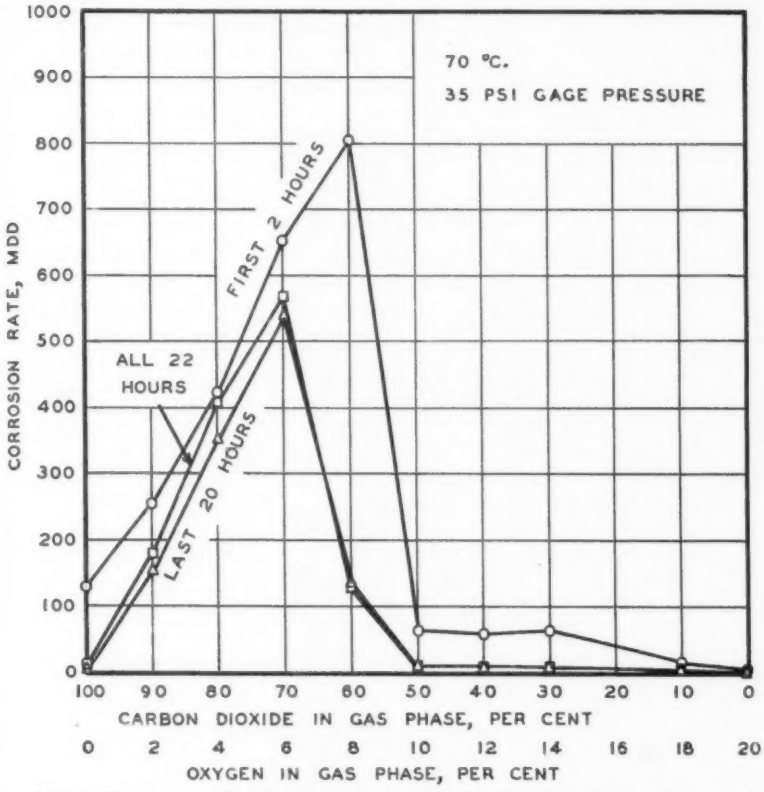

FIG. 3. Effect of composition of non-condensable gases on corrosion of nickel in steam condensate at 70°C.

At 120°C. and 35 psi gage pressure, the corrosion behavior for the first 2 hr. was similar to that at 70°C., although the rates were generally somewhat lower. However, the corrosion practically stopped after 2 hr.

It can be concluded that at 35 psi, the most corrosive conditions for nickel are 70°C. and 70 per cent carbon dioxide. Corrosion rates well over 100 mdd were encountered in the range 55° to 100°C. and 90 to 60 per cent carbon dioxide (or 2 to 8 per cent oxygen). At all temperatures, the cor-

rosion rate was small at 100 per cent carbon dioxide and with less than 50 per cent carbon dioxide.

EFFECT OF TIME

The corrosion rate of nickel was determined at 70°C. and 80 per cent carbon dioxide in experiments lasting up to 72 hr. In some of these tests, the apparatus was opened at 2 hr. just as in the standard procedure, and in others the exposure was continuous. The results are plotted in Fig. 5.

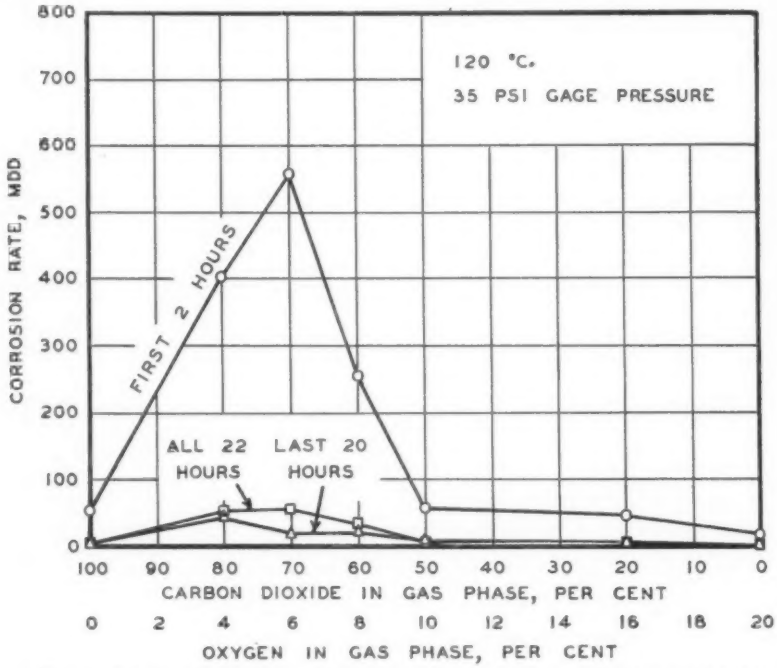

FIG. 4. Effect of composition of non-condensable gases on corrosion of nickel in steam condensate at 120°C.

It is apparent that even under these severe corrosive conditions the corrosion rate of nickel decreased with time. Under less corrosive conditions, much more marked decreases in corrosion rate have already been noted. In the figure, as time increases, the rate of change decreases and the corrosion rate tends to become more constant. Nevertheless, the corrosion rates obtained in short time tests must be regarded as higher than those which would be obtained with long exposure under plant conditions.

The decrease in corrosion rate with time is regarded as due to the building up of protective films and the accumulation of corrosion product on

the specimens. It might also be due to changes taking place in the water in the corrosion chamber. In plant operation the film of condensate on nickel tubes is continuously replaced with fresh condensate.

EFFECT OF PRESSURE

A few runs were made by the standard procedure except that the gage pressure was dropped to 10 psi. This decreased the corrosion considerably. At 85°C., variations in the amount of carbon dioxide in the noncondensable gas produced 2 hr. curves similar to those of Fig. 3 and 4, except that the corrosion rates were lower, and the peak was shifted to 494

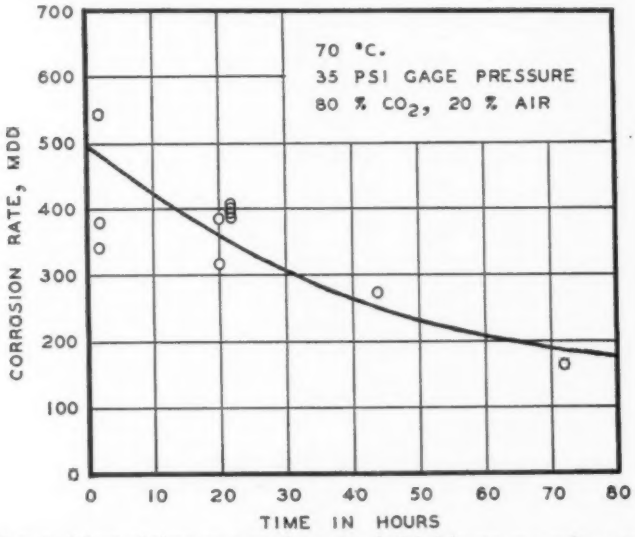

FIG. 5. Effect of time on corrosion rate of nickel in steam condensate

mdd at 50 per cent carbon dioxide. The decrease in corrosion rate with time was intermediate between Fig. 3 and 4. Practically no corrosion occurred at 100 or below 40 per cent carbon dioxide.

PASSIVITY OF NICKEL IN STEAM CONDENSATE

In the results described so far, all the nickel specimens were cut from one sheet of commercial A-Nickel. In general, the corrosion behavior of these nickel specimens was consistent and reproducible. However, occasionally a specimen was passive and had a weight loss much lower than expected. These instances of passivity were easily isolated and have not been included in the graphs.

Aside from these instances of passivity, the reproducibility of the results was satisfactory. The weight losses on duplicate specimens in individual runs usually checked each other very closely. Thus, the average per cent

deviation from the mean on duplicate specimens in all runs where the corrosion rate was greater than 20 mdd was about 4 per cent. In 27 repeat runs, the average deviation from the mean was 9 per cent. Table II illustrates the reproducibility of the results in repeat runs. The meaning of the designation, iron present or absent, is explained below.

Table III illustrates instances of passivity. In these illustrations, one nickel specimen corroded at a high rate while a duplicate specimen in the same run suffered practically no corrosion at all. There is no difficulty distinguishing between the passivity shown by Table III and the normal

TABLE II. *Illustrations of reproducibility of results on nickel*

Each line represents a separate run.
Pressure: 35 psi gage pressure
Specimen area: 0.305 sq. dm.

Conditions			Average weight loss, mg.		
Temp. °C.	CO_2 % by volume	Iron present or absent	First 2 hr.	Last 20 hr.	All 22 hr.
70	80	Absent	13.9	97.3	115.4
			8.7	81.4	113.6
70	50	Present	7.6	130.6	115.8
			9.1	128.2	140.2
100	60	Present	15.0	108.6	129.4
			17.2	94.3	119.1
120	50	Present	20.1	43.3	22.5
			21.6	22.8	25.9

TABLE III. *Illustrations of passivity of nickel in steam condensate*

Pressure: 35 psi gage
Time: 20 hr.
Specimen area: 0.305 sq. dm.

Conditions			Weight losses on duplicate specimens, mg.	
Temp. °C.	CO_2 % by volume	Iron present or absent	Passive specimen	Corroded specimen
70	50	present	4.7	115.8
70	60	present	2.7	91.3
120	60	present	0.6	99.9

scatter shown by Table II. Occasionally all the specimens in a run remained passive, low weight losses being obtained under conditions where normally high corrosion rates would be expected.

In time, the first sheet of A-Nickel was used up, and specimens were cut from a second sheet. Specimens from the second sheet were much more prone to remain passive than specimens from the first sheet. The reason for the difference in behavior of the two sheets was not known. The passivity of the second sheet is illustrated in Table IV. Under the conditions in the table, the 5 liters of solution in the corrosion chamber accumulated enough nickel bicarbonate in solution to indicate that the nickel parts of the equipment were corroding at high rates.

It must be concluded that the corrosion of nickel differs with specimens from different sources and that the behavior of nickel is erratic in that individual specimens may remain completely passive even when the conditions are very corrosive to other specimens. This phenomenon is not new and was not entirely unexpected in the corrosion of nickel by steam condensate.

It has already been pointed out that under many condensate conditions nickel appeared to owe its resistance to attack to the development of a protective film. Quite often the initial rate of attack was rapid, but by 2 hr. corrosion had practically ceased. The protective film was usually invisible, and perhaps it was related to the same sort of "oxide" film considered present on passive nickel.

CORROSION RATE OF NICKEL IN PRESENCE OF IRON

If the corrosion resistance and passivity of nickel were due to the formation of a protective film, anything which interfered with the development

TABLE IV. *Illustration of comparative behavior of two nickel sheets*

Pressure: 35 psi gage
Time: 72 hr.
Specimen area: 0.305 sq. dm.

Conditions			Individual weight losses, mg.	
Temp. °C.	CO_2 % by volume	Iron present or absent	Sheet 1	Sheet 2
70	80	Absent	147.5	
			147.7	17.1
			152.6	14.8
			153.2	20.8
			144.2	13.4
			150.6	

of this film should increase the tendency of nickel to corrode. Iron tube sheets may be present in caustic evaporators and, accordingly, it seemed desirable to determine what effect the presence of iron and its corrosion products might have on the corrosion of nickel.

To do this, ingot iron specimens were included in the runs. The iron specimens were similar in size, shape, and manner of mounting to the nickel specimens. Under these conditions, the corrosion rate of nickel was determined by the standard procedure with exactly the same ranges of temperature and concentration of carbon dioxide as before.

The general effect of the presence of iron was to extend the range of conditions under which high corrosion rates of nickel were encountered. Thus, in Fig. 3 the effect of iron was to extend the range of corrosion of nickel into lower carbon dioxide percentages. Rates in excess of 500 mdd were obtained at 60 and 50 per cent carbon dioxide for both the 20 and 22 hr. tests. In Fig. 4, the maximum 2 hr. rate was shifted and raised to 1055 mdd at 40 per cent carbon dioxide. Also, in Fig. 4, the development of a protective film was prevented at the higher concentrations of carbon

dioxide, so that at 90 per cent carbon dioxide, the 2 hr. rate was 89 mdd and the 20 and 22 hr. rates about 106 mdd.

The effect of iron is summarized in Fig. 6. Zone 1 indicates high corrosion rates of nickel in pure condensate, and zone 2 indicates high rates in the presence of iron. With iron present, 20 and 22 hr. corrosion rates greater than 100 mdd were encountered in the range of 90 to 50 per cent carbon dioxide and 30° to 135°C. At all temperatures the corrosion rate was small

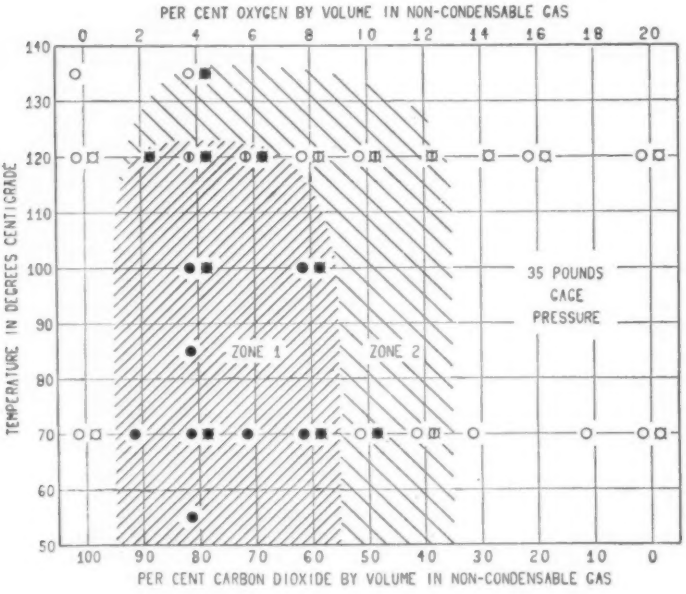
PER CENT OXYGEN BY VOLUME IN NON-CONDENSABLE GAS
0 2 4 6 8 10 12 14 16 18 20
140 130 120 110 100 90 80 70 60 50
TEMPERATURE IN DEGREES CENTIGRADE
35 POUNDS GAGE PRESSURE
ZONE 1
ZONE 2
100 90 80 70 60 50 40 30 20 10 0
PER CENT CARBON DIOXIDE BY VOLUME IN NON-CONDENSABLE GAS
PURE CONDENSATE
IRON PRESENT
CORROSION RATE LESS THAN 50 MDD. IN 20 OR 22 HOUR TEST
CORROSION RATE FROM 50 TO 100 MDD. IN 20 OR 22 HOUR TEST
CORROSION RATE ABOVE 100 MDD. IN 20 OR 22 HOUR TEST

FIG. 6. Corrosion of nickel in steam condensate containing carbon dioxide and air. Zone 1, corrosion of nickel occurs in pure condensate; zone 2, corrosion of nickel occurs provided the formation of its protective film is prevented by presence of iron or other interfering impurities in the condensate.

at 100 and below 30 per cent carbon dioxide. The most corrosive conditions for nickel in the presence of iron were 70°C. and 60 per cent carbon dioxide, the pressure being 35 psi gage reading.

Careful study of the data led to the conclusion that the presence of iron did not accelerate the rate of corrosion of nickel unless conditions were such that nickel tended to develop a protective film. Iron corrosion products precipitated on the nickel specimens, and the effect of these corrosion

products must have been simply interference with the formation of the nickel protective film. Whether the interference was purely mechanical in nature or involved some chemical reaction was not certain.

EFFECT OF PURITY OF CONDENSATE

After it was found that iron influenced the corrosion rate of nickel, a few tests were made to determine the effect of other substances. The steam in evaporators might contain impurities carried over from the boiler by priming and foaming or picked up along the way. Experimental runs were made in which sodium chloride, sodium sulfate, and magnesium chloride were dissolved in the distilled water in the corrosion chamber. Also, runs were made in condensate collected from a commercial evaporator, in tap water, and in a spring water.

The results showed differences which were greater than experimental error. Thus, at 120°C., 60 per cent carbon dioxide, 35 psi, and iron present, 20 hr. corrosion rates were obtained which ranged from 57 to 280 mdd depending on the purity of the water.

CORROSION PRODUCT

In those runs where corrosion of nickel occurred in the absence of iron, the solution in the corrosion chamber at the end of the run was clear and light green due to nickel bicarbonate in solution. Analysis of one of these solutions showed 570 ppm of nickel. The nickel specimens when corroded were irregularly covered with a thin, loose, black film, which was probably nickel oxide in such form as to be poorly protective. Those portions of the specimens not covered by the film appeared unattacked.

When iron was present, the solution at the end of a run contained much precipitate. At 2 hr., the color of the precipitate was yellow, but its color at 22 hr. depended on the composition of the gas. When air was present, the precipitate was dark colored. When the carbon dioxide was high but less than 100 per cent the precipitate was bright red. When the carbon dioxide content was low, the precipitate was rust colored. All the precipitates except the red one tended to remain in suspension. Underneath the deposited red precipitate, corroded nickel specimens were coated with a black film.

CORROSION OF IRON IN STEAM CONDENSATE

The ingot iron specimens included in some of the runs were handled by the standard procedure exactly as described for the nickel specimens. Thus, weight losses were obtained for 2, 20, and 22 hr. under the same ranges of temperature and concentration of carbon dioxide as considered hitherto. Unfortunately, most of these results were not accurate because the iron specimens became coated with a nickel plate.

The character and protective value of the nickel plate depended mainly on the amount of nickel in solution in the water in the corrosion chamber. Under those conditions where appreciable nickel was in solution, fairly thick bright plates were obtained. At 70°C. and 60 per cent carbon dioxide, the nickel plate became 0.6 mil thick! The nickel plates were brittle and not very adherent, but tests with potassium ferricyanide in agar agar gel showed them to be of surprisingly low porosity.

The weight losses showed that iron was susceptible to severe corrosion in steam condensate. At 120°C. the 2 hr. rates averaged over 2,000 mdd, and at 70°C. they averaged over 1,300 mdd. Owing to the nickel plate, the rates dropped off rapidly with time and developed considerable scatter. The 22 hr. rates were published by W. Z. Friend (3) but must be regarded as being much lower than would be obtained in a nickel-free apparatus. Since the protective character of the nickel plate varied with conditions, it is difficult to draw any definite conclusions. At 70°C., there was some support for the statement of Skaperdas and Uhlig (6) that exposure to carbon dioxide and oxygen simultaneously was more corrosive than exposure to the two gases individually. At 120°C., the highest 22 hr. rates were obtained with pure air, but it still seemed probable that there was a separate peak in the region of mixed gases.

CORROSION OF INCONEL

Inconel specimens (80Fe, 13Cr, 6Fe) were included in all the runs made on nickel. They were handled according to the standard procedure and were similar to the nickel specimens. In only one instance was the 20 or 22 hr. corrosion rate greater than 1 mdd, and, in this instance, it was only 4 mdd. Hence, the conclusion is inevitable that Inconel does not corrode in steam condensate under the conditions of these experiments. This supports data reported by L. F. Collins (1).

In anticipation of the possibility that it might be desirable to use Inconel tubes in the first effect of caustic evaporators in plants where condensate corrosion was severe with nickel, the corrosion rate of Inconel in unaerated 50 per cent technical sodium hydroxide at 100°C. and 1 atm. pressure was determined. A corrosion rate of 1.2 mdd was obtained in a 20 hr. test, which was identical with the corrosion rate of nickel specimens in the same test. Since then, Inconel tubes have been used successfully in service.

CORROSION OF OTHER METALS

Although the objective of this project was to explain the behavior of nickel, a few corrosion tests were performed to give some idea of the relative losses in weight of some other materials. The results of these tests are presented in Table V. Where the run number is the same for several metals in that table, those specimens were present simultaneously in the corrosion chamber. Care was taken to have no metallic contact between the test pieces since that would have introduced galvanic corrosion.

Copper alloys were included because they were known to have corroded in steam condensate. Tin was studied because it might have been practical to coat the nickel tubes on the condensate side with tin, stainless steel because it might become a competitive alloy, and zinc to see whether it became nickel-plated in a manner similar to iron. Under the corrosive conditions studied, tin, stainless steel, and Inconel were very resistant but zinc suffered severe corrosion. Nickel could be detected by qualitative analysis of the surface of the zinc but did not form a bright deposit as in the case of iron.

In condensate saturated with a 30 per cent carbon dioxide gas phase, a condition frequently met in industry, the copper alloys corroded at a

moderately high rate whereas nickel was very resistant. Shifting the non-condensable gas composition to 70 per cent carbon dioxide caused a high rate of attack of nickel as before but lowered the rates for the copper alloys.

Inasmuch as there is no reason to believe that the particular conditions selected for these tests were the most corrosive ones for the metals other

TABLE V. *Corrosion of various metals*

22 hour runs interrupted at end of 2 hours
Rates shown are average for duplicate specimens.

% CO_2 in entering gas		30		70		80		80	
Temperature, °C		70		70		100		135	
Gage pressure, psi		35		35		35		35	
Metal	Exposure time in hours	Run	Wt. loss mdd	Run	Wt. loss mdd	Run	Wt. loss mdd	Run	Wt. loss mdd
Tin	First 2	1	−4	5	20				
	Last 20		−1		4				
	All 22		−1		−3				
Stainless steel Type 302	First 2	1	8	5	0				
	Last 20		1		0				
	All 22		1		0				
Inconel	First 2	2	12	6	0				
	Last 20		1		1	9		12	
	All 22		1		1		1		1
Nickel	First 2	3	63	7	652		374		325
	Last 20		7		538	10	154	13	12
	All 22		6		568		266		30
Monel metal	First 2	2	602	6	169		319		197
	Last 20		45		355	11	185	14	21
	All 22		55		370		197		32
45Ni:55Cu	First 2	2	606	6	134				
	Last 20		86		72				
	All 22		106		86				
30Ni:70Cu	First 2	4	311	8	366				
	Last 20		72		70				
	All 22		72		64				
Copper	First 2	4	209	8	154		138		191
	Last 20		119		43	11	41	14	33
	All 22		145		44		50		33
Yellow brass	First 2	4	417	8	319				
	Last 20		116		87				
	All 22		127		104				
Zinc	First 2	1	1,660	5	984				
	Last 20		257		267				
	All 22		341		422				

than nickel, evaluation of the relative resistance of these materials must be confined to the conditions represented.

PREVENTING CONDENSATE CORROSION OF NICKEL TUBES

With only a few exceptions, all the results discussed in this report were obtained according to a standard procedure and by using specimens cut

from the same nickel sheet. This makes the data comparable, but three factors render doubtful any attempt to use them to predict actual corrosion rates in the field. First, the corrosion rate decreased with time; second, nickel may become passive; and third, different corrosion rates were obtained with nickel from different heats. Nevertheless, it is believed that Fig. 6 shows graphically the conditions of temperature, pressure, and non-condensable gas composition under which the greatest danger of corrosion of nickel exists and also the conditions under which nickel does not corrode.

The corrosion of nickel is negligible at all temperatures when the non-condensable gases contain from 0 to 30 per cent carbon dioxide or 100 per cent carbon dioxide. Any treatment of the steam which would keep the composition of the non-condensable gases in the safe range of carbon dioxide content should prevent corrosion of nickel. This could be accomplished by complete removal of all gases, complete removal of oxygen or reduction of carbon dioxide content to below 30 per cent. Since the time at which the work described in this report was done, great progress has been made in design of commercial deaerators so that these can be used to prevent corrosion of nickel. In one installation, the ratio of oxygen to carbon dioxide content of the non-condensable gas was reduced to 0.023 and nickel tubes no longer corrode there. In other cases, it has been possible to reduce the carbon dioxide content by altering the chemical treatment of the boiler feed water. Other means to reduce either carbon dioxide or air contents of steam are discussed in the "Corrosion Handbook" (7).

CONCLUSIONS

1. Corrosion of nickel in steam condensate is due to the presence in the steam supply of carbon dioxide and air in a critical ratio. The corrosive range of non-condensable gas compositions is from about 55 to 90 per cent carbon dioxide by volume.

2. In the critical range, the corrosion rate of nickel reaches a maximum between 55° and 85°C. at a gage pressure of 35 psi.

3. The corrosion rate of nickel, except under the most critical conditions, decreases rapidly with time due to formation of a protective film. Nickel specimens from different sources behaved differently and pieces sometimes became completely passive.

4. The presence of iron corrosion products and possibly other impurities in the steam condensate affected the corrosion rate by interfering with the development of the protective film. In the presence of such products, the region of appreciable corrosion of nickel is broadened to include the range from 40 to over 90 per cent carbon dioxide in the non-condensable gases.

5. Inconel and stainless steel remained unaffected by the steam condensate under all conditions tested. Tin showed no loss in weight and was only tarnished by the exposure.

6. Nickel carbonate is soluble in carbon dioxide solutions under pressure. It forms a clear light green solution containing as much as 570 parts per million of nickel.

Any discussion of this paper will appear in the discussion section of Volume 95 of the TRANSACTIONS of the Society.

REFERENCES

1. L. F. Collins, "Corrosion Handbook," p. 538, The Electrochemical Society, John Wiley & Sons, New York (1948).
2. F. Rhodes and J. Clark, *Ind. Eng. Chem.*, **28**, 1078 (1936).
3. W. Z. Friend, "Corrosion Handbook," pp. 254–256, The Electrochemical Society, John Wiley & Sons, New York (1948).
4. F. L. LaQue, *Modern Power and Eng.*, **41**, 47 (1947).
5. C. D. Hodgman, "Handbook of Chemistry and Physics," 21st Ed., p. 936, Cleveland, Chemical Rubber Publishing Co. (1936).
6. G. T. Skaperdas and H. H. Uhlig, *Ind. Eng. Chem.*, **34**, 748 (1942).
7. "Corrosion Handbook," pp. 540 and 506, The Electrochemical Society, John Wiley & Sons, New York (1948).
8. W. Z. Friend and F. L. LaQue, *Trans. Am. Inst. Chem. Engrs.*, **42**, 849 (1946).
9. W. A. Wesley, "Corrosion Handbook," p. 962, Fig. 5, The Electrochemical Society, John Wiley & Sons, New York (1948).

THE LONG-TERM DETERIORATION IN CERTAIN PHOSPHORS EXPOSED TO THE LOW PRESSURE MERCURY ARC[1]

ERWIN F. LOWRY

Sylvania Electric Products, Inc., Salem, Massachusetts

ABSTRACT

An expression for the decay in lumen efficiency of phosphors exposed to a mercury vapor discharge has been developed. It turns out that this expression is of the form commonly associated with first order chemical reactions. This is of considerable physical and chemical significance since it permits one to speculate on the phenomena responsible for the decay. While it may be argued that a three term exponential equation is sufficiently flexible to fit most any set of data, a careful study indicates that variations in the coefficients alone account for all the differences encountered between good and poor lumen maintenance.

Several experiments are described which substantiate these speculations and show that the decay in fluorescent efficiency is caused by at least three more or less independent reactions of widely different velocities.

It is common knowledge among workers in the field of luminescence that fluorescent lamps undergo a deterioration in luminescent efficiency during exposure to a mercury arc. This decline in efficiency must not be confused with the very rapid decay in luminescence which normally occurs immediately after the termination of excitation. The process with which we are here concerned is a very slow deterioration in phosphor efficiency which continues for many thousands of hours. A careful study of the rate of this deterioration has been made for thousands of fluorescent lamps of varying quality.

For various reasons, the standard 40 watt White fluorescent lamp has been chosen for use in the experiments to be described in this report. This lamp has a 45 inch (114.3 cm.) arc length, is 1.5 inches (3.8 cm.) in diameter, and is coated with an 88/12 blend of zinc-beryllium-manganese silicate and magnesium tungstate. All the lamps have been operated at 410 $\pm$ 10 ma. arc current on standard commercial ballasting equipment on an intermittent duty cycle of 180 minutes on, 20 minutes off. Only the actual burning time was recorded. Photometric measurements were made in a 96 inch Ulbrecht sphere after the lamps had been "warmed up" by burning at rated load for about five minutes. The photometric laboratory and the sphere were maintained at a constant temperature of 80° $\pm$ 1°F. for all measurements. Unless otherwise noted, each plotted point on the various curves is the average of measurements made on a group of five lamps.

[1] Manuscript received January 10, 1949. This paper prepared for delivery before the Philadelphia Meeting of the Society, May 4 to 7, 1949.

THE LUMEN MAINTENANCE EQUATION

As a result of this study, certain definite characteristics of the deterioration in lumen efficiency with operating time have been established. A mathematical expression has been arrived at by Dr. Keith H. Butler of these laboratories, and the writer who describes this deterioration accurately and completely. This equation is as follows:

$$L_0 - L_T = A(1 - \epsilon^{-aT}) + B(1 - \epsilon^{-bT}) + C(1 - \epsilon^{-cT})$$

where L_0 is the initial efficiency in lumens per watt
L_T is the efficiency at time T
T is the operating time in hundreds of hours
A, B, and C have the dimensions of L.P.W.
and a, b, and c are quantities which represent the velocity at which the decay approaches a limiting value.

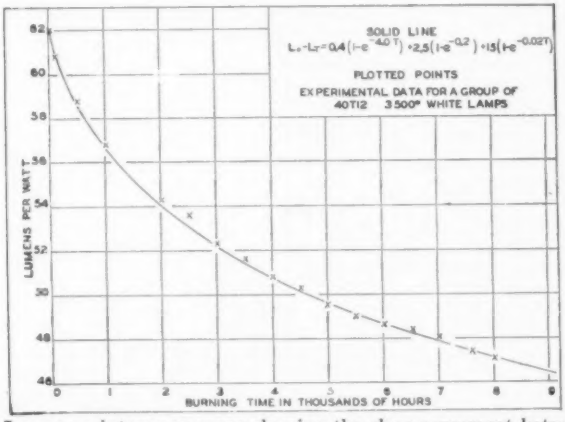

FIG. 1. Lumen maintenance curve showing the close agreement between experimental data and the maintenance equation.

For brevity the three terms on the right-hand side of the equation will hereinafter be referred to simply as the A, B, and C terms.

Fig. 1 illustrates how accurately this equation expresses the behavior of a group of 20 lamps throughout an operating life of 8000 hours. The solid line is obtained from the equation with the values of coefficients and exponents shown in the legend. Plotted points are the experimental measurements. Attention is directed particularly to the values of the exponential quantities a, b, and c since it has been found that, with one exception to be discussed later, they are constants for all 40T12 white lamps studied to date. Obviously, we have to do with a sum of three separate and distinct rates of decay. Mathematically, at least, they are independent and have velocities differing by about one order of magnitude. The first or "A" term approaches A as a limit in 100–200 hours. The "B" term reaches its practical limit in about 2000 hours, while the "C"

term continues to function for something over 20,000 hours before the factors causing the deterioration become ineffective. The maximum loss in lumen output from all factors now recognized is the sum of the coefficients *A*, *B*, and *C*. In this particular instance these amount roughly to 18 L.P.W. so that the lumen output of these lamps approaches 44 L.P.W. as a limit. This is of academic interest only since the cathodes will undoubtedly become deactivated and the lamps cease to function before this limit is reached. The point to be emphasized is, that phosphors exposed to the low pressure mercury discharge will retain an appreciable portion of their initial efficiency indefinitely, unless some further factor not now apparent enters the picture later on.

In Fig. 2 are plotted lumen maintenance curves for four groups of 40 watt fluorescent lamps of varying quality. Again the solid lines are drawn

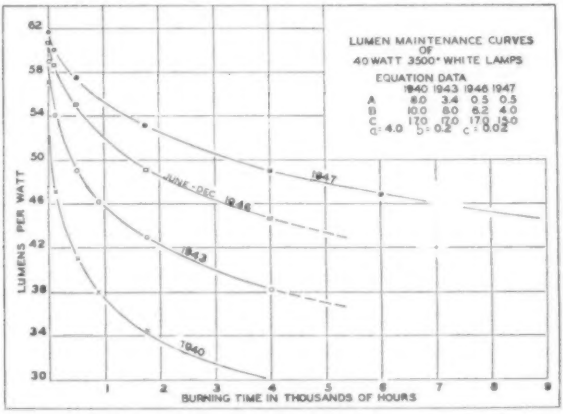

FIG. 2. Lumen maintenance curves of fluorescent lamps of varying quality. The legend indicates the changes in the coefficients of the maintenance equation corresponding to changes in maintenance.

from the equation, using the values of coefficients shown in the legend. The plotted points were obtained from photometric measurements. Readings on about 500 lamps were averaged to obtain the points for each curve. While these curves show the tremendous improvement in phosphors and in processing techniques achieved since the prewar period of 1940, the point of interest for this discussion is the accuracy with which the equation follows the experimental data for all groups. The values of the constants in the equation are also deserving of particular attention. First of all, it will be noted that there is no change in the values of the exponents. "*a*" is 4.0, "*b*" is 0.2 and "*c*" is 0.02 for all the curves which means that there has been no change in the rates of the deteriorations taking place in any of the groups. There has, however, been an important change in the *amount* of these declines as indicated by the differences in the coefficients *A*, *B*, and *C*, particularly in the first two. "*A*," which controls the loss during the first hundred hours, has been reduced from 8.0 to 0.5. "*B*,"

the coefficient of the second term, has been reduced from a value of 10.0 to one of 4.0 and "C" which remained constant from 1940 to December, 1946, shows a small but definite decrease for the year 1947.

EFFECT OF LAMP LOADING

Let us now look at some of the factors which have a bearing on the problem: One of these factors is the matter of lamp loading. The more intense the bombardment of the phosphor with ions, electrons, and high energy quanta, the more rapid the loss in efficiency. As shown in Fig. 3, the percentage loss in lumen output for a given exposure time is directly proportional to the arc watts consumed in the discharge per unit area of the phosphor. In this figure the lumen maintenance of several common types of fluorescent lamps, expressed in percentage of the 100 hour value, is plotted against arc watts per square inch of phosphor area for two different periods

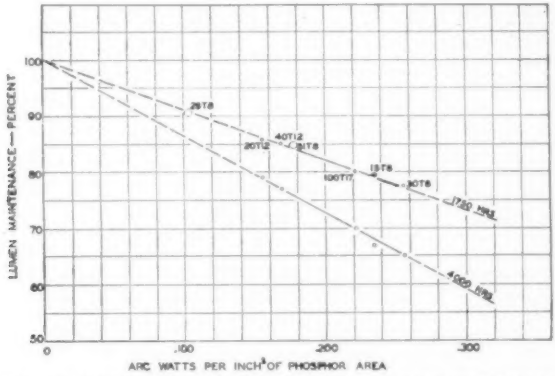

FIG. 3. Curves showing the relation between per cent maintenance and lamp loading.

of operation. In both cases straight lines drawn through the points extrapolate to 100 per cent for 0 loading. This is one of the reasons why all the lamps discussed in this paper are of the same size and operated at the same wattage.

EFFECT OF ARGON PRESSURE

In so far as the writer is aware, all fluorescent lamps are filled with a mixture of rare gas and mercury, usually argon and mercury. The function of the argon is to afford ease in starting and to protect the cathodes from mercury ion bombardment. At low argon pressures cathode erosion by ion bombardment is greatly accelerated, so much so that if no argon is introduced the cathodes may be entirely ruined in a few hours. It turns out that the presence of argon is also essential to good lumen maintenance. Fig. 4 illustrates this effect. At low pressures of argon the initial efficiency is high, corresponding to the increased mean free path and resulting higher electron temperatures obtained. This initial advantage is lost very rapidly

and after about 200 hours of burning the lamps having the higher argon pressure also have higher efficiency. This advantage is maintained throughout life. While the constants of the equation have not been calculated, it is apparent that most of the improvement has been in the early

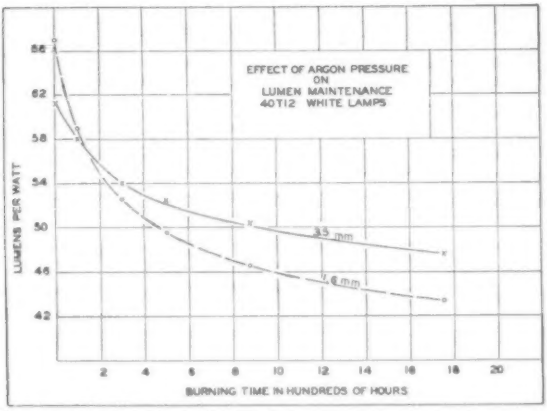

FIG. 4. Curves showing the relation between argon pressure and lumen maintenance.

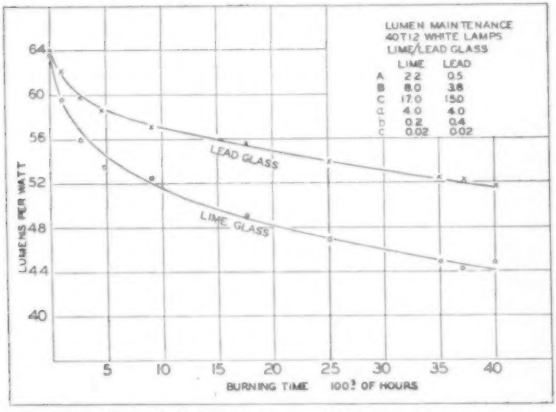

FIG. 5. Curves showing effect of the type of glass envelope on the phosphor efficiency.

depreciation. The two curves are nearly parallel after 1000 hours indicating that the coefficient C has not been affected.

EFFECT OF THE GLASS ENVELOPE

The type of glass upon which the phosphor is spread has long been known to have an effect on lumen maintenance. Fig. 5 shows the tremendous

difference in maintenance between two groups of lamps which are identical in all respects except for the glass of which the envelope is composed. The essential difference between the two glasses is, of course, in their lead and sodium content. A listing of the equation constants is given in the legend. It will be noted that all three of the coefficients are improved in the case of lead glass, particularly the value of "*B*." There is also a difference in the exponent "*b*," indicating a more rapid rate of depreciation. Additional data must be secured before the latter change can be relied upon. As mentioned in a previous paragraph, this is the only instance which has come to the writer's attention when the value of any of the exponents has been found to vary from the "standard" values determined for 40 watt lamps coated with a zinc-beryllium silicate and magnesium tungstate mixture blended to give 3500° white color.

For some time it was questionable whether the difference in maintenance between lead and lime glasses was caused by a deleterious effect of sodium or a favorable reaction with lead. The experiments now to be described should aid in clarification.

RESULTS OBTAINED WITH A "PROTECTIVE COATING"

Some years ago Mr. Arthur Roy and Mr. Robert Ives of our laboratories discovered that the addition of a small amount of certain antimony compounds to the finished phosphor had the effect of reducing the decline in efficiency during operation. A series of experiments was started to determine the effectiveness of this addition. For the purposes of this discussion, we will confine ourselves to those in which antimony trioxide (Sb_2O_3) was the additive.

One of the first of this series of experiments was carried out as follows: A group of lime glass bulbs such as are used in 40 watt lamps was coated for one half their length with a standard white phosphor. The other half was coated with the same phosphor, to which 0.05 per cent of Sb_2O_3 had been added. This group of bulbs was then divided into two subgroups and put through a lehr for removal of the binder as indicated in Fig. 6. Subgroup A was put through the lehr with a stream of air passing through the bulbs so that the air stream passed first over the untreated phosphor and then over the treated phosphor. The direction of air flow was reversed for the bulbs of group "B." The bulbs were then made into lamps and life tested. The curves of the figure indicate the results of photometric measurements of the treated and untreated halves of these lamps. The treated phosphors have a slightly lower initial efficiency than the untreated and very similar maintenance curves regardless of the direction of air flow during baking. In the case of the untreated phosphors, however, the direction of air flow makes a marked difference in performance. In group "A" the phosphor shows about the decline to be expected for an untreated phosphor on lime glass, indicating that there is no essential diffusion of the antimony oxide in the discharge. In case "B," however, it is obvious that some of the Sb_2O_3 has vaporized during baking and that some of this vapor has been carried by the air stream and deposited on the untreated phosphor.

Another experiment is illustrated by the curves of Fig. 7. In this experiment three groups of lamps were tested. In one group the bulbs were coated with untreated phosphor. In a second group 0.05 per cent NaOH was added to the phosphor prior to coating. In the third group 0.3 per cent

Sb_2O_3 was added to the phosphor containing the NaOH. The lumen maintenance curves demonstrate that the NaOH not only decreased the initial efficiency of the phosphor by 2.6 L.P.W., but also increased the decline in efficiency. When 0.3 per cent Sb_2O_3 was added to this contami-

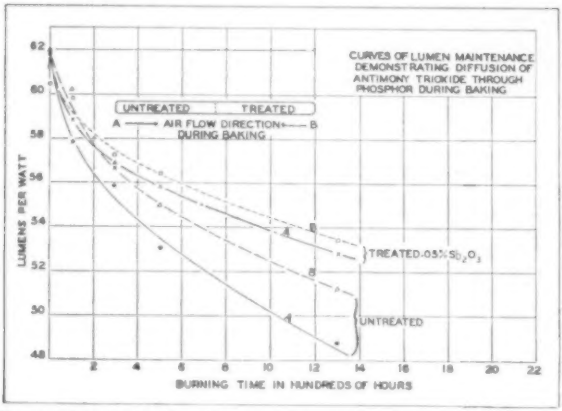
CURVES OF LUMEN MAINTENANCE DEMONSTRATING DIFFUSION OF ANTIMONY TRICKIDE THROUGH PHOSPHOR DURING BAKING
UNTREATED
TREATED
A ——— AIR FLOW DIRECTION DURING BAKING ——— B
TREATED-05% Sb2O3
UNTREATED
LUMENS PER WATT
BURNING TIME IN HUNDREDS OF HOURS

FIG. 6. Curves demonstrating the improvement in lumen maintenance resulting from the addition of Sb_2O_3 to the phosphor.

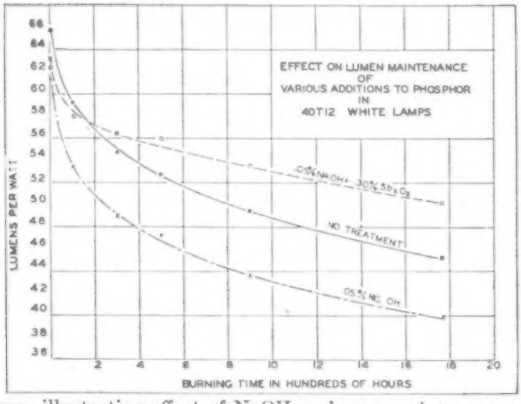
EFFECT ON LUMEN MAINTENANCE OF VARIOUS ADDITIONS TO PHOSPHOR IN 40T12 WHITE LAMPS
05% NaOH + 30% Sb2O3
NO TREATMENT
05% NaOH
LUMENS PER WATT
BURNING TIME IN HUNDREDS OF HOURS

FIG. 7. Curves illustrating effect of NaOH on lumen maintenance and the neutralization of this effect by Sb_2O_3.

nated phosphor, however, the maintenance was improved to such an extent that after about 200 hours the efficiency of these lamps was better than that of the lamps containing the untreated phosphor. Other experiments using Na_2CO_3 instead of NaOH as the impurity addition gave similar results.

It next becomes of interest to inquire whether the effect of Sb_2O_3 results from a reaction with the glass or with the phosphor. To test this question a group of lime glass bulbs were coated with a suspension containing 10 grams of Sb_2O_3 per gallon of vehicle. This suspension was flowed on the inside surface of the bulb and allowed to drain and dry. The bulbs were then put through the lehr just as in the normal processing of phosphor coated bulbs. After baking they were thoroughly washed with hot water, dried, and coated with phosphor. Half of the bulbs were coated with untreated phosphor and half with phosphor to which had been added 0.1 per cent of Sb_2O_3. These coated bulbs were then made up into lamps and life tested as usual. Fig. 8 shows the results of this experiment. Curve X represents the data obtained from lamps with treated bulbs only. Curve Y was obtained with the lamps whose phosphor also contained Sb_2O_3. The initial and 4000 hour values of L.P.W. for curve X are almost exactly

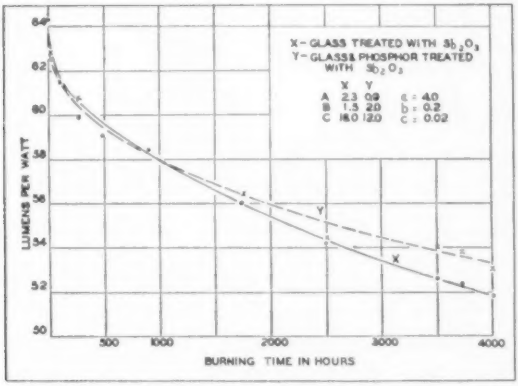

FIG. 8. Curves showing effects of treating glass or glass and phosphor with Sb_2O_3.

the same as for the lead glass curve given in a previous figure although the coefficients of the equation are slightly different. There is a considerable difference between the coefficients of the X and Y curves, particularly the C coefficient, indicating that the Sb_2O_3 has appreciably decreased the long term deterioration.

Fig. 9 illustrates the effects obtained in another experiment in which the amount of Sb_2O_3 added to the phosphor was varied in three groups of lamps. To the phosphor of one group was added 0.05 per cent, to another 0.10 per cent, and to a third 0.30 per cent. The coefficients of the equation as determined for these three groups show that increasing amounts of antimony oxide have little additional effect on the *A* and *B* values but markedly improve the *C* value.

In an effort to shed light on the way in which the Sb_2O_3 protects the phosphor, particularly over long time exposures, several bulbs of ultraviolet transmitting glass were coated with a suspension of this material as described in a previous section. The transmission of these bulbs for

2537Å and 1849Å radiation was then measured. It was found that their transmission of 2537Å was decreased about 5 per cent, but for 1849Å radiation by about 25 per cent.

Experiments previously described by the author (1) have shown that there is no decrease in the generation of 2537Å radiation during long periods of operation, and that at least 98 per cent of the ultraviolet energy generated is absorbed by the phosphor.

It has been well established by numerous tests that lumen maintenance is materially affected by particle size. Phosphors with a large average particle size have a better maintenance than those of small size. In other words the maintenance is a function of the specific area.

Mercury wets the surface of poorly reacted phosphors such as those represented by curve "1940," Fig. 3, resulting in a gray appearance of the un-

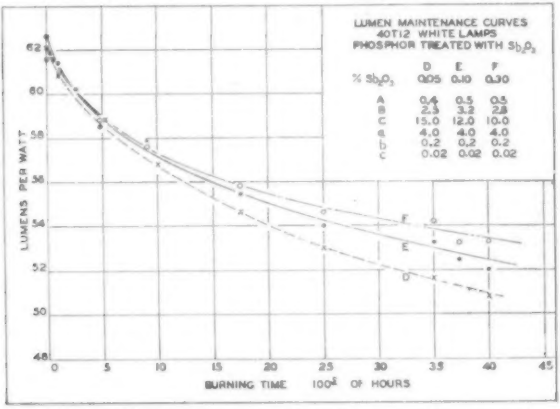

FIG. 9. Curves showing the improvement in long term lumen maintenance as a function of the amount of Sb_2O_3 added to the phosphor.

lighted lamp after rather short burning intervals. It does not wet well-reacted or stabilized phosphors.

SUMMARY

Let us now review the evidence and endeavor to establish some sort of working hypothesis regarding the factors which govern the luminescent deterioration resulting from exposure to the low pressure mercury discharge.

1. The deterioration in lumen efficiency with time of exposure can be completely and accurately described as the sum of three simultaneous exponential expressions.

2. These three exponentials are independent of each other and are of widely different velocities.

3. Complete reaction of the phosphor and improved lamp processing decrease the A and B coefficients but have no effect on the C coefficient.

4. The per cent loss in efficiency is directly proportional to lamp loading.

5. The lumen maintenance is materially affected by the argon pressure which in turn determines the electron temperature.

6. The maintenance is affected by the particle size of the phosphor and hence by its specific surface.

7. The type of glass upon which the phosphor is spread is an important factor, probably due to release of sodium compounds.

8. Treatment of certain glasses with a glass forming material such as Sb_2O_3 improves the maintenance, particularly the "*B*" term.

9. Addition of Sb_2O_3 to the phosphor further improves the maintenance, affecting not only the "*B*" but the "*C*" terms also.

10. The long or "*C*" term maintenance improves progressively with increasing amounts of Sb_2O_3 additions.

11. Treatment of ultraviolet transmitting glass with a thin film of Sb_2O_3 serves to decrease appreciably the transmission of 1849Å without a comparable effect on the transmission of 2537Å radiation.

12. There is no measurable depreciation in the rate of generation of 2537Å radiation during long periods of operation.

CONCLUSIONS

There is much other corroborative evidence, but the above should be sufficient to permit one to make a few fundamental assumptions and draw some conclusions regarding the mechanism of phosphor deterioration. The phosphor crystal is normally some two or three microns in diameter and, therefore, is made up of many thousands of elementary fluorescent units or centers. Let us assume that these centers either fluoresce with unit quantum efficiency or do not fluoresce at all. A loss in lumen efficiency would then be directly proportional to the number of active centers or luminescent units deactivated by some agency, a chemical reaction for example. If a chemical reaction were involved, one would expect the centers on or near the surface of the crystal to be preferentially affected. A situation of this sort would result in building up an inert layer on the surface of the crystal. While such a layer would reduce the fluorescence of the crystal, it could well act as a protective coating for other active centers beneath. A similar process would be expected to result from bombardment of the crystal with high energy photons or other energy bearing components of the discharge.

Some such protective mechanism must be involved, otherwise one would expect the deterioration of the phosphor to continue until its fluorescence was entirely destroyed, particularly if high energy photons were responsible (impurities in the gas or phosphor might be consumed before complete deactivation was reached). This definitely does not occur. As a matter of fact one group of lamps now on test in our laboratory has shown no change in efficiency whatever for the last 2000 hours of operation. It has been shown in previous paragraphs that such a protective layer can be formed by the deposition on the phosphor crystal of a very thin film of a glass forming material such as antimony trioxide. Such a film not only minimizes the reaction of certain ingredients in the glass with the phosphor but has the property of preventing the transmission of at least part of the 1849Å radiation which would otherwise bombard the phosphor crystal.

A well known chemical principle states that if a small amount of a sub-

stance I is in the process of reacting with a large amount of another substance P, the reaction proceeds in accordance with the simple equation:

$$I_T = I_0 e^{-aT}$$

where I_T is the amount of substance I available for reaction at time T
I_0 is the amount of substance I available initially
and a is a quantity representing the velocity at which the reaction proceeds.

It follows immediately that at time T the amount of I which has been consumed is:

$$I_0 - I_T = I_0(1 - e^{-aT})$$

This is exactly the type of equation which has been found to fit the luminescent deterioration situation. If one assumes, as has been done, that the loss in lumen efficiency is proportional to the number of active centers destroyed, it follows at once that the coefficients A, B, and C in the maintenance equation represent the amounts of certain reagents present in the lamp which are capable of deactivating the fluorescent centers. So far as has been determined there are three types of these reagents each of which reacts with the phosphor at a widely different velocity.

Reagent A reacts rapidly and is all or nearly all consumed in about 100 hours. A typical reagent of this type is mercury which will wet a poorly reacted phosphor. Although not specifically discussed here, other gases and vapors are known to behave in similar fashion.

Reagent B reacts much more slowly. Typical of this class is sodium from the glass. Other solid impurities would also be expected to have a slow rate of diffusion and reaction with the phosphor.

The type of efficiency loss represented by the C term of the equation is probably the result of destruction of active centers by 1849A radiation. A review of the data shows that this decline was constant for lamps of all qualities with the single exception of those whose phosphor was covered, or partially covered, with a thin film of antimony trioxide. The amount of improvement in this particular depreciation was roughly proportional to the amount of protective film deposited.

These reagents act independently and the experiments described demonstrate that they can be treated separately. It seems reasonable to conclude, therefore, that the deterioration in certain phosphors exposed to a low pressure mercury arc is caused by a series of "first order" chemical reactions. These are three in number: (1) A rapid "gas phase" reaction between the phosphor and mercury vapor or some gaseous impurity in the lamp; (2) A much slower "solid phase" reaction such as that between the phosphor and a sodium compound released from the glass wall; (3) An extremely slow reaction probably due to the direct action of high energy quanta on the phosphor.

ACKNOWLEDGMENTS

The author wishes to express his thanks to Dr. Keith Butler who suggested the type of equation found so useful in this study and to Mr. Eric Mager and Mr. Arthur Roy who performed much of the experimental

work. He is deeply indebted to Mr. John Merrill and the Engineering Staff of the Sylvania Chemical Division who furnished all the phosphors used in this work and whose cooperation has been invaluable. He also wishes to express his appreciation of the enthusiastic support of Mr. Howard Biggs, Chief Engineer of the Lamp Division.

Any discussion of this paper will appear in the discussion section of Volume 95 of the TRANSACTIONS of the Society.

REFERENCES

1. E. F. LOWRY, *Illum. Eng.*, **43**, 141 (1948).
2. E. F. LOWRY, *Illum. Eng.*, **41**, 859 (1946).
3. C. KENTY AND J. R. COOPER, *Trans. Electrochem. Soc.*, **87**, 397 (1945).
4. H. C. FROELICH, *Trans. Electrochem. Soc.*, **87**, 429 (1945); *J. Applied Phys.*, **17**, 573 (1946).
5. G. MEISTER AND R. NAGY, *J. Optical Soc. Am.*, **36**, 696 (1946).
6. J. W. MARDEN, N. C. BEESE, AND G. MEISTER, *J. Optical Soc. Am.*, **30**, 184, (1940).
7. C. J. LEBEL (To Raytheon) U. S. Pat. 2,126,787, Aug. 16, 1938.
8. E. L. MAGER (To Sylvania Electric Products, Inc.) U. S. Pat. 2,419,902, Apr. 29, 1947.

DOUBLE AND TRIPLE ACTIVATED MAGNESIUM PYROPHOSPHATE PHOSPHORS[1]

HERMAN C. FROELICH

Lamp Development Laboratory, General Electric Company, Cleveland, Ohio

ABSTRACT

Magnesium pyrophosphate, double activated with cerium and thorium, has been developed as an ultraviolet emitting phosphor having considerably greater powder brightness than standard 360 BL phosphor. The peak of emission occurs between 3440 and 3560 Å, depending upon composition, as compared with 3600 Å for 360 BL. All data refer to excitation with λ 2537. With increasing thorium content, the brightness is increased and the peak emission displaced toward longer wavelengths. The increase in brightness compared with the single activated parent phosphors is more than additive and may be interpreted as being due to sensitization of Th by Ce.

The phosphors are made more friable through addition of a few per cent of silica before firing. They are very susceptible to oxidation at elevated temperatures and, for this reason, have not given outputs in lamps as high as expected from powder brightness data.

The further addition of manganese resulted in a novel system of triple activated phosphors, $Mg_2P_2O_7$: (Ce, Th, Mn), with relatively bright emission in the visible, plus variable amounts of ultraviolet. Color and brightness of these phosphors are a function of the concentration of all three activators, as shown in graphs and tables. The maximum brightness attained so far was of the order of two-thirds of that of ZnBeSilicates of corresponding color. These phosphors, too, are improved by silica and show high sensitivity to oxidation at elevated temperatures. They produced lamps of lower lumen output than was expected from powder brightness data.

INTRODUCTION

The addition of small amounts of thorium in the preparation of cerium activated calcium phosphate (360 BL) phosphors resulted in an appreciable brightness gain (1). This suggested a study of the activator pair Ce-Th in other matrices. Thus the brightness of $AlPO_4$:Ce, a phosphor of inconsequential efficiency, could also be brought up to the level of 360 BL phosphor with the incorporation of some thorium. On the other hand, several silicates with the activator pair Ce-Th gave only poor ultraviolet (UV) emitting phosphors over the range of compositions and firing conditions studied.

One of the more promising matrices was magnesium pyrophosphate. Double activation with Ce-Th produced phosphors of considerably greater brightness compared with standard 360 BL. This work is described in part I below. Orthophosphates prepared synthetically from MgO and H_3PO_4 gave only low brightness phosphors (of the order of 15% of 360 BL).

[1] Manuscript received January 12, 1949. This paper prepared for delivery before the Philadelphia Meeting, May 4 to 7, 1949.

Experiments on the further addition of manganese as a third activator led to the discovery of a new and rather complicated phosphor system with emission in the visible. This is described in part II below.

I. $Mg_2P_2O_7$: (Ce, Th)—UV PHOSPHORS

Preparation.—Magnesium pyrophosphate is conveniently prepared by ignition of $MgNH_4PO_4$. Its formation is analogous to the formation of $Ca_2P_2O_7$ by ignition of $CaHPO_4$ in air. Firing in an atmosphere of wet hydrogen leads to the formation of $Ca_3(PO_4)_2$ from $CaHPO_4$ (1). It was unexpected, therefore, to find that $Mg_2P_2O_7$ is formed and survives the treatment when $MgNH_4PO_4$ is fired in steam and hydrogen as well as in air. Dry hydrogen, however, produced some phosphine and magnesium phosphide (as observed by Struve in 1860) and inactive phosphors.

The preparation of the phosphors is very simple. A cold solution of magnesium nitrate, of about 25 per cent strength, is prepared with the required amounts of the activators added also in form of nitrates. A slight excess of a 20 per cent solution of $(NH_4)_2HPO_4$ is added under vigorous stirring. This is followed by the addition of concentrated ammonia, about the same number of cc. as the weight of the phosphate in grams. After some standing the finely crystalline precipitate is filtered, washed, dried, sieved, then fired in an atmosphere of much steam and little hydrogen, for about 1 hour at 1050° to 1100°C. After cooling in hydrogen and sieving, the phosphor is ready for use.

Commercial Reagent Grade chemicals were used without further purification and seemed adequate for the purpose. More careful purification might improve the efficiency of the phosphors somewhat. Modifications of the above method might yield particles of even smaller size.

In exploratory work, phosphors were fired in atmospheres of nitrogen and hydrogen, respectively, and with and without steam, at temperatures from 900° to 1200°C. All samples fired in dry hydrogen were dead and gave indication of some reduction to P compounds of valence lower than 5. Samples fired in wet or dry nitrogen were of very weak fluorescence. Thereafter, the phosphors were fired only in steam and hydrogen. In general the brightness increased with firing temperature. However, the degree of sintering increased also with firing temperature so that the range from about 1050° to 1100°C. seemed to strike the best compromise of all important factors to be considered. All brightness measurements were made with filtered λ 2537 as exciting source, as described in (1).

The powder qualities of the phosphors (friability, particle size, etc.) could be improved with the addition of some silica before firing. Two to five per cent were effective, yet amounts of 10 per cent by weight gave no reduction in powder brightness (samples P 284 and P 285 in Table I). Brightness differentials may be found, however, if the phosphors are compared after some hard grinding.

The silica may be added in several ways. For example, fine, hydrated silica (Mallinckrodt) may be suspended in the solution of the nitrates prior to precipitation; ethyl silicate solution may be mixed with the nitrates and hydrolyzed during or after addition of phosphate and ammonia; silica may be mixed with the dried phosphor intermediate before firing. It was not ascertained whether the silica remained free in the powder after firing or whether it formed $MgSiO_3$ or a double compound with the phosphate.

In lamps made with the conventional suspension coating method, the phosphors proved somewhat disappointing. The cerium (3+) activator was found to be very susceptible to oxidation at elevated temperatures. This resulted in a considerable brightness loss of the phosphor in lamp lehring. In two cases checked, the combined brightness losses due to grinding and lehring amounted to 30 and 45 per cent, respectively. Electrostatic coating application would give more favorable results.

Characteristics.—Cerium alone gave a fairly strong emission, increasing with the Ce content, and with a maximum of brightness in the broad range of about 10 to 30 mols Ce_2O_3 per 100 mols $Mg_2P_2O_7$ (see Table I). The absorption of λ 2537 of all these phosphors was high. Thorium alone gave only very weak fluorescence, whether excited by cathode rays or by λ 2537.

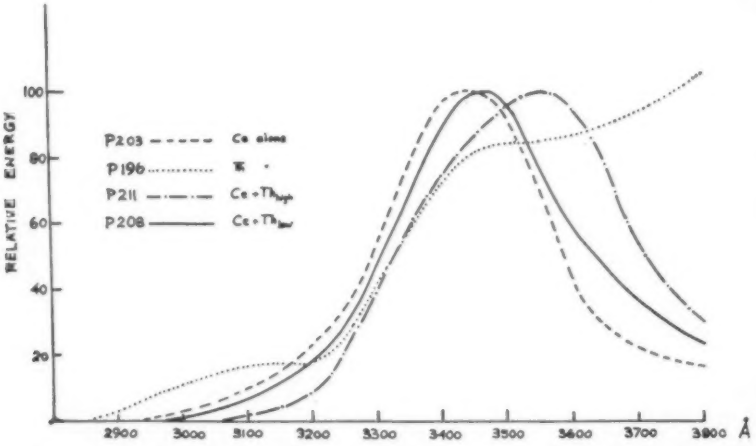

FIG. 1. Spectral energy distribution of $Mg_2P_2O_7$ phosphors single and double activated with Ce and Th. Concentrations are given in Table I.

Because of its low intensity, the accuracy of curve P 196 in Fig. 1 is not as great as that of the others. The low intensity of the thorium activated phosphors is due, in part, to the absence of a strong absorption band in the region of λ 2537. This was demonstrated qualitatively by the strong excitation of zinc silicate phosphor with 2537 radiation which passed through a layer of $Mg_2P_2O_7$:Th. The phosphors activated with cerium alone gave no or feeble excitation of the zinc silicate under like conditions, indicating strong absorption (and scattering) of λ 2537.

Most combinations of the two activators, however, resulted in phosphors whose brightness was considerably greater than the sum of the brightness of single activated phosphors having like concentrations of Ce and Th, respectively. This appears to be a case of true sensitization. Many combinations gave phosphors of considerably higher brightness than the standard 360 BL phosphor. Small amounts of thorium in combination with about 10 to 15 mols Ce_2O_3 for 100 mols $Mg_2P_2O_7$ gave the brightest

phosphors, up to 147 per cent in terms of 360 BL. This, however, does not imply a corresponding increase in quantum efficiency since the powder brightness measurements were not corrected for the changing photocell sensitivity for powders with different spectral distribution and quantitative absorption data were not obtained. Table I gives a brief survey of a number of compositions studied.

The concentrations were calculated under the assumptions that (1) all magnesium introduced as nitrate is eventually recovered as $Mg_2P_2O_7$, and (2) that all cerium and all thorium introduced as nitrates are also recovered

TABLE I

No.	Mols/100 mols $Mg_2P_2O_7$			Per cent brightness against 360 BL, after firing at:		
	Ce_2O_3	ThO_2	SiO_2	1000°C.	1100°C.	1200°C.
P 181	0.13			15	50	
P 182	1.34			24	90	
P 183	10.7			50	105	
P 224	13.4			120	116	
P 205	16.1				112	
P 203	27.0			112	113	
P 223	54.0			100	98	
P 227	∞ (= $CePO_4$)				60	
P 196		1.6		7		7
P 214		16.6			2	
P 190	0.13	1.67		34	54	57
P 191	1.34	1.67		87	79	107
P 212	1.36	16.7			108	
P 192	10.7	1.67		128	134	140
P 225	13.4	0.084			130	
P 208	13.6	0.152			139	
P 226	13.4	0.168			140	
P 209	13.6	1.52			142	
P 210	13.6	7.6			146	
P 211	13.6	15.2			145	
P 206	16.1	2.0			145	
P 204	27.0	2.0			145	
P 284	13.7	16.7			147	
P 295	13.7	16.7	23.4		147	

as phosphates. Thus, while the activator concentrations are listed in terms of oxides, it is assumed that the activators are actually present as phosphates. Because of the high atomic weight of Ce and Th, errors due to slight deviations from assumption (2) would in this case be of secondary importance. Chemical analyses of finished phosphors were not considered important enough to be made.

Fig. 1 shows the emission of a few typical phosphors as measured by E. S. Steeb, Jr. of this laboratory, with the quartz double monochromator described in reference 1. The measurements were made on powders, not lamps. The emission band of the single activated Ce phosphor P 203 with 27 mol per cent Ce_2O_3 shows a maximum at about 3440 A which compares with 3600 Å for the peak emission of cerium activated calcium phosphate.

Thus the particular crystal field afforded by the magnesium phosphate matrix caused a displacement of the cerium emission toward shorter wavelengths. The shape of the curve and the peak position were fully identical with those of a single activated Ce phosphor with much lower cerium content (P 182 with 1.34% Ce_2O_3). Therefore, except for intensity, the emission of the single activated Ce phosphors may be considered invariant with concentration.

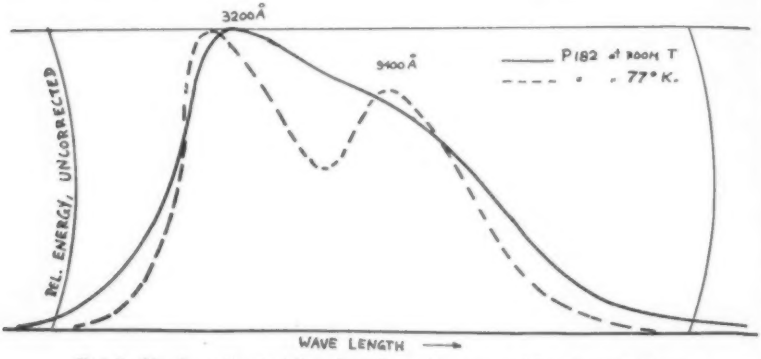

FIG 2. Single activated Ce phosphor at room and low temperatures

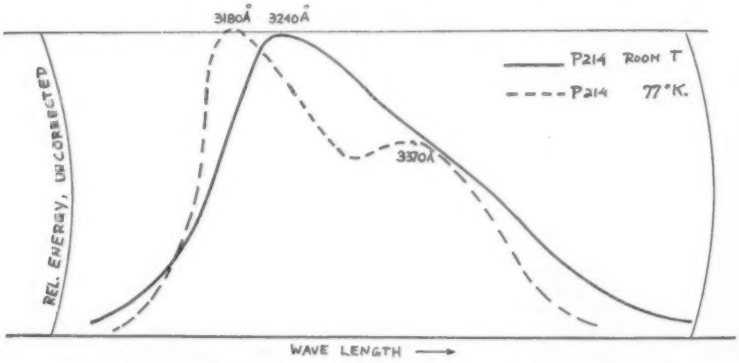

FIG. 3. Single activated Th phosphor at room and low temperatures

At liquid air temperature, the familiar split of the cerium band may be observed, giving two component bands which lie so close together as to be unresolved at room temperature. This is shown in Fig. 2 for phosphor P 182. The graph is a tracing from recorded curves obtained by Dr. F. J. Studer of the General Electric Research Laboratory, with a grating spectrograph and phototube pickup. The ordinates have not been corrected for tube sensitivity to obtain true energies. The ensuing distortion may be judged by comparing the curves for sample P 211 in Fig. 1 and 4. They

show an apparent complete reversal of intensities of the two main component bands. The traced curves do not give the true peak positions of the emission bands. They serve merely to demonstrate the split in two at low temperatures. Numerous reflected low and higher order Hg lines have not been reproduced in the tracings.

The weak emission of thorium alone is also shown in Fig. 1 (on a relative scale), for sample P 196 with 1.6 mol per cent ThO_2. Sample P 214 with 10

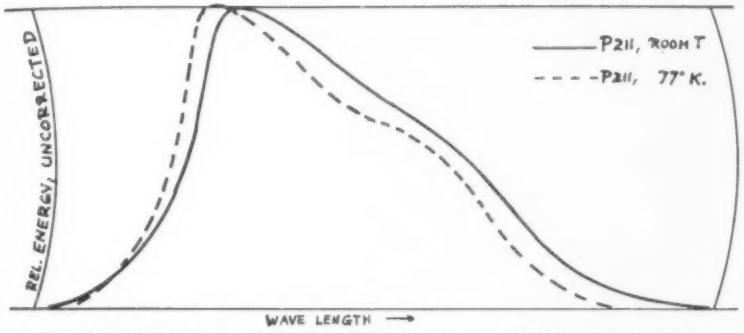

FIG. 4. Double activated Ce-Th phosphor at room and low temperatures

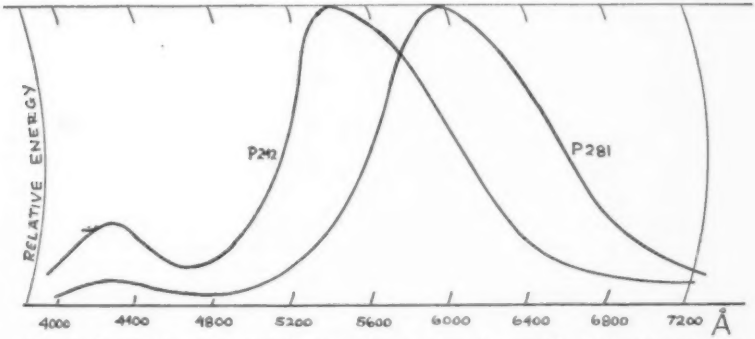

FIG. 5. Spectral energy distribution of a green and a red $Mg_2P_2O_7$:(Ce, Th, Mn) phosphor.

times as much ThO_2 gave likewise a curve of identical shape and peak location, showing independence of the emission of the thorium content. Because of low intensity, these curves are not too accurate. Two bands are prominent, one in the UV in the vicinity of 3500 Å, the other in the visible at 4300 Å. Low temperature excitation of these phosphors reveals again a doublet nature for the UV band due to Th (Fig. 3). The existence of the 4300 Å band is indicated by the rising branch of the curve in Fig. 1; it may be seen more clearly in Fig. 5 to 8. While the absolute intensity of the thorium activated phosphors is very low, their quantum efficiency with

respect to the actually absorbed amount of λ 2537 radiation may still be high. It was pointed out above that they are quite transparent to λ 2537. In addition to these two emission bands, there appears to be another third band of very low intensity at about 3130 Å.

Kröger (2) has reported a blue band obtained with unactivated $Mg_2P_2O_7$ phosphors under cathode ray excitation. He attributes it to fluorescence

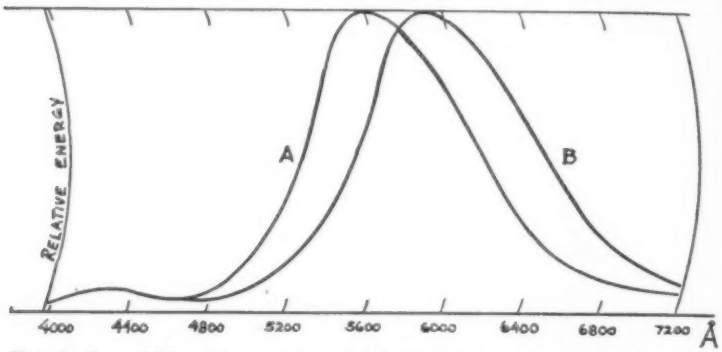

FIG. 6. Ce and Mn constant, Th in "B" (P 246) four times as high as in "A" (P 245).

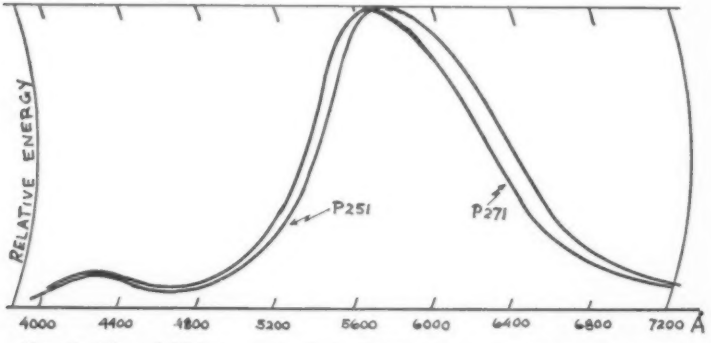

FIG. 7. Th and Mn constant, Ce in P 251 4.5 times as high as in P 271

of the PO_4 group as such, possibly to a lower valent P compound. Similar phosphors without added activators, prepared by the author, did not give a measurable blue emission with λ 2537 excitation. It seems probable, therefore, that, in the phosphors prepared with added thorium, its origin lies in Th centers.

It is not clear whether the emission of the double activated phosphors originates in Ce centers, in Th centers, or both, additively or otherwise. Considerations below lead to preference for Th emission with increasing Th content. The intensities, however, and thus the efficiencies of con-

version, are certainly more than additive. Fig. 1 shows that the peak position becomes displaced toward longer wave lengths with increasing amounts of thorium.

Several explanations might be considered for this shift toward longer wave lengths. One of these is that the intensity of the longer wave band of the Ce emission becomes considerably increased as a result of the presence of Th. This would amount to sensitization of Ce by Th. In other words, the probability of the transition from $^2F_{7/2}$ would become considerably greater than that from $^2F_{5/2}$, (3), increasing even further with the Th content. This does not seem to be very likely. Increased self-absorption of the shorter wave length Ce band would result in an apparent shift toward longer wave lengths but would not be consistent with the observed actual increase in brightness. It is quite unlikely that the shift could be due to a build-up in intensity of the 4300 Å band because of its lack of width and its remoteness from the 3500 Å band. A simple explanation would be that the

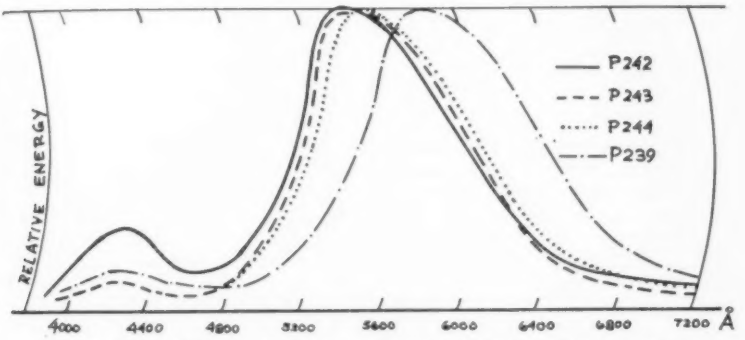

FIG. 8. Ce and Th constant, Mn increased 80 fold from P 242 to P 239

incorporation of thorium so changes the particular crystal field afforded by the $Mg_2P_2O_7$:Ce matrix that the emission due to Ce would originate in surroundings more closely approximating those prevailing in $Ca_3(PO_4)_2$:Ce. This, however, makes it difficult to explain why very small amounts of thorium, such as 0.1 per cent or one atom of Th for several hundred atoms of Ce, already cause a marked shift and, in particular, why this is accompanied by a considerable increase in brightness (of the order of 25% or more).

While the exact position of the ultraviolet Th emission is not too certain, as pointed out above, it would appear from Fig. 1 that a very considerable increase of its intensity should result in an emission whose peak position moves toward longer wavelengths with increasing Th content. This is observed in samples P 208 and P 211 with a hundred fold increase of the Th content for a given Ce concentration (Fig. 1). Thus the emission of the double activated phosphors would be due to sensitization of the Th emission by Ce. At present, this appears to be the most plausible interpretation for both the observed emission shift and the brightness increase. With Th as

chief or sole emitter, no difficulty is presented in accounting for high phosphor brightness with even low Th contents such as 0.1 per cent, in the presence of 100 times as much Ce as sensitizer. It is believed that this view might still hold even if closely coupled Ce-Th pairs should be formed, a condition which would be favored at high Ce and Th contents.

In contrast to $CaSiO_3$: (Pb, Mn) (4), this would be a case of true sensitization. In the calcium silicate phosphor, the exciting energy (λ 2537) is absorbed by Pb and, in the absence of Mn, emitted as long UV. This finds its parallel in $Mg_2P_2O_7$: Ce. With increasing Mn content the emission due to Pb is decreased in intensity and the visible emisison due to Mn is correspondingly increased. The Mn emission, however, is already latent in phosphors containing only Mn and no Pb, as evidenced by their strong emission of the Mn fluorescence with excitation of greater energy such as cathode rays.

In $Mg_2P_2O_7$: Th an emission due to Th alone is not latent because it is not excited in any strength by either cathode rays or UV energy. It is considered to appear only in the presence of the sensitizer, Ce. The emission not only appears, but has an intensity much greater than would be predicted from additive brightnesses. For this reason, the term "sensitized" appears to be proper in this case. This may also be the correct interpretation for the brightness increase observed in $Ce_3(PO_4)_2$ and in $AlPO_4$ with the activator pair Ce-Th.

At low temperatures, one would expect the appearance of three or four bands if the emissions were simply additive and independent of one another. Due to the close proximity of the Ce and Th bands, however, such fine structure would be beyond the resolution of our instruments and a split in two major bands may be all that can be realized. Actually, as shown in Fig. 4, there is only a slight narrowing into two bands observed at 77° K., much less than with the individual activators alone as in Fig. 2 and 3. This could be taken as an indication of direct and close coupling between Ce-Th "pairs," in line with the above. It could be confirmed if excitation at much lower temperatures should fail to show a further increase in fine structure.

II. $Mg_2P_2O_7$: (Ce, Th, Mn) PHOSPHORS

Magnesium pyrophosphate, single activated with manganese and prepared as described above, gave a cathode ray response of yellow-green color for very low concentrations of Mn and orange for high Mn, the change being continuous with concentration. The phosphors did not respond to λ 2537.

Phosphors prepared with additional cerium gave about the same colors under cathode rays, as determined by the manganese content, but did not fluoresce more than faintly under λ 2537 excitation. Fluorescence was absent in spite of their strong absorption of the exciting radiation. This is in contrast to the double activated $Ca_3(PO_4)_2$: (Ce, Mn) phosphor which fluoresces bright deep red with λ 2537 excitation (5). It serves to demonstrate that strong absorption of exciting radiation is only one prerequisite for fluorescence and does not necessarily lead to it. It also shows that phosphor behavior can not be predicted, else the activator pair Ce-Mn would respond similarly in the calcium and the magnesium phosphate matrices.

Samples made with 13.6 mols Ce_2O_3 and from 0.34 to 56.4 mols MnO for 100 mols pyrophosphate, for example, gave only long UV emission decreasing in intensity from 122 to 51, and a very weak deep red emission with λ 3650 excitation. Phosphors prepared with only thorium and manganese activators gave the characteristic Mn emission under cathode rays, but neither UV nor visible light under λ 2537 excitation. Lack of fluorescence of the Ce-Mn and Th-Mn phosphors is not due to temperature quenching, for excitation at liquid air temperature did not increase the intensity of emission.

Phosphors prepared with all three activators, Ce, Th and Mn, present simultaneously, gave strong visible response to excitation with λ 2537. The color of these triple activated phosphors was determined chiefly by the concentrations of both, thorium and manganese, although the emission undoubtedly originates in the Mn centers alone. In general, the color became redder with increasing Th content, increasing Mn content, and increasing firing temperature. Most phosphors described here were fired for one hour at 1100°C., in atmospheres of steam and hydrogen.

The cathode ray excited emission was about the same as that of the corresponding single activated Mn phosphors. With λ 3650 excitation they showed a weak deep red emission whose intensity could be changed with the concentration of the activators, whose position, however, was apparently not changed. Thus some curious phosphors were produced which fluoresced light green under λ 2537 and deep red under λ 3650 excitation, at room or low temperatures. This could indicate the presence of two matrix phases[2] or of two species of Mn centers, both containing Mn^{2+} ions. Formation of any high valent manganese (4+ or 7+) was excluded with the preparative conditions. The red emission, therefore, can not be due to "manganate" centers as suggested by Szigeti *et al.* (6) and by Makai (7) for manganese activated phosphors showing red emission.

The λ 2537-excited emission consists of three bands. There is a UV band near 3500 Å whose intensity decreases with increasing thorium and manganese contents. Ideally it should be reduced to zero to allow complete utilization of the absorbed exciting energy in form of visible light. Actually, it was of the order of 1 to 10 per cent (in terms of 360 BL) in phosphors of useful colors. The second band is a blue band at 4300 Å

[2] During the review of this paper it was suggested that x-ray diffraction patterns of the phosphors should be taken in order to establish whether they are truly single phase materials with different response to short and long UV excitation, respectively.

The author had planned a separate study of the structures involved, but deferred it for some later date in anticipation of possible difficulties with complicated or mixed phase structures. This was expected from some preliminary work done with the recording instrument of the North American Philips Co.

The first recorded patterns indicated that all phosphors show principally the structure of magnesium pyrophosphate, and that some unidentified phases were present as impurities especially in the samples with high cerium or thorium contents. These phases were not ThO_2 or Ce_2O_3, but possibly phosphates other than pyro. It is, therefore, possible that the origin of the 3650 Å-excited fluorescence lies in a small amount of a different phase than the 2537 Å-excited strong fluorescence of the main phase. In view of the above it may be associated with Ce-Mn centers which are devoid of Th or thorium influence.

Mrs. Beulah F. Decker of the General Electric Research Laboratory carried out this preliminary diffraction work which is here gratefully acknowledged.

which is attributed to thorium. Its intensity was low and was reduced with increasing manganese content, as shown in Fig. 5 and 8. Its position, however, was invariant with activator concentrations.

The third and most prominent of the emission bands lies entirely in the visible. Apparently it is a single band, for neither change of concentration nor low temperature excitation resolved it into more than one band. Its location is not defined by the manganese content alone as is true with most other phosphors. It is a function of what might be called the "effective" manganese concentration, which depends also upon the thorium content. At best it is equal to, but generally lower than, the absolute concentration of manganese. Within reasonable limits it does not depend upon the cerium content. Thus, the same color of, say, orange fluorescence may be obtained with low concentration of Th and high Mn, compared with high Th and low Mn, for a given content of Ce. However, the brightness of phosphors having the higher Th content was generally greater.

The brightness of the phosphors has reached about two-thirds or slightly more of that of ZnBeSilicates of corresponding color. The good or excellent brightness of $CaSiO_3$: (Pb, Mn) and of Sb-Mn activated halophosphate phosphors has shown that lower brightness is not fundamental to double activation. For this reason, lower brightness of triple activated phosphors is not believed to be an inherent consequence of the cooperation of three activators. The lower brightness of these $Mg_2P_2O_7$: (Ce, Th, Mn) phosphors may be due simply to concentration quenching, since they require relatively large amounts of activators in the brightest samples. While measurements were not made, qualitative observation showed that their brightness increased with excitation at liquid air temperature. In that case, however, it is not clear why phosphors with lower activator contents were not more efficient at room temperature.

The following figures and Table II will illustrate the color variability of the system by means of a few examples. The figures, again recorder curves with true energy as ordinate, show only the continuous phosphor radiation. Reflected Hg lines have been omitted in the tracings. Fig. 5 shows one of the greenest (P 242) and one of the reddest (P 281) phosphors that have so far been made. The cerium content was held constant in these phosphors, thorium increased about twofold, and manganese increased about fourfold in P 281. This resulted in a shift of peak from 5400 to nearly 6000 Å, a range which seems to cover the useful colors produced by the system. The shape of the two curves is not precisely the same, only very nearly so. This could leave some doubt as to the true single band nature of the emission.

Fig. 6 illustrates the emission of two phosphors prepared with the same amounts of cerium and manganese, but a fourfold increase of thorium in "B" (P 246) over "A" (P 245). This resulted in a considerable shift (370 Å) toward the red.

For the phosphors shown in Fig. 7, the content of thorium and manganese was held constant, and cerium increased 4.5 fold in P 251 over P 271. This resulted in only a minor change of color.

Finally, Fig. 8 illustrates the case for one constant amount of cerium and thorium, and increasing manganese. Again there is a large change of color (some 400 Å) attendent with an 80 fold increase in the manganese

content. Concurrently, the blue Th emission is depressed. A recorded curve is not available for sample P 237 to show how it fits in with the other curves drawn. For the particular Ce and Th contents chosen, the brightness of the phosphors goes through a maximum for contents of 5 to 15 mol per cent MnO.

The amounts of activators which could be incorporated in the $Mg_2P_2O_7$ matrix were higher than usual. For this reason it seemed of interest

TABLE II

No.	Mols, per 100 mols $Mg_2P_2O_7$, of			Brightness* under λ 2537	Green/red ratio†	Peak emission (Å)	UV‡
	Ce_2O_3	ThO_2	MnO				
P 230	13.6	—	0.68	—			122
P 238	13.4	—	56.4	—			51
P 219	—	8.4	6.4	—			0
P 270	1.46	8.4	4.2	73	5.5	5570	32
P 280	1.50	12.6	4.3	91	4.65	5600	27
P 251	1.46	8.4	8.4	70	3.0	5700	14
P 254	1.58	9.2	14.0	64	1.76	5800	1
P 282	1.61	12.7	8.4	85	2.85	5870	11
P 291	2.2	19.1	8.5	70	2.4	5800	15
P 271	3.2	8.4	8.4	69	3.7	5570	10
P 241	13.6	17.0	0.34	Faint	—	—	113
P 242	13.6	17.0	0.68	34	10.0	5400	104
P 243	13.6	17.0	2.8	68	7.9	5470	57
P 244	13.6	17.0	14.2	72	5.3	5550	13
P 237	13.4	17.0	28.2	67	2.2	5800	1
P 239	13.4	17.0	56.4	46	1.43	5900	1
P 283	13.6	23.9	14.1	76	2.4	5720	11
P 247	13.8	20.0	17.6	77	3.45	5600	11
P 240	13.4	1.74	28.2	37	6.6	—	56
P 245	13.6	8.6	28.2	80	4.45	5530	14
P 246	13.6	34.0	28.2	63	1.5	5900	1
P 281	13.6	33.3	28.2	63	1.3	5950	1

* In terms of a certain ZnBe Silicate of orange color.

† Ratio of intensities at the red and green ends of the emission band, measured with suitable though arbitrary red and green filters placed over the photocell. This value is often useful for the prediction of fluorescent lamp colors.

‡ In terms of 360 BL standard.

to determine whether the magnesium phosphate is really a necessary part of the phosphors. Thus some phosphors such as thorium phosphate activated with Ce and Mn, or cerium phosphate activated with Th and Mn, were prepared. Their fluorescence with λ 2537 excitation was only weak or faint. This would justify considering the phosphors described as triple activated magnesium phosphates.

A few minor inconsistencies between color or brightness and composition may be found in the data of Table II. These are attributed to uncontrolled variabilities in the preparation of different phosphor samples.

As in the case of the UV emitting phosphors, the addition of some

silica improved the powder characteristics without affecting the brightness adversely. (A few of the samples listed in Table II were prepared with SiO_2.) Likewise, the temperature stability in air was found to be rather poor. Thus the combined grinding and lehring losses of one sample used for lamp making amounted to as much as 42 per cent. While the phosphors are suitable for the production of "white" fluorescent lamps of various shades, their commercial use will probably be quite small because of lower brightness, poorer stability, and much higher cost. From a theoretical point of view, however, they ought to prove quite interesting.

Any discussion of this paper will appear in the discussion section of Volume 95 of the TRANSACTIONS of the Society.

REFERENCES

1. H. C. FROELICH, *Trans. Electrochem. Soc.*, **91**, 161 (1947).
2. F. A. KRÖGER, "Some Aspects of the Luminescence of Solids," p. 59–60. Elsevier Publishing Co., New York (1948).
3. F. A. KRÖGER AND J. BAKKER, *Physica*, **8**, 628 (1941).
4. H. C. FROELICH, *J. Electrochem. Soc.*, **93**, 101 (1948); J. B. MERRILL AND J. H. SCHULMAN, *J. Optical Soc. Am.*, **38**, 471 (1948).
5. G. B. BUCK AND H. C. FROELICH, *Illum. Eng.*, **XLIII**, 27 (1948).
6. G. SZIGETI, E. NAGY, AND E. MAKAI, *J. Chem. Phys.*, **15**, 881 (1947).
7. E. MAKAI, *J. Electrochem. Soc.*, **95**, 107 (1949).

THE FLUORESCENCE OF SILICATE PHOSPHORS
III. APPLICATION OF POTENTIAL ENERGY CURVES[1]

KEITH H. BUTLER
Sylvania Electric Products, Inc., Salem, Massachusetts

ABSTRACT

The fluorescence of silicate phosphors is discussed on the basis of a potential energy curve model and it is shown that Gaussian distributions of the energy bands in excitation and emission spectra can be expected from this model. The model is applied to manganese activated phosphors and an attempt is made to explain the long decay time of these phosphors. Lead activated silicates are discussed and reasons for assuming divalent lead to be the activator are brought out.

The mechanism of sensitized luminescence is treated briefly in terms of the model, as well as the ways in which radiationless energy dissipation may take place.

INTRODUCTION

In discussions of the fluorescence of the inorganic crystalline phosphors, an energy band model is very commonly used with the location of activator levels being shown between the bands representing the energy levels of the matrix. In this model, the crystal is considered to be an entity with little possibility of assigning electrons to specific atoms. This simple model has both advantages and defects when compared to the other model, less frequently used in current literature, in which the effect of configuration, or atomic spacing, on the potential energy is represented as potential curves.

The mechanism of fluorescence is a complex one for which any one model can represent only an over-simplified outline of the true state of the crystal, and only by using many models will it be possible to get an explanation of the involved experimental data. The phosphors excited by mercury resonance radiation of 2537 Å wavelength are almost exclusively of the substitutional type, in which the activator is present in large amount and is an integral part of the crystal matrix. It is believed that a clearer picture of the performance of this type of phosphor can be obtained from the potential curve model than from the energy band model. Recent papers (1, 2, 3, 4) have presented experimental data and theoretical discussions on various phosphors. The present paper[2] will attempt to interpret these and other data using the potential curve model.

ENERGY LEVELS OF MOLECULES

In Herzberg's (5) discussion of the energy levels of diatomic molecules, as determined by the states of the separated atoms, it is clearly evident

[1] Manuscript received January 10, 1949. This paper prepared for delivery before the Philadelphia Meeting, May 4 to 7, 1949.

[2] References 11 and 4 are the first and second papers dealing with the fluorescence of silicate phosphors.

that certain of the molecular energy levels can be attributed to the presence of excited states of one of the atoms, that other levels are due to excited states of the other atom, and that the remaining energy levels of the molecule require that both of the atoms be excited above their normal states. This discussion lays particular emphasis on molecules in which the bonding is homopolar, and in this type of bonding the electrons belong to the molecule as a whole. In contrast, molecules showing ionic bonding are held together simply by the electrostatic attraction between oppositely charged atoms. With this type of bond the electrons are much more localized on the individual atoms and, while the interaction between the ions greatly affects the potential energy levels, it is reasonable to assume that each ion possesses a distinct and different set of energy levels or potential energy curves. We can, therefore, consider independently the excitation of the electrons of one ion.

POTENTIAL ENERGY CURVES OF MANGANESE

One of the most useful equations giving an approximation to the shape of the potential energy curve for solids is that of Born and Mayer (6). This equation is:

$$U = Ae^2/r + B \exp. (-r/\rho) \tag{1}$$

where U is the potential energy
r is the interatomic spacing between cation and anion
A is the Madelung constant, dependent on crystal geometry and valence of the ions
e is the charge on the electron
B is a constant dependent on crystal geometry
ρ is a constant (0.345 Angstrom units)

From equation (1) an expression can be derived for U_0, the equilibrium energy:

$$U_0 = \frac{-Ae^2}{r_0}\left(1 - \frac{\rho}{r_0}\right) \tag{2}$$

Thus the value of U_0 is dependent both on A and on r_0. It is found also that:

$$B = \frac{\rho A e^2}{r_0^2} \exp. (r_0/\rho) \tag{3}$$

Here it can be seen that B, due to the exponential factor, is determined largely by the value of r_0, but is also affected by the value of the Madelung constant, A.

Values of A have been calculated for simple crystals and typical values are listed in Table I to show the effect of ionic valence.

The value of B can be readily calculated by equation (3) if we know the equilibrium spacing, r_0, at which U has its minimum value.

For MnO, which crystallizes in a cubic lattice, many of the values needed in the calculation are known or can be assumed. The potential energy curve for this material is shown as curve I in Fig. 1. For the purpose of discussion it can be assumed that this curve represents, as a rough ap-

proximation, the shape of the potential energy curve for divalent manganese ions in their unexcited state, when these ions are bound to oxygen ions in an ionic lattice. Thus it will represent the behavior of manganese as it exists in most phosphors.

TABLE I

Crystal	A	Type of ions
NaCl	1.75	Both monovalent
ZnS	1.64	Both divalent
CaF_2	5.04	One mono-, one divalent
TiO_2	4.82	One di-, one tetravalent

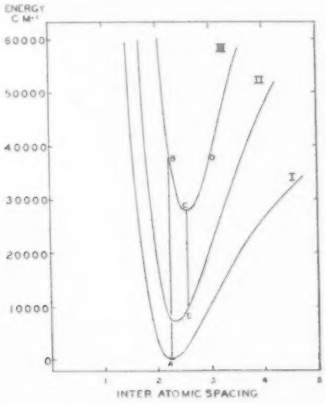

FIG. 1. Potential energy curves for MnO. I, Unexcited manganese ion; II, manganese ion in first excited state (even); III, manganese ion in second excited state (odd).

The outer shell of the divalent manganese ion (7) has the following electronic distribution and normal state:

$$3s^2 3p^6 3d^5 \qquad {}^6S_{5/2}$$

This is spectrographically an even level. When this is excited (8) the first excitation level is an even level with the configuration:

$$3s^2 3p^6 3d^4 4s \qquad {}^6D_J \text{ } (J \text{ variable})$$

On further excitation to the first odd level the configuration becomes:

$$3s^2 3p^6 3d^4 4p \qquad {}^6F_J{}^0 \text{ } (J \text{ variable})$$

Other states with different multiplicity and orbital moment have been found for both of these levels (8), but the electron configuration remains unchanged.

Considering now the effect of these electron configurations on the properties of the manganese ion, the unexcited ion with six $3p$ electrons and

five $3d$ electrons will have a reasonably symmetrical electron distribution and can be considered spherical. In the first even level, one electron has been moved into the $4s$ orbit, thus resulting in an appreciable expansion of the effective radius of the ion, which remains however essentially spherical (9). In the first odd level, one electron enters the $4p$ orbit and as a result the expanded ion loses its symmetrical structure and becomes non-spherical. Due to the expansion of the ion, with a single electron occupying the outermost orbit, the Born-Mayer equation will be appreciably changed. The value of r_0 will obviously increase and, in addition, it can be assumed that the excited ion will exert greater attractive and repulsive forces than the unexcited ion due to distortion of the crystal effectively changing the crystal symmetry. This will materially increase the value of A. Unfortunately, it is not possible to assign values to either A or r_0 for the excited ion[3], hence only schematic curves can be drawn for the potential energy of the excited Mn ion.

Due to the increase in A and r_0 the value of U_0 become much larger and the widely separated energy levels of the free ion approach more closely. Another effect is that the slope of the curves on each side of the minimum becomes steeper. The schematic curves, which might represent the behavior of the excited manganese ion, are shown as curves II and III in Fig. 1.

Using the curves of Fig. 1, the energy transitions responsible for excitation and fluorescent emission of manganese ions can be explained. The unexcited Mn ion at point A on curve I absorbs a photon of ultraviolet radiation and according to the Franck-Condon principle is excited to point B on curve II. Following the transition, lattice vibrations start along BCD with the interatomic spacing changing between the limits B and D on curve III and the potential energy between the limits B or D and C. Vibrational energy is lost with the system coming to equilibrium at point C on curve III. From this point, there is again a sudden transition with the emission of visible light, to point E on curve II, whence the system returns to the normal state by transitions which do not result in visible light. These may be facilitated by Stark levels between the normal and the first excited state.

EFFECT OF THERMAL VIBRATION[4]

It has been found experimentally that both the excitation and the emission spectra of manganese activated zinc orthosilicate can be represented quite closely by Gaussian distributions. If we take thermal vibration into account, the potential energy curves serve to explain the cause of the Gaussian distribution.

In the preceding section, the energy and position of the unexcited manganese atom was assumed fixed at point A in Fig. 1. Actually the system vibrates and it has been established that the probability distribution of position is given by a Gaussian error function (10). Consequently, the system actually vibrates between points A and B on curve I of Fig. 2

[3] Calculations for r_0 have been reported by F. E. Williams, *Phys. Rev.*, **73**, 1257 (1948).

[4] Mott and Gurney, "Electronic Processes in Ionic Crystals," p. 11, have presented a similar derivation.

with the Gaussian distribution of the vibration being shown in curve III. If this Gaussian curve is "reflected" in curve II, representing the excited state, the energy distribution resulting is that shown in curve IV and the possible energy variation is shown by points C and D on curve II. Thus the thermal vibration of the crystal accounts for the Gaussian distribution of the excitation spectrum if curve II approximates to a straight line between points C and D.

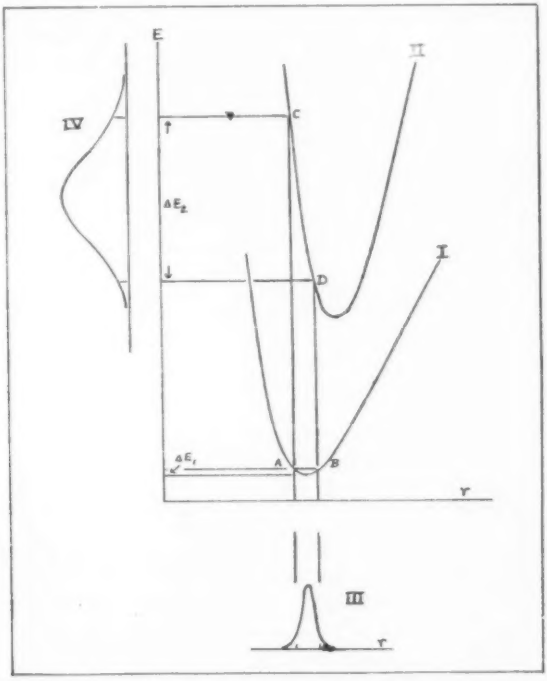

FIG. 2. Origin of Gaussian distribution of energy spectrum. I, II, Potential energy curves of MnO; III, Gaussian probability curve for position in unexcited state; IV, Gaussian probability curve of energy in excited state.

It is obvious that a similar relation must hold for the emission spectrum, with the excited manganese ion having vibrational energy with a Gaussian distribution of position. Since the potential curve of the lower state has rather a steep slope at the point below the minimum of the excited state (see Fig. 1), the energy spread will be rather broad and will approximate a Gaussian distribution. The accuracy of this approximation will depend on how closely the lower curve approaches a straight line. It is apparent also that the Gaussian will be narrower for the emission than for the excitation spectrum for two reasons: (a) the minimum of the potential curve is narrower for the excited than for the unexcited state, and (b)

the left sides of the potential curve are always very steep while the right sides may have a lower slope.

Near the minimum, the potential energy curve approaches the shape of a parabola with $U = nx^2$. It is also true that the average energy is given by the

$$U = U_0 + 3/2\, kT \tag{4}$$

Hence $x\alpha(c + T)^{1/2}$ or the average displacement varies as the square root of the temperature plus a constant, with the constant being dependent on the zero point energy of the system. From this we conclude that the width of the Gaussian distribution will be related to temperature by an equation which is roughly:

$$\sigma = a(b + T)^{1/2} \tag{5}$$

This will apply both to the excitation and the emission spectra with different values for the arbitrary constants, a and b.

TABLE II

T(°K.)	b	1000/b
100	293	3.41
300	165	6.06
378	129	7.75
418	104	9.60
468	79	12.7
518	60	16.7
623	32	31.3
648	27.5	36.4

The only available experimental data to check this prediction is that of Szigeti and Nagy on the emission from zinc orthosilicate (2). The Gaussian used is of such a form that their constant $b \propto 1/\sigma^2$. The values in Table II are calculated from data and figures in their paper. These data, plotted in Fig. 3, show a more complex temperature dependence than the simple theory presented here would predict and they give an equation which is equivalent to:

$$\sigma = a + bT^{3/2} \tag{6}$$

As Fig. 3 shows, the band width remains finite at 0°K. and is not much narrower than at 100°K. This more complex temperature dependence may result from the actual curvature in the lower potential energy curve. A curvature in the proper direction would lead to a wider energy distribution, as is seen in Fig. 4 and would also lead to departure from a true Gaussian curve. This indicates a need for precise measurement of spectral energy distribution on phosphors at various temperatures.

EMISSION SPECTRA OF ZINC SILICATES

The emission spectrum of zinc orthosilicate activated by manganese is relatively simple, consisting of a strong green band with a slightly asymmetrical distribution. Analyses of the emission curves (2, 4) have

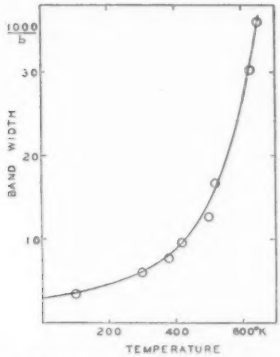

FIG. 3. Effect of temperature on band width for zinc orthosilicate

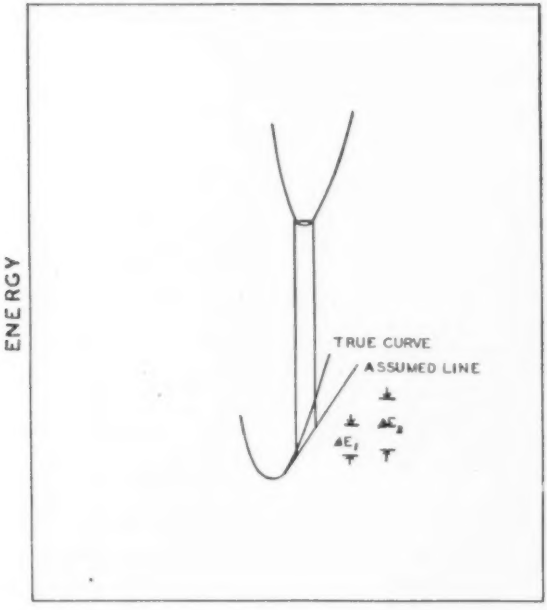

FIG. 4. Effect of curvature of potential energy curves on band width

shown them to be the sum of three components having Gaussian distributions, with one being predominant. The intensity of these components varies with the manganese content, but the location of the peaks is not

shifted (4). To explain satisfactorily the existence of more than one band with fixed locations, but with varying amplitude, it is necessary to assume that more than one energy level is present in the excited manganese ion. A previous paper in this series (11) has discussed briefly the reason for this multiplicity of energy states. It was suggested that the radiating transition was from a $3d^4 4p$ excited odd level to a $3d^4 4s$ even level rather than to the normal unexcited $3d^5$ even level. It is felt that the existence of this intermediate level to which transitions might occur is in itself sufficient evidence that this transition should be incorporated into the suggested mechanism of fluorescence.

One major difficulty with the assignment of levels in the previous paper lies in the fact that the suggested transitions are "allowed" in the spectrographic sense; consequently the life time of the excited state should be low and the decay rate of fluorescence should be lower than the actual observed value. Several possible explanations can be found to resolve this problem.

The simplest of these calls for the existence of *a* ^2D state with the $3d^4 4s$ configuration, which has not been observed spectroscopically for manganese. This level should lie at a somewhat higher energy value than the ^4D and ^6D states and, if it exists for the manganese ion bound in the crystal, it would involve the least energy change on emission and would lead to slower decay rates. With this hypothesis it is difficult, however, to explain why the "allowed" transitions to ^4D and ^6D states should not occur.

A more complex explanation would call for the existence of excited odd levels having a multiplicity of two, e.g., $^2P^0$, $^2D^0$, $^2F^0$, with the $3d^4 4p$ configuration, but lying at a lower energy value than the levels with multiplicity of 4 or 6. This seems possible, though it probably requires a crossing of the odd energy levels, and would account for the observed decay rate. Transition from these three levels to the ^4D and ^6D levels would give six possible energy values for the emission spectrum. With this hypothesis it is necessary to assume also that ^2D levels with the $3d^4 4s$ configuration do not exist; but, in spite of this difficulty, it seems the more reasonable hypotheses. A possible diagram of the potential energy curves of the excited odd levels is shown in Fig. 5, and with this situation an electron initially excited to the $^6D^0$ level might readily cross over to the $^2D^0$ level.

When beryllium is introduced into the zinc orthosilicate lattice as a replacement for zinc, the color of the fluorescent light changes rather rapidly at first to a yellow and then more slowly to a reddish buff as the beryllium concentration increases. The analyses of the emission spectrum has shown that the location of the band centers is invariant and that the σ values are also invariant with composition, but that the amplitude of various components varies systematically. Table III shows the values of the various parameters (4). It is obvious that the transitions responsible for the three high frequency bands must have a different final potential energy curve than the band at 16,400 cm.$^{-1}$, if the previous discussion of the reason for Gaussian distributions of emitted energy is correct. This is an additional justification for the assumption that the $3d^4 4s$ level is involved in the emission. Also there must be at least three separate states from which the transitions initiate. It is tentatively suggested that the σ value

for the last band at 15,300 cm.$^{-1}$ has been incorrectly chosen, and that the true value approaches 1000. Table III also lists possible transitions on the assumption that the excited odd level has a multiplicity of two. These differ from the original assignments because of the new assumption as to the odd level involved. Transitions to the ^4D state may have a different decay time from those involving the ^6D state and measurements of the decay time as affected by beryllium content would be of considerable interest.

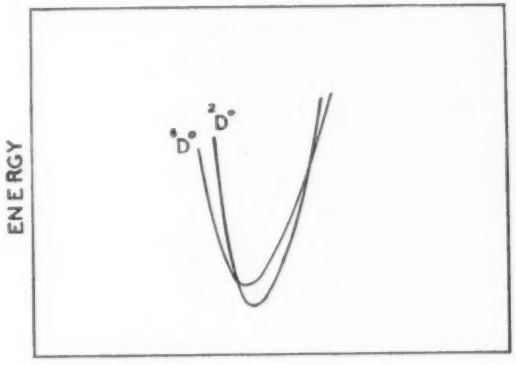

FIG. 5. Possible energy curves for excited manganese ion with varying multiplicity

TABLE III

$1/\lambda_s$ band center	σ	Compositions of phosphor				Transition	
19,080	550	A	B	C	D	$2D^e$	$6D$
18,300	550	A	B	C	D	$2P^e$	$6D$
17,300	600	A	B	C	D	$2p^6$	$6D$
16,400	1000			C	D	$2D^e$	$4D$
15,300	650 (?)				D	$2P^e$	$4D$

A.—Zinc orthosilicate. B.—Zinc beryllium silicate, low Be, low Mn. C.—Zinc beryllium silicate, high Be low Mn. D.—Zinc beryllium silicate, high Be high Mn.

EMISSION SPECTRUM OF LEAD ACTIVATED SILICATES

The emission spectrum of lead activated calcium metasilicate (12, 13) is simple, being a broad band peaked in the ultraviolet at about 3300 Å. Barium disilicate (13), activated by lead, also has a simple spectrum consisting of a slightly narrower band peaked at about 3500 Å. When the relative intensity is plotted on a frequency scale, it is seen that both of these phosphors have bands consisting of a single component with a Gaussian distribution. The parameters are:

	Peak $1/\lambda$	σ
Calcium metasilicate	30,000 cm.$^{-1}$	2800 cm.$^{-1}$
Barium disilicate	28,500 cm.$^{-1}$	1500 cm.$^{-1}$

The emission is decidedly different from that of manganese activated zinc silicate in the σ value of the emission band. The decay rate is rapid for lead activated compounds so it is probable that both the states involved in emission have the same multiplicity. There are three possible interpretations of this on the potential energy curve model, as shown in Fig. 6A, 6B, and 6C. In Fig. 6A, curve 1 represents the state of lead ion after emission, while curves 2 and 3 are two possible locations of the excited state. With curve 2 a "normal" value is obtained while with curve 3 a wide spread in emitted energy would be caused by the thermal vibrations in the excited state. This difference is indicated by the projections *a-b*

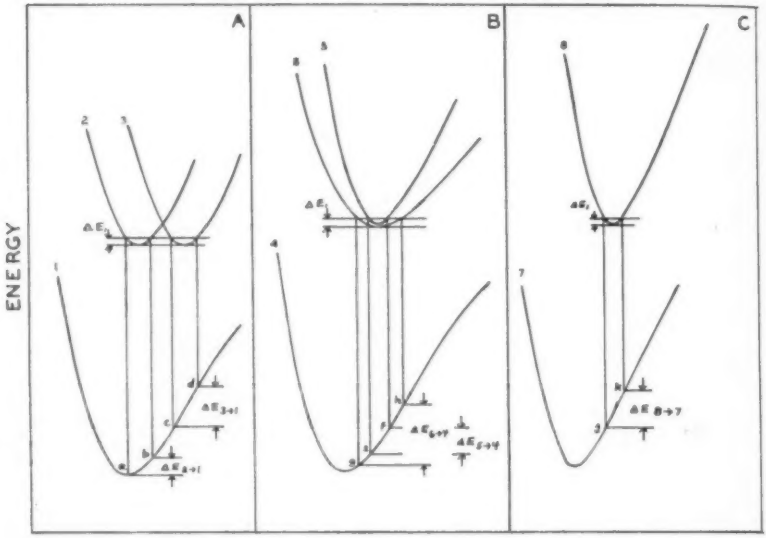

FIG. 6. Potential energy curves of lead ion. A, effect of different interatomic spacings on band width of emission spectrum; B, effect of different shapes of excited curves on band width; C, effect of a deep minimum in energy curve on band width.

and *c-d* on curve 1. A curve of type 3 would be obtained if the ion contracts considerably when going from the excited state to the state after emission.

In Fig. 6B, curve 4 again represents the state after emission while curves 5 and 6 are energy curves for the excited state which would give narrow and wide emission bands as shown by *e-f* and *g-h* respectively. A curve of type 6 would be obtained if the equilibrium interatomic spacing were large and the Madelung constant small.

In Fig. 6C, curve 7 represents the state after emission and curve 8 the excited state. On both of these the right-hand side of the potential energy curve rises sharply. This shape is obtained only if the Madelung

constant is large and the equilibrium interatomic spacing small. The wide energy band obtained is shown by j-k.

If it is assumed that lead enters the lattice as a divalent atom occupying atomic positions ordinarily taken by calcium or barium, the configuration of the lead ion and the atomic radius is given by:

	Configuration				State	Radius
Pb unexcited	$5s^2$	$5p^6$	$5d^{10}$	$6s^2$	^1s	1.32
Pb excited	$5s^2$	$5p^6$	$5d^{10}$	$6s\ 6p$	$^1p_0$	—

The spectrographic data show no intermediate even level is possible, though $^3p^0$ levels exist, and the assumption then required is that the emission involves a transition from the $6s6p$ configuration to the $6s^2$. The constants for the Pb-O system are close to those for the Mn-O system; therefore, the shape of the potential energy curves of the unexcited ions will be similar.

The equilibrium spacing r_0 is about 2.64 for unexcited lead as compared to 2.23 for unexcited manganese, with the values for the excited ions being larger. There is also only a small change in electron density as we go from the $6s^2$ to the $6s6p$ configuration, hence the Madelung constant for the excited ion should be small. We have, therefore, the situation described in Fig. 6B with a flat potential energy curve for the excited ion resulting in a broad emission band. The large change in equilibrium spacing required for Fig. 6A is not likely with divalent lead as there will be relatively little change in effective ionic radius between the $6s^2$ and the $6s6p$ configurations.

The second possibility which should be considered is that lead substitutes for silicon as a tetravalent ion with the parameters (7) being:

	Configuration				State	Radius
Pb unexcited	$5s^2$	$5p^6$	$5d^{10}$		^1s	0.84
Pb excited	$5s^2$	$5p^6$	$5d^9$	$6s$	even	—
Pb excited	$5s^2$	$5p^6$	$5d^9$	$6p$	odd	—

Here the picture fits Fig. 6C since r_0 is small, comparable with MnO, and there is a marked change in configuration as a $5d$ electron goes into the $6p$ orbit so that the electron density changes considerably affecting the attractive and repulsive forces. The observed spectra can then be explained by potential energy curves with a large U_0 from equation (2) and steep slopes on both sides of the sharp minimum.

The energy levels of tetravalent lead (14) are rather complex and would lead to an emission spectrum with several bands, so that it does not seem probable that tetravalent lead is involved in the emission.

While both of these ultraviolet emitting phosphors are alkaline earth silicates, the emission bands have quite different values of σ, indicating a decided difference in the potential energy curves caused by a difference in crystal structure, so that the fact that they both show ultraviolet emission is purely a coincidence. Other barium silicate phosphors (15), activated by lead, are known and these emit visible blue light with a wide spectral energy distribution (i.e., large value of σ). The same mechanism can be applied to explain the observed emission of these phosphors, with the actual location of the emission band being determined by the crystal

structure of the compound. The common characteristic of these phosphors is the simple spectrum given by lead serving as the activator.

MECHANISM OF SENSITIZED ACTIVATION

During the last few years, the phenomenon of sensitized luminescence has been receiving a considerable amount of attention and several phosphors have been developed, which are becoming of practical importance. This phenomenon involves the use of two activators to form a phosphor, emitting visible light characteristic of one activator, and excited by short-wave ultraviolet energy which will not cause luminescence if the emitting activator is used alone. One representative of this type of phosphor is calcium metasilicate (16, 18) activated by lead and manganese. The characteristics of this material are shown in Table IV.

It has been well established that lead is responsible for the excitation by 2537 and that the manganese content determines the emission spectrum. As the lead content changes, the efficiency of the phosphor is affected, but the color remains unchanged. In contrast, as the manganese content increases, the emission band due to lead is gradually suppressed and

TABLE IV

Activation	Emission on excitation by:		
	Cathode rays	1850 Å	2537 Å
Pb	Ultraviolet	?	Ultraviolet
Mn	Good orange	Weak orange	None
Pb + Mn	Good orange	Weak orange	Good orange

that due to manganese becomes stronger. The emission band due to manganese has been shown (4) to be formed of three components with Gaussian distribution. The amount of lead required for activation is less than 10 mol per cent of the manganese content.

To explain the behavior of this phosphor, it can be assumed that both lead and manganese substitute for calcium. As the first step in the activation of the compound by 2537 radiation, a lead ion absorbs a quantum, one electron is excited to the $6p$ orbit, and the ion expands, thus setting up vibrations in the crystal with the excess energy being transmitted to adjoining ions until the new equilibrium value of the interatomic spacing is reached. In the crystal structure of this compound, each calcium is bonded directly to eight oxygen atoms and each of these is bonded to four calcium atoms. Therefore, if the oxygen linked to lead is also linked to manganese, this bond will receive some of the vibrational energy, and, as shown in Fig. 7, the average potential energy of the manganese ion may shift from point A to point B. At this latter position, it is capable of directly absorbing 2537 energy and making a transition to point D. The direct transition from A to C requires more energy than is present in the 2537 quantum, but will take place with 1850 or with cathode rays.

With this mechanism it is readily seen that exciting one lead atom may sensitize many manganese ions by direct transfer of vibrational energy and, if sufficient energy is released, it may sensitize other indirectly linked

manganese ions. When the excited lead ion emits, it again sets up vibrations in the crystal and, consequently, the emission step also serves to sensitize manganese ions.

With a low concentration of manganese ions the probability of having Pb and Mn linked to the same oxygen is low; consequently the manganese is poorly sensitized and the lead emission band is very marked. As the manganese concentration increases, the probability of a common oxygen held between Pb and Mn rises rapidly so that activation of a single lead atom will sensitize many manganese atoms; consequently the ratio of lead emission to manganese emission becomes quite low.

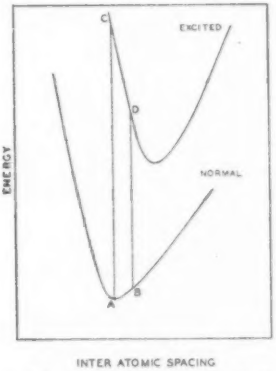

FIG. 7. Mechanism of sensitized luminescence. A–C, normal transition; B–D, transition after sensitization.

RADIATIONLESS ENERGY DISSIPATION

One of the general characteristics, common to all phosphors, is that the efficiency falls off rapidly with rising temperature after some critical temperature is reached. Previous discussions (3) have assumed that the potential energy curves of the excited and the normal states cross and that the transfer of energy without emission of radiation can take place if the energy barrier can be surmounted.

It has been shown by Kröger (1) that the efficiency of a phosphor is given by:

$$\eta = p \frac{K_f}{K_f + k_d}$$

where p is the fraction of the exciting energy actually absorbed by the activator, K_f is the probability of the fluorescent transition, and K_d that of the dissipation process. The discussion showed also that K_d is related to temperature by the formula:

$$K_d = S \exp. (-\epsilon/k_T)$$

where ϵ is an activation energy of about 0.7 electron volt or 5000–7000 cm.$^{-1}$. The implicit assumption is that the excited electron gains sufficient energy

from thermal vibration to pass the energy barrier, ϵ, between the excited and the normal state. A little consideration of Fig. 1 will show that the excess energy possessed by the excited ion immediately after activation is far greater than the energy barrier of 5000–7000 cm.$^{-1}$. Consequently, very large numbers of the excited ions should immediately pass over the potential barrier and enter the normal state without radiating.

A clue to the true mechanism is given by Szigeti and Nagy (2) in their recent paper on zinc silicate. It is shown in this paper that unexcited zinc silicate shows increasing conductivity as the temperature is raised above a critical temperature which is identical with the critical temperature for loss of fluorescence. The conductivity is also shown to vary exponentially with temperature. If it be assumed that free electrons are present in the phosphor, derived from some other source than the activator ion, then the number having an energy ϵ will be given by:

$$N_e = S \exp. (-\epsilon/kT)$$

where ϵ is the energy needed to liberate the free electrons and S is a constant of the order of the frequency of lattice vibration. These free electrons will then account for the conductivity of the unexcited phosphor.

The next assumption is that the free electron can absorb the energy of an excited manganese ion and return it to the normal state without emitting radiation by a process equivalent to a collision of the second kind. If this is correct then the probability of a radiationless dissipation of energy is given by:

$$K = cN_c N_e = CSN_c \exp. (-\epsilon/kT)$$

where C is a constant
N_c is the number of excited activator ions
N_e is the number of free electrons of energy ϵ
S is a constant

With this proposed mechanism all phosphors should show a temperature dependent conductivity when unexcited, and the critical temperature should be approximately the same for loss of fluorescence and for increase of conductivity. Increasing the concentration of activator should drop the critical temperature for loss of fluorescence. Phosphors with a large concentration of excited atoms should show a lower critical temperature than those with only a low concentration. Thus decay rate and critical temperature may be related. A further corollary is that all phosphors should show photoconductivity since a part of the vibrational energy liberated during excitation and emission will undoubtedly be transferred to the conductivity centers and liberate free electrons. This proposed mechanism makes a definite distinction between luminescent centers and conductivity centers, though the two may interact.

CONCLUSION

The behavior of phosphors activated by manganese or lead or by a combination of these two activators has been discussed on the basis of potential energy curves. These curves lead to a reasonable explanation of the existence of emission bands having a Gaussian distribution of energy with frequency and also to a possible explanation of the mechanism of

sensitized fluorescence. The application of potential energy curves leads to a simpler explanation of the emission behavior of lead than that previously proposed.

The assumptions proposed in this paper are capable of experimental proof in several instances and it is hoped to present this evidence in a later paper.

ACKNOWLEDGMENT

The author is particularly indebted to Dr. E. F. Lowry and Mr. O. H. Biggs for helpful discussions of the theories presented in the present paper.

Any discussion of this paper will appear in the discussion section of Volume 95 of the TRANSACTIONS of the Society.

REFERENCES

1. F. A. KRÖGER, *et al.*, *Physica*, **14**, 81 (1948).
2. G. SZIGETI AND E. NAGY, Public. Univ. for Technical Sciences, Budapest #3 (1948).
3. F. E. WILLIAMS AND H. EYRING, *J. Chem. Phys.*, **15**, 289 (1947).
4. K. H. BUTLER, *Electrochem. Soc.*, **93**, 143 (1948).
5. G. HERZBERG, "Molecular Spectra," p. 336, Prentice Hall, New York (1939).
6. M. BORN AND J. E. MAYER, *Z. Physik*, **75**, 1 (1932).
7. R. F. BACHER AND S. A. GOUDSMIT, "Atomic Energy States," McGraw-Hill Book Co., New York (1931).
8. H. T. GILROY, *Phys. Rev.*, **38**, 2217 (1931).
9. H. E. WHITE, "Introduction to Atomic Spectra," p. 63, McGraw-Hill Book Co., New York (1934).
10. G. HERZBERG, *loc. cit.*, p. 83.
11. K. H. BUTLER, *J. Optical Soc. Am.*, **37**, 566 (1947).
12. F. J. STUDER AND G. R. FONDA, *Bull. Amer. Phys. Soc.*, **23**, 48 (April, 1948).
13. R. H. CLAPP AND R. J. GINTHER, *J. Optical Soc. Am.*, **37**, 355 (1947).
14. J. E. MACK AND M. FROMER, *Phys. Rev.*, **48**, 357 (1935).
15. K. H. BUTLER, *Trans. Electrochem. Soc.*, **91**, 265 (1947).
16. H. C. FROELICH, *J. Electrochem. Soc.*, **93**, 101 (1948).
17. J. B. MERRILL AND J. H. SCHULMAN, *J. Optical Soc. Amer.*, **38**, 471 (1948).
18. G. R. FONDA AND H. C. FROELICH, *J. Electrochem. Soc.*, **93**, 114 (1948).

THE ELECTRON AFFINITY OF THE CARBON ATOM[1]

GEO. GLOCKLER AND JOSEPH W. SAUSVILLE[2]
State University of Iowa, Iowa City, Iowa

ABSTRACT

The electron affinity of the carbon atom is estimated to be 2.2 e.v. from linear extrapolation of the ionization potentials of the isoelectronic sequence C^-, N, O^+, F^{++}, and Ne^{+++}.

Experimentally it is shown that a carbon filament above 1850°K. gives off negative ions under proper conditions. Assuming that these ions are C^- ions, the electron affinity of the carbon atom is determined to be $\sim 2.8 \pm 0.3$ e.v. if the heat of sublimation of carbon is taken to be 136 kg.-cal. and $\sim 2.1 \pm 0.3$ e.v. if the heat of sublimation of carbon is 124 kg.-cal.

INTRODUCTION

Electron affinities of atoms and molecules have been determined by a variety of methods (1). In the case of the carbon atom only an estimate was available (2), based on an empirical relation between ionization potentials and atomic number of the isoelectronic sequence C^-, N, O^+, F^{++}, and Ne^{+++}. A similar consideration using a different empirical relation is as follows:

$$I^a = bZ + c \tag{1}$$

where I is the ionization potentlia in e.v., Z is the atomic number, and a, b, and c are constants. The results yielded are shown in Fig. 1 and Table I. For the isoelectronic series just mentioned

$$a = 0.575,\ b = 3.07, \text{ and } c = 16.828.$$

From column 5 of Table I it can be seen that equation (1) reproduces the ionization potentials of N, O^+, F^{++}, and Ne^{+++} to a high degree of accuracy. Hence the extrapolated value for the ionization potential of negative carbon atomic ions is very likely a pretty good estimate and

$$C + E^- \rightarrow C^-;\ EA(C) = 2.2 \text{ e.v.} \tag{2}$$

In these calculations the latest spectroscopic information was used as given by Herzberg (3).

On the experimental side there are available a number of methods (1). Since the first object of the study was to discover under what conditions negative carbon ions (C^-) will leave a hot filament it was decided that the

[1] Manuscript received November 21, 1948. This paper, which was submitted by Joseph W. Sausville to the Graduate College of the State University of Iowa in partial fulfillment of the requirements of the degree of Doctor of Philosophy, January, 1948, prepared for delivery before the Philadelphia Meeting, May 4 to 7, 1949.

[2] Present address: Department of Chemistry, University of Cincinnati, Cincinnati, Ohio.

magnetron method of Sutton and Mayer (4) would afford the simplest way, short of a mass-spectrograph, of attaining this end. The experimental arrangement included a straight carbon filament which, however, was found to have a rather large voltage drop over its length. It caused a complicating feature in the behavior of the experimental tube. Positively charged atomic ions (probably C^+) appeared under certain conditions of operation. Their number was much inferior to the number of electrons leaving the filament but of the same order as the negative ions.

In the usual method of determining electron affinity by the hot wire method, a carrier gas, for example, molecular iodine (I_2) is used to produce the corresponding atoms (I) on the surface of the hot filament (usually tungsten). In the present experiments it was expected that *the carbon filament itself would evaporate at a sufficient rate to produce a cloud of carbon atoms near its surface* and that some of these carbon atoms would unite with electrons and hence leave the filament surface as negative carbon ions. This expectation seemed indeed to have been fulfilled. It is, of course, well known, from the work of Marshall and Norton (5), for example, that carbon rings will lose weight by sublimation when brought to a high

TABLE I. *Ionization potentials of seven electron systems*

($I^{0.876} = 3.0699\ Z - 16.8283$ (e.v.))

	Z	I(expt.)(e.v.)	I(calc'd.)(e.v.)	% error
C^-	6	2.8 ±0.3	2.24	−20
N	7	14.545	14.544	−0.01
O^+	8	35.082	35.057	−0.08
F^{++}	9	62.647	62.716	+0.11
Ne^{+++}	10	96.897	96.889	−0.01

temperature. It was assumed that the vapor pressure of monatomic carbon would develop on the surface of the carbon filament in accordance with its temperature. If it is then supposed that equilibrium is reached on the surface of the filament (at temperature T) for the reaction

$$C^- \rightarrow C + E^-$$

then the well known thermodynamic equations

$$\Delta F^0 = \Delta H^0 - T\Delta S^0 = -RT\ln K_p \qquad (3)$$

apply. (ΔF^0 = standard free energy change, ΔH^0 = standard enthalpy change, ΔS^0 = standard entropy change, R = gas constant in calories per mol per degree, and K_p = equilibrium constant in terms of pressures.) In terms of the electron affinity (ΔE_0^0) these equations become

$$\Delta E_0^0 + 5/2\ RT - T\Delta S^0 = -RT\ln[(p_{E^-} \cdot p_{C^-})/p_{C^-}] \qquad (4)$$

where the p's refer to vapor pressures. Using the kinetic theory relation

$$p = Z(2\Pi mkT)^{1/2} \qquad (5)$$

where Z = number of atoms leaving unit area in unit time, m = mass of one atom, and k = Boltzmann's constant for one atom, and the well-

known expression for the entropy of a monatomic gas, it is found that the equation

$$\Delta E_0^0(\text{e.v.}) = 198 \times T \times 10^{-4} \times [5/2 \log T + \log (i_{C^-}/i_{E^-}) - \log P_C(\text{atm}) - 3.66] \quad (6)$$

gives the value of the electron affinity of carbon, ΔE_0^0 (the energy change in e.v. accompanying the above reaction at 0°K.), in terms of the ratio of ions to electrons, i_{C^-}/i_{E^-}, leaving the filament surface at an absolute temperature, T, and the pressure, P_C (in atmospheres), of monatomic carbon vapor at the filament surface. Three assumptions were made in the derivation of equation (6): (a) the reflection coefficient for all atomic species at the filament surface is zero; (b) the temperature of the gaseous carbon atoms leaving the filament surface is that of the filament; and (c)

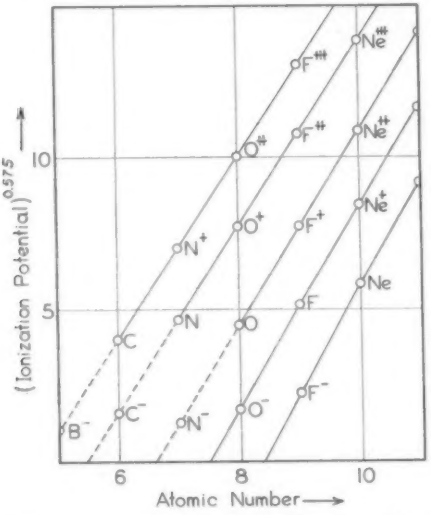

FIG. 1. Ionization potentials of several isoelectronic sequences

the ground state of the C^- ion is a $^4S_{3/2}$ state with a multiplicity of four similar to that of the nitrogen atom.

APPARATUS

Fig. 2 shows a schematic diagram of the experimental tube and the electrical circuits used in the experiments. The tube jacket, J, consisted of the outer half of a 71/60 pyrex ground glass joint increased to a total length of 45 cm. A glass thimble, T, holding the tungsten element supports was sealed at its base to the inner portion of the 71/60 joint. The side-arm, V, connected to the vacuum system. Copper wire leads soldered to the tungsten element supports were led through glass guides held at the base of the tube by a rubber stopper.

Commercial carbon filaments of several diameters from five to twenty mils and carbon clamping paste were kindly supplied by the Euclid Lamp Works of the General Electric Co. The filaments were analyzed spectrographically. The only contaminant non-volatile at normal filament operation temperatures was silicon which was present in trace amounts.

Five mil diameter filaments (F, Fig. 2) 7.5 cm. long were used in the experiments. These were fastened at either end to a nickel and stainless

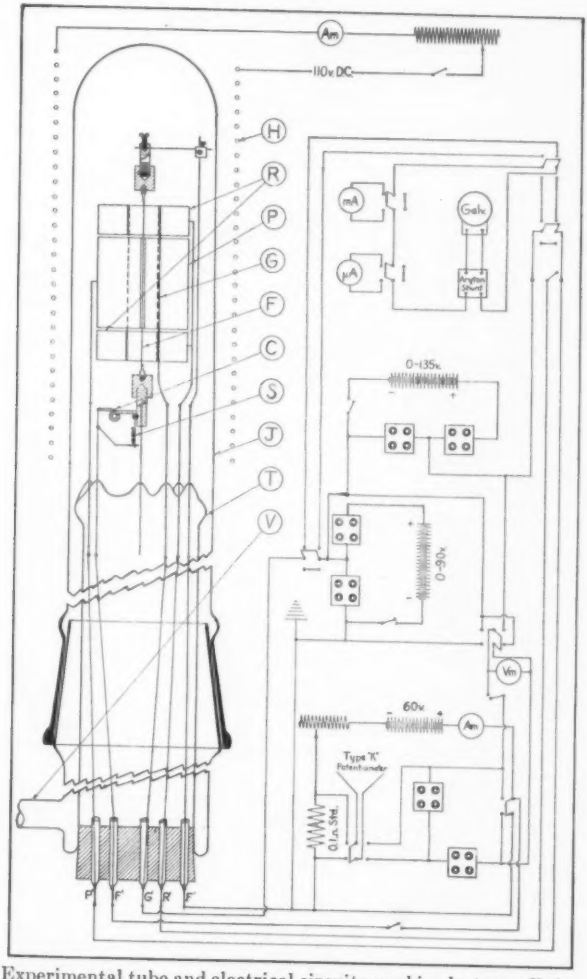

FIG. 2. Experimental tube and electrical circuits used in electron affinity measurements.

steel end block by means of clamping paste. The upper end block was supported by a tungsten wire and brass connector which also served as a means for centering the filament axially and longitudinally with respect to the plate. The lower end block was drilled to fit over a central tungsten wire guide. The filament was maintained taut by a spring, S, acting vertically upon a screwhead projecting from the lower end block. A heavy, semi-flexible copper wire, C, connected to the end block carried the filament current.

The guard rings, R, were of 15 gauge tantalum sheet 40 mm. in diameter and 13 mm. long. These were separated from the plate, P, by a distance of 0.5 mm. The plate, also of tantalum, was 40 mm. in diameter and 40 mm. long and differed from the usual in that the metal did not form a complete ring. The ends of the tantalum were separated by a 1 mm. gap which served as a slit through which the filament could be viewed for temperature measurement. To minimize plate current loss and to decrease field distortion caused by the slit, thin nickel sheets were spot-welded to the tantalum and bent so as to provide a tunnel at the slit 1 mm. wide and 5 mm. long along the entire length of the plate.

The grid, G, was 13 mm. in diameter and 68 mm. long. A 40 mm. long central portion aligned vertically with the plate was 24 mesh, 8.5 mil nickel wire gauze, and the rest of the length was covered with a thin outer layer of nickel sheet 14 mm. long at either end.

The solenoid, H, consisted of ten layers of No. 15 single-cotton covered, enameled copper wire with fifteen turns per inch over an 8 in. long brass core. The core, 3 in. inside diameter by 3.5 in. outside diameter, was made of two concentric brass cylinders separated by a space of 0.125 in. through which cooling water flowed. The solenoid was suspended on a pulley directly over the experimental tube and was counterweighted for convenience in lifting or lowering.

Plate currents, depending upon their magnitude, were measured by means of a milliameter, mA, a microammeter, μA, or an Aryton shunt-D'Arsonval galvanometer combination. The galvanometer used was a Leeds and Northrup instrument, Type "R," with a sensitivity of 7,860 mm./microamp. which was calibrated in conjunction with the Aryton shunt in a high resistance series circuit including a standard resistance shunted by a Type "K" potentiometer. In the experimental measurements, the Type "K" potentiometer was used to measure the filament current by the drop across a standard resistance, and filament, plate, and grid potentials through a volt box arrangement and suitable switches. Rough meters were also used for measuring these quantities approximately in order to avoid harsh treatment of the potentiometer.

Measurements of filament temperature were made with a Leeds and Northrup triple-range optical pyrometer for temperatures from 750°-2800°C. All three scales of the pyrometer were calibrated against a tungsten ribbon filament lamp recently standardized by the National Bureau of Standards. The true temperature, T, of the carbon filaments in the experimental tube was calculated from the apparent brightness temperature, T_a, as indicated by the pyrometer, using the Wien equation,

$$\frac{1}{T} - \frac{1}{T_a} = \frac{\lambda \cdot 2.303 \log \epsilon}{14{,}330}. \tag{7}$$

A value of 0.654 was used for λ, the effective wave length of the pyrometer screen. The Prescott and Hincke (6) value of $\epsilon = 0.98^{\frac{1}{4}} - 5.8 \times 10^{-5}T$ was taken for the spectral emissivity of carbon.

EXPERIMENTAL PROCEDURE

When the tube elements were properly positioned, the ground joint was lubricated on both freshly cleaned ground faces with picein wax, and the union made while the wax was warm. The top of the waxed joint was 9 cm. below the top of the thimble and over 13 cm. from the connections between the tube elements and tungsten supports; thus the wax was completely free from radiative or conductive heat from the tube elements when operating. At no time during the experimental determinations could any difference in temperature between the ground joint and the outside surroundings be noted. Thus the absence of detectable quantities of vapor from the wax was assured.

When the experimental tube had been assembled in preparation for a run, it was evacuated and the portion of the tube above the ground joint was flamed with a hand torch for twenty minutes. When the pressure in the vacuum system had decreased to 10^{-5} mm. Hg, the tube was flamed for another twenty minute period. Immediately after the second flaming the filament was heated to approximately 1750°K. while the grid was held at a positive potential of 20–30 volts with respect to the negative end of the filament, and the plate was maintained 40–50 volts positive with respect to the grid. The tube was allowed to operate in this condition with the pumps running continuously and until the following criteria were met: (a) with the tube operating under the above mentioned conditions, the pressure in the system had to remain less than 10^{-5} mm. Hg; (b) the plate currents obtained for fixed filament temperature and grid and plate voltage must be reproducible with time.

When the tube was in satisfactory operating condition, the filament temperature was measured with the pyrometer and the solenoid then lowered to a position around the tube such that its center coincided with the center of the plate. With a positive potential on the grid and a small positive drift potential on the plate, the plate current, i_{po}, of the triode was measured in the absence of the magnetic field. Current was then allowed to flow through the solenoid and measurements were made of the plate current, i_{ps}, for increasing values of solenoid current, I_{sol}, up to 15 amp. At the conclusion of a series of measurements at any one temperature, the solenoid was raised and readings again taken of the filament temperature.

EXPERIMENTAL RESULTS

The experimental measurements obtained were interpreted by plotting $\log (i_{ps}/i_{po})$ against $(I_{sol})^{-1/2}$. In several cases the plate current became positive in sign for a certain range of solenoid current values. These positive currents are represented in the lower portion of Fig. 4. The appearance of positive currents is understandable upon consideration of the fact that, depending upon the temperature of the filament, the potential drop across it was large, 45–60 volts, in comparison with the ionization potential of carbon, 11.2 volts (7) and under these conditions positive ions can be formed.

The shape of the resulting curves for any given temperature depended to a considerable extent upon the values used for the grid and plate potential during the experiments. Fig. 3 shows curves obtained for varying plate potential and a large grid potential of 37.8 volts. Fig. 4 represents results obtained at a constant plate potential of 2.06 volts and two different grid voltages, 19.29 and 25.79 volts. In each case, the conditions conducive to the production of positive plate currents yielded curves below, or more "positive" than those obtained for larger positive grid or plate potentials.

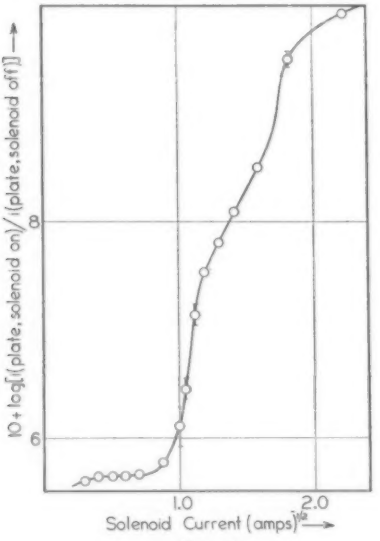

FIG. 3

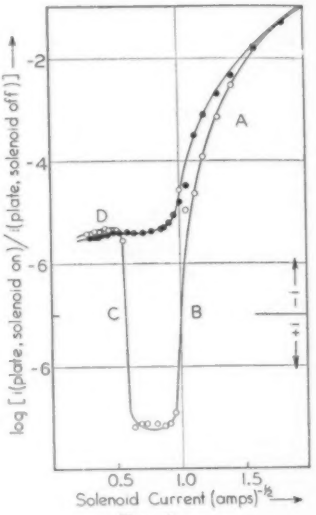

FIG. 4

FIG. 3. Ratio of ion current to electron stream to the plate as a function of magnetic field; grid potential 37.80 volts; plate potentials 0.50, 1.10 and 2.15 volts; T = 1926°K.

FIG. 4. Ratio of ion current to electron stream to the plate as a function of magnetic field; grid potential 19.29 volts (open circles); grid potential 25.79 volts (full circles); plate potential 2.06 volts; T = 2057°K.

The interpretation of the most complicated curves obtained, such as those in Fig. 4, depends upon consideration of three factors: (a) the relative masses of the charged particles in the tube, (b) the repressive effect of the solenoid on plate current of either sign, and (c) the action of the grid and plate in tending to repress positive plate current and to increase negative plate current. For low values of solenoid current the field acts to suppress electron current only because of the extremely small electronic mass, and the A portion of the curves in Fig. 4 results. When the electron current has been decreased by the field to an insignificant quantity in comparison with the concentration of the heavier C^+ ions, the curve B is obtained.

Part C results through the mutually cooperative action of the increasing field and the repelling action of the positively charged grid and plate upon the positive carbon ions. The plateau at D represents current due to negative ions insufficiently influenced by the field as a consequence of the accelerating effect of the grid and plate upon the negative particles. For still higher solenoid currents, a section of curve of decreasing slope results with decreasing negative ion current (Fig. 3 and 4).

Sets of curves similar to those of Fig. 3 and 4 were obtained at five temperatures from 1853°–2154°K. The plateau values representing the log of the ratio of the negative ion current to electron current are presented in Table II with the corresponding temperature values.

TABLE II. *Plateau values for log* (i_{p_2}/i_{p_0}) *at different temperatures*

T(°K.)	log (i_{p_2}/i_{p_0})
1853	−4.20
1930	−4.35
1971	−4.60
2057	−5.36
2154	−5.34

TABLE III. *Calculated values of the electron affinity of carbon in e.v. corresponding to different vapor pressure curves of carbon*

T(°K.)	$-\Delta E_0^0$(A)	$-\Delta E_0^0$(B)	$-\Delta E_0^0$(C)	$-\Delta E_0^0$(D)
L(C) kg.-cal.	169	136	124	107
1853	4.5	3.3	2.5	1.9
1930	4.3	3.1	2.4	1.7
1971	4.1	2.9	2.2	1.5
2057	3.7	2.5	1.8	1.1
2154	3.6	2.4	1.6	1.0
Mean	4.0	2.8	2.1	1.4

Upon the assumption that the particles comprising the negative ion currents observed in the experiments were C^- ions, calculation of the electron affinity of carbon was made using equation 6. Because of the uncertainty of values given in the literature for the vapor pressure of carbon as a function of temperature, calculations of ΔE_0^0 were made corresponding to four different vapor pressure curves. The values so obtained are presented in Table III.

The values of ΔE_0^0 given in columns A, C, and D in Table III were obtained using vapor pressure curves by Goldfinger and Jeunehomme (8) calculated with values for the heat of sublimation of carbon into atoms of 169, 124, and 107 kg.-cal. respectively. The vapor pressure curve used to obtain the B column was a hypothetical one calculated by means of the Clausius-Clapeyron equation assuming the temperature of sublimation of carbon to be 4000°K. and using 136 kg.-cal. for the heat of sublimation (9).

DISCUSSION OF RESULTS

The results presented in Table III show the effect upon ΔE_0^0 of the choice made for the pressure of carbon vapor as a function of temperature. It will be noted that the values in all four columns show a decrease with temperature. A consideration of the effect of the presence of positive carbon ions on the ion-electron ratio shows that they are responsible for this temperature trend. It was not possible to allow for this positive current properly, but further refinements of these experiments, including the use of an equipotential carbon emitting surface, avoiding thereby the large filament drop and its attendant complications, will very likely yield better results. It is interesting to note that the empirically determined electron affinity (2.2 e.v.) mentioned earlier checks the values given in columns 3 and 4 of Table III better than the values of columns 2 and 5. Hence a heat of sublimation of carbon of 136 or 124 kg.-cal. is indicated. A number of arguments for the 136 kg.-cal. value have been presented lately by one of us (10).

Consideration must be given to the possibility of the presence of detectable quantities of C_2^-, Ni^-, O_2^-, O^-, N_2^-, N^-, and Hg^- ions in the experimental tube. The pressure of C_2, Hg, or Ni molecules could not have been high enough to produce measurable quantities of ions. Since the experimental tube was not sealed off, but was operated with the pumps running continuously, the effect of the presence of air at a pressure as high as 10^{-5} mm. Hg was determined. The results of Metlay and Kimball (11) in the determination of the electron affinity of the oxygen atom using N_2O as carrier gas indicate that the effect of the presence of N_2 is negligible. Hence both N_2^- and N^- ions are excluded as possible interfering ion sources.

Possible ion currents produced by O_2^- ions were calculated using a value of 65.5 kg.-cal. for the electron affinity of the oxygen molecule as apparently indicated by the measurements of Metlay and Kimball. These currents were negligible in comparison with those obtained in the present experiments. Similarly, O^- ion currents were found to be negligible when calculated using the value 53.8 kg.-cal. for the electron affinity of the oxygen atom. This figure was obtained by Metlay and Kimball using N_2O as carrier gas, and it is in good agreement with those obtained by other investigators (12, 13). An average of apparent values for the electron affinity of the oxygen atom determined by the same investigators using oxygen as carrier gas, 65.5 kg.-cal., was also used for a calculation of O^- ion currents. The values obtained in this way were smaller than the measured currents, but of the same order of magnitude. These calculated O^- ion current values were subtracted from the experimental ion currents, and the differences were used to recalculate values of ΔE_0^0 for carbon. The change produced in the values of ΔE_0^0 for carbon ranged from only 0.04 to 0.20 e.v. In view of the above considerations, therefore, it appears likely that the chief contributor to the negative ion currents measured in the present experiments was the C^- ion.

Any discussion of this paper will appear in the discussion section of Volume 95 of the TRANSACTIONS of the Society.

REFERENCES

1. GEO. GLOCKLER AND S. C. LIND, "The Electrochemistry of Gases and other Dielectrics," John Wiley and Sons, Inc., New York (1939).

2. GEO. GLOCKLER, *Phys. Rev.*, **45**, 111 (1934).
3. G. HERZBERG, "Atomic Spectra and Atomic Structure," Dover Publ., New York (1944).
4. P. P. SUTTON AND J. E. MAYER, *J. Chem. Phys.*, **3**, 20 (1935).
5. A. L. MARSHALL AND F. J. NORTON, *J. Am. Chem. Soc.*, **55**, 431 (1933).
6. C. H. PRESCOTT AND W. B. HINCKE, *Phys. Rev.*, **31**, 130 (1928).
7. R. F. BACHER AND S. GOUDSMIT, "Atomic Energy States," McGraw-Hill Book Co., New York (1932).
8. P. GOLDFINGER AND W. JEUNEHOMME, *Trans. Faraday Soc.*, **32**, 1591 (1936).
9. H. D. HAGSTRUM, *Phys. Rev.*, **72**, 947 (1947).
10. GEO. GLOCKLER, *J. Chem. Phys.*, **16**, 842 (1948).
11. M. METLAY AND G. E. KIMBALL, *J. Chem. Phys.*, **16**, 774 (1948).
12. W. LOZIER, *Phys. Rev.*, **46**, 268 (1934).
13. G. HANSON, *Phys. Rev.*, **45**, 476 (1935).

THERMIONIC EMISSION FROM CARBON[1]

GEO. GLOCKLER AND JOSEPH W. SAUSVILLE[2]
State University of Iowa, Iowa City, Iowa

ABSTRACT

Measurements of the work function of carbon have yielded the value 4.35 ± 0.06 e.v. The constant A of the Richardson equation was found to be 48 ± 25 amp./cm.^{2}/deg.^{2} These results are in accordance with the latest values reported in the literature.

INTRODUCTION

Experimental values of the thermionic work function, Φ, of carbon reported in the literature and presented in Table I are discordant. Similarly those values for the constant A of the well known Richardson equation

$$I = AT^2e^{-\Phi/kT}$$

which are available show lack of agreement. The success of such experiments depends on the purity of the carbon filament and on the need of thoroughly outgassing it. Both these conditions are not easy to attain as they require extreme care and patience. For this reason, it was considered valuable to attempt another measurement of Φ and A for carbon.

EXPERIMENTAL PROCEDURE

The experimental tube used in the present investigation was a diode with a filament of carbon and a plate and guard rings of tantalum sheet. The tube was the same as that described in the preceding paper (8) except for the grid which was removed for the purpose of the present experiments. The electrical apparatus and circuits were the same as those mentioned in the prior paper except that the grid and solenoid circuits were eliminated. Filaments of 5 and 9 mils diameter and 7.5 cm. long were used throughout. Measurements of filament temperature were made with an optical pyrometer.

Once assembled, the experimental tube was outgassed by flaming the portion of the tube above the joint for twenty minutes. When the pressure had decreased to 10^{-5} mm. Hg, the tube was again flamed for twenty minutes. The filament was then heated to 1750°K. while plate and guard rings were kept at a potential of 90 volts positive to the negative terminal of the filament. After at least twelve hours of operation under these conditions with constant pumping, checks were made of the pressure and the thermionic current. After the pressure was less than 10^{-5} mm. Hg and thermionic currents were reproducible, measurements were begun.

[1] Manuscript received November 21, 1948. This paper, which was submitted by Joseph W. Sausville to the Graduate College of the State University of Iowa in partial fulfillment of the requirements for the degree of Doctor of Philosophy, January, 1948, prepared for delivery before the Philadelphia Meeting, May 4 to 7, 1949.

[2] Present address: Department of Chemistry, University of Cincinnati, Cincinnati, Ohio.

Saturated plate current was measured as a function of filament temperature from 1350°–2100°K. for plate potentials in the range 70–90 volts positive to the negative filament terminal. Guard rings were maintained at the same potential as the plate, but guard ring currents were by-passed to the potential source whereas the plate current reached the battery through the Aryton shunt-galvanometer combination.

TABLE I. *Literature values for the thermionic work function of carbon*

Investigator*	Φ	A
	e.v.	*amp./cm.² deg.²*
Deininger	4.4	—
Langmuir	2.5	$5. \times 10^{-4}$
Langmuir	3.88	—
Lester‡	4.52	—
Langmuir	3.94	5.93
Reimann	4.34	30.

* References 1–6.

‡ Lester measured the latent heat of evaporation of electrons from carbon, and Becker and Brattain (7) have demonstrated that this quantity is the same as the work function.

TABLE II. *Experimental values of Φ and A and associated data*

Run	Φ	$p\Phi$	$\Delta\Phi$	Log A	A	ΔA
	e.v.	*e.v.*	*e.v.*		*amp./cm.² deg.²*	*amp./cm.² deg.²*
1	4.17	0.034	0.18	1.193	15.6	32.2
2	4.34	0.004	0.01	1.787	61.2	13.4
3	4.36	0.026	0.01	1.904	80.2	32.4
4	4.40	0.006	0.05	1.953	89.7	41.9
5	4.46	0.006	0.11	1.779	60.1	12.3
6	4.36	0.006	0.01	1.456	28.6	19.2
Av. mean....	4.35	0.014	0.06	1.679	47.8*	25

* The mean value of A is the geometric mean of the values for A given in the table. This results from taking the antilogarithm of the arithmetic mean of the values found for log A.

EXPERIMENTAL RESULTS

Constants for the (2 log T − log I) *vs.* $1/T$ curves for six runs were calculated by the method of least squares, and the value of Φ and of A determined therefrom. The values obtained are given in Table II.

In the table, $\Delta\Phi$ and ΔA are the deviations of Φ and A from the mean. $p\Phi$ is the probable error of Φ based upon the precision of the data for each individual run. The average deviation of the Φ values from the mean, however, presents a more reliable picture of the precision of the measurements. The probable error in the temperature measurements ranged from about 10° at 1500°K. to 15° at 2000°K. The corresponding uncertainty reflected in Φ ranges from 0.40 e.v. at 1500°K. to 0.45 e.v. at 2000°K. The probable error in current measurements was approximately 0.5 per cent. For an error of this magnitude in I, that reflected in Φ at 1500°K. is 0.008 e.v. and at 2000°K. is 0.010 e.v. Thus the probable error of the

average Φ ranged from 0.048 to 0.055 e.v., which approximates the precision of the average value. Similarly, the precision of the mean value for A approximates the accuracy of this value. The results here presented are seen to be in good agreement with the Reimann value (6) which is the most recent determination reported in the literature.

Any discussion of this paper will appear in the discussion section of Volume 95 of the TRANSACTIONS of the Society.

REFERENCES

1. F. DEININGER, *Ann. Phys.*, **25**, 285 (1908).
2. I. LANGMUIR, *Phys. Rev.*, **2**, 329, 450 (1913).
3. I. LANGMUIR, *Trans. Am. Electrochem. Soc.*, **29**, 125 (1916).
4. H. LESTER, *Phil. Mag.*, **31**, 197 (1916).
5. O. W. RICHARDSON, "Emission of Electricity from Hot Bodies," 2nd Ed., p. 81, Longmans Green and Co., London (1921).
6. A. L. REIMANN, *Proc. Phys. Soc. (London)*, **50**, 496 (1938).
7. J. A. BECKER AND W. H. BRATTAIN, *Phys. Rev.*, **45**, 694 (1934).
8. G. GLOCKLER AND J. W. SAUSVILLE, *Trans. Electrochem. Soc.*, **95**, 282 (1949).